ZEROS OF EIGENFUNCTIONS OF THE SCHRÖDINGER OPERATOR ON GRAPHS AND THEIR RELATION TO THE SPECTRUM OF THE MAGNETIC SCHRÖDINGER OPERATOR

A Dissertation

by

TRACY KATHLEEN WEYAND

Submitted to the Office of Graduate and Professional Studies of
Texas A&M University
in partial fulfillment of the requirements for the degree of

DOCTOR OF PHILOSOPHY

Chair of Committee,	Gregory Berkolaiko
Co-Chair of Committee,	Peter Kuchment
Committee Members,	Joseph H. Ross, Jr.
	Jay R. Walton
Department Head,	Emil Straube

August 2014

Major Subject: Mathematics

ABSTRACT

In this dissertation, we analyze characteristics of eigenfunctions of the Schrödinger operator on graphs. In particular, we are interested in the zeros of the eigenfunctions and their relation to the spectrum of the magnetic Schrödinger operator.

We begin by studying the nodal count on finite quantum graphs, analyzing both the number and location of the zeros of eigenfunctions. This question was completely solved by Sturm in one dimension. In higher dimensions (including domains and graphs), we only know bounds for the nodal count. We discover more information about the nodal count on quantum graphs while analyzing eigenvalues of the magnetic Schrödinger operator. In particular, we show a relation between the stability of eigenvalues of the magnetic Schrödinger operator with respect to magnetic flux and the number of zeros of the corresponding eigenfunctions. We also study the location of the zeros of eigenfunctions while analyzing partitions. Specifically, we show that the critical points of the energy functional are the nodal partitions corresponding to zeros of an eigenfunction and that the stability of these critical points is related to the nodal count.

Then using Floquet-Bloch theory, we study the spectrum of the Schrödinger operator on infinite periodic graphs by analyzing the eigenvalues of the magnetic Schrödinger operator on a fundamental domain. Here we consider both discrete and quantum graphs. We find a characterization of critical points of the dispersion relation that occur inside the Brillouin zone under certain conditions on the graph. In particular, we show that if the fundamental domain is a tree, then the eigenfunction corresponding to an interior critical point must be zero on a vertex.

Finally, we use the results from infinite periodic graphs to study the magnetic Schrödinger operator on a finite quantum d-mandarin graph. We find that extremal points of the disper-

sion surface occur inside the Brillouin zone where two surfaces touch and the corresponding eigenfunction is zero on a vertex.

DEDICATION

To my parents,

who have supported me every step of the way.

ACKNOWLEDGEMENTS

First I would like to thank my advisor Dr. Gregory Berkolaiko for his guidance, insight, and most of all, patience. Thanks to you, not only have my research and technical writing skills improved tremendously, but my refined presentation skills earned me an award. During this entire process, I have been thankful for an advisor who is always willing to find time for me in his busy schedule.

I would also like to thank the rest of my Ph.D. committee. Dr. Peter Kuchment's assistance began when I was searching for a research topic and has continued all these years. He is one of the few Distinguished Professors I know who enjoys opening his home to his students. Thank you for the insight gained from our conversations and your continued support; I truly enjoyed getting to know you. Dr. Jay Walton invited me to join the NSF IGERT program at TAMU when I was visiting as a prospective student, and Dr. Joseph Ross was the principal investigator for this program. I would like to take this opportunity to thank both of you for that wonderful opportunity and experience.

I have discovered that it truly takes an entire department to have a Ph.D. student graduate with a job. Dr. Peter Howard, I don't even know where to begin. Thank you for being a mentor to me. Thank you for providing me opportunities to use and improve both my leadership and teaching skills. I am thankful for my teaching mentor Dr. Harold Boas who helped ensure I would be a well-rounded job candidate. I am grateful to Monique Stewart, the one person who always knows what to do. I appreciated the support of female faculty, especially Dr. Sue Geller and Dr. Jean Marie Linhart; you have both been an inspiration. I am also grateful to the other graduate students. Whether it was help with homework or LaTeX, a joke in the middle of the afternoon, a night out after a tense week, or simply someone to "vent" to, thank you for being there when I needed you. Paul Bruillard and Jennifer Webster, thank you for leaving me with such an amazing dissertation template.

Finally, I would like to thank my parents. Thank you for raising me to be an independent hard-working dreamer, as earning a doctoral degree required all of those qualities. Most days you cannot understand what I am doing, but you always try to understand what I am going through. You had faith in me when I lost faith in myself. You have been the biggest supporter of not only what I am doing, but the person I am. There is no way I could have accomplished this without you.

TABLE OF CONTENTS

LIST OF FIGURES

CHAPTER I

INTRODUCTION

In the most general sense, a graph represents a relationship between a set of objects. Applications appear in chemistry, physics, engineering, computer science, and social science to name a few. For example, graphs have been used to model roads, computer networks, and molecular and crystal structures. In applications, the relationship between objects (vertices) is represented by an operator that acts on functions whose domain is the graph. There has been extensive interest in the spetra of such operators. This chapter provides a summary of applications and current topics of interest.

The first use of a differential operator on a metric graph (i.e., a quantum graph) is attributed to Pauling while he was studying free electrons in organic molecules [80]. Graphs have subsequently been used to study such questions as the quantum Hall effect [25, 41, 56] and Anderson localization [5, 46, 57, 58, 77, 78]. Specifically, it has been shown that extended states exist on discrete [54, 55] and quantum [1, 2] trees. Kottos and Smilansky were the first to use quantum graphs to study quantum chaos [63, 64]; the interested reader should see the review [38] for more information.

Quantum graphs have also been used to model thin structures. Ruedenberg and Scherr were the first to consider graphs an idealized network of wires [87]. The wires have a finite diameter that is much smaller than any other length. These so called *fat quantum graphs* or *quantum wires* have been an important topic in mathematical physics [31, 68, 72, 83, 89]. Applications include thin superconductive materials [3, 85] and photonic crystals [35, 67, 70].

Quantum graphs have been simulated experimentally. Oheh, Ławniczak, Bauch, and Sirko used a microwave network to construct quantum graphs with time reversal symmetry and

then analyzed the spectral statistics [49]. Further work has considered directed networks, in which case the simulated quantum graphs do not have time reversal symmetry [48, 73], and these experimental results are in close agreement with the random matrix theory predictions [74].

Recently there has been much interest in carbon nanostructures due to their unique properties [53, 76, 88]. Quantum graphs have been actively used to model such structures [4, 61]. In particular, the spectra of graphene [71], graphyne [29], and carbon nanotubes [50, 60, 61, 71] have been analyzed using quantum graphs.

I.1 Magnetic Schrödinger Operator

The analysis of operators acting on functions whose domain is a graph began with the Laplace operator and then extended to the Schrödinger operator (i.e., the Laplace operator with electric potential). Later, applications arose that required analyzing the effect of a magnetic potential on a graph. One of the first such applications involved analyzing the free electrons in a metal in the presence of a uniform magnetic field. Harper modeled the metal as a two-dimensional lattice, which is equivalent to a discrete graph [42]. Hofstadter then studied the eigenvalues of this discrete graph in the presence of a magnetic field, discovering an amazingly rich fractal structure (before the word "fractal" was formally defined) [47]. The so-called "Harper model" and "Hofstader butterfly" are still active areas of study; see, for example, [59, 65]. A review of the discrete magnetic Schrödinger operator can be found in [94].

It has been shown that the spectrum of the magnetic Schrödinger operator on a graph depends only on the total magnetic potential through each cycle, which we call the magnetic flux [62]. On a discrete graph, "total" refers to the sum of the magnetic potential on each edge of a cycle, and it refers to the integral of the magnetic potential around a cycle on a quantum graph. Therefore, one can define an equivalence class of magnetic potentials such that the magnetic Schrödinger operator has the same spectrum for any magnetic potentials

from the same equivalence class. The eigenvalues can then be viewed as a function of β parameters that represent magnetic flux through a set of basis cycles where β is the first Betti number of the graph [62].

I.2 Nodal Count

One particular area of interest in mathematical physics has been the relation between the sequential number of the eigenfunction and the number of its zeros. This question goes back to Sturm in the nineteenth century. Sturm's Oscillation Theorem states that in one dimension the nth eigenfunction of the self-adjoint Laplace operator (or more generally, the Schrödinger operator) has $n-1$ zeros that when removed breaks the interval into n subintervals which we will call nodal domains [93]. However, this fact does not generally hold in higher dimensions, and we usually only know an upper bound on the number of nodal domains. In particular, the Courant Nodal Theorem states that in any dimension, the maximum number of nodal domains of the nth eigenfunction is n [27]. Pleijel demonstrated that in dimensions higher than one, this upper bound can only be achieved for a finite number of eigenfunctions [81] which are referred to as Courant sharp eigenfunctions.

Interest in this area was stimulated when Blum, Gnutzmann, and Smilansky demonstrated that nodal count statistics are important in the study of quantum chaos [21]. Bogomolny and Schmit introduced a percolation model for nodal domains of random wavefunctions that allows analytical calculations [22, 23]. It was then shown by Nazarov and Sodin that on $\mathbb{S}^2$, the number of nodal domains increases linearly with n [75]. Let ϕ_n denote the number of zeros of the nth eigenfunction. It has been shown that the sequence $\{\phi_n\}$ contains geometrical information about the domain [37]. Lower bounds have been found on the volume of the set of zeros of the nth eigenfunction [45, 91].

More recently, nodal counts have been analyzed on graphs. Both discrete [20] and quantum [90] tree graphs satisfy Sturm's Theorem, or in other words the nth eigenfunction has $n-1$ zeros that break the tree into n nodal domains, as long as the graph is generic; that is,

the eigenvalues are simple and the corresponding eigenfunctions are nonzero on vertices. We let ν_n denote the number of nodal domains corresponding to the nth eigenfunction. Courant's Nodal Theorem for domains in $\mathbb{R}^n$ was adapted to generic quantum graphs by Gnutzmann, Smilansky, and Weber [40], which gives us the upper bound $\nu_n \leq n$. It has also been shown that in the generic case, the minimum number of nodal domains is $n - \beta$ where β is the first Betti number of the graph [12]. If the eigenvalue is multiple, Courant's Theorem must be adjusted for the multiplicity; namely, $\nu_n \leq n + m - 1$ where m is the multiplicity of the nth eigenvalue [28]. It was conjectured that for a self-adjoint operator on a generic graph every possible nodal domain count was obtained, or in other words, for every integer $z \in [0, \beta]$, there exists n such that the nodal deficiency $n - \nu_n$ is equal to z. Recent counterexamples have demonstrated that this is not true for every generic graph.

An application of nodal domains has arisen in attempting to solve the inverse spectral problem on graphs. The famous question by Mark Kac "Can one hear the shape of a drum?"(see [51]) has been addressed on finite graphs; namely, given the spectrum, can one reconstruct the graph uniquely? The answer is no; many examples of isospectral graphs (i.e., different graphs with the same spectrum) have been found. In the discrete case, one can determine the number of edges, vertices, components, and spanning trees [95], but one cannot uniquely determine bipartiteness or planarity. Examples by Band, Ben-Shach, and Parzanchevski demonstrate that in the quantum case, one cannot uniquely determine the number of vertices or edges and hence, the first Betti number, given only the spectrum [11, 79].

Additional information about the structure of a quantum graph can be found from the Bloch spectrum of the graph. The Bloch spectrum can be viewed as the union of the spectrum of the magnetic Schrödinger operator over all possible magnetic fluxes. In particular, the Bloch spectrum uniquely determines the block structure and planarity of a graph [86].

Since the eigenvalues alone do not provide enough information to reconstruct the graph

uniquely, people have begun looking at the eigenfunctions with hope that they can provide additional information about a graph's structure. In particular, the question has been rephrased to "Can one count the shape of a graph?" It has been observed that on quantum graphs the nodal count complements the information contained in the spectrum, and in some cases the nodal count does resolve the isospectral problem [39]. Additionally, the nodal count contains information about the geometry of the graph [8, 10]. These and other results emphasize the importance of the nodal count. Recently, a relation has been found between the nodal count and the stability of eigenvalues with respect to perturbing a magnetic field; this is the focus of Chapter III.

Another way to approach the question of zeros of an eigenfunction is via the study of partitions. Informally speaking, a partition is simply a set of points. One question of interest is the following: which partitions correspond to the zeros of an eigenfunction? To answer this question, Helffer, Hoffmann-Ostenhof, and Terracini began analyzing minimal partitions on a domain. In particular, they define the energy functional Λ on the set of partitions as the maximum first eigenvalue over all the subdomains formed by removing the partition points from the original domain. A bipartite partition is a partition such that all subdomains can be labeled with $+$ or $-$ and no neighboring subdomains have the same sign. It was shown that a partition that minimizes Λ is bipartite if and only if it corresponds to the set of zeros of a Courant sharp eigenfunction [44].

Later the concept of partitions was extended to and analyzed on graphs, which in turn led to substantial progress in the study of the energy functional Λ on manifolds. It was first shown on quantum graphs that if one restricts the domain of Λ to the set of equipartitions, or partitions in which every subdomain has the same first eigenvalue, then the partitions corresponding to the zeros of eigenfunctions are the critical points of the energy functional Λ. Furthermore, the Morse index of these critical points is equal to the corresponding nodal deficiency [7]. This result was then extended to discrete graphs [18] and bounded domains in $\mathbb{R}^n$ [16]. The result of [7] will be strengthened in Section III.3.

I.3 Critical Points of the Dispersion Relation

Many physical systems, such as crystal structures, are modeled by infinite periodic graphs. We define a fundamental domain (or Wigner-Seitz cell) of an infinite period graph as a minimal subgraph that can generate the entire graph under the action of the group of periods. On external vertices of the fundamental domain we impose quasi-periodic boundary conditions parameterized by quasi-momenta. The Brillouin zone is the set of all quasi-momenta, which we will take to be $B = [-\pi, \pi]^k$ for a $\mathbb{Z}^k$-periodic graph. By standard Floquet-Bloch theory (see e.g., [15, 66, 84]), we know that the spectrum of an elliptic self-adjoint operator can be found by calculating the spectrum on a fundamental domain for a specific quasi-momentum and then taking the union of the resulting spectra over the entire Brillouin zone.

We define the jth spectral band as the set of all the jth eigenvalues over the entire Brillouin zone, or in other words $\{\lambda_j(\boldsymbol{\alpha})|\boldsymbol{\alpha} \in [-\pi, \pi]^k\}$. The spectrum σ of the infinite periodic graph is the union of all spectral bands. The dispersion relation is the multi-valued function $\boldsymbol{\alpha} \in B \to \sigma$, and the minimum and maximum of each spectral band is called a spectral edge. Therefore, spectral edges can be viewed as extremal points of the dispersion relation. One question that has been raised on infinite periodic graphs is the location of these spectral edges. In particular, where in the Brillouin zone do the spectral edges occur? As spectral edges correspond to minimum and maximum points, this question is essentially equivalent to considering the eigenvalues as functions of the quasi-momenta parameters and locating the extremal points. It is known that in one dimension the extrema occur on the boundary of the Brillouin zone (see e.g., [84]). Numerically, this is often the case in higher dimensions as well. However, some counterexamples have been found, proving that this is not always the case in higher dimensions, in particular with discrete or quantum graphs [30, 43].

In the process of studying the spectra of such operators, the graphs of the spectral bands (i.e., dispersion surfaces) sometimes touch (which can be viewed as degenerate eigenvalues

on the fundamental domain), and in particular conical Dirac points have been observed. Such points occurred when using quantum graphs to model the structures of graphene [32, 71, 76] and graphyne [29]. We study properties of the eigenfunctions corresponding to these touching points in Chapter IV and then use this information to construct explicit examples in which dispersion surfaces touch in Chapter V.

I.4   Outline

In this dissertation, we analyze properties of the spectra of both discrete and quantum graphs as well as properties of the corresponding eigenfunctions. We introduce the concept of operators and functions acting on discrete and metric graphs in Chapter II. Here we introduce definitions, notation, and preliminary results that will be used in subsequent chapters. In Chapter III, we present results relating the nodal count to the stability of an eigenvalue with respect to magnetic perturbation. In particular, the Morse index of the eigenvalue at a symmetric point is equal to the nodal surplus of the corresponding eigenfunction. In the quantum graph case, details of the proof are provided. Consequences of this relation will also be discussed, one of which involves partitions. Specifically, we show that the partition defined by the zeros of an eigenfunction is a critical point of the energy functional Λ, and the Morse index of this critical point is equal to the nodal deficiency.

In Chapter IV, we switch the focus to infinite periodic graphs. We say a point $\boldsymbol{\alpha} \in [-\pi, \pi]^k$ is a nonsymmetric point, or a point in the interior of the Brillouin zone, if there exists j such that $\alpha_j \neq 0, \pm\pi$. We demonstrate that if the eigenvalue $\lambda_n(\boldsymbol{\alpha})$ has a critical point at a nonsymmetric point of the Brillouin zone and the fundamental domain is a tree, then the corresponding eigenfunction must be zero at an internal vertex.

Finally, we use the previous results to analyze extremal points of dispersion surfaces of finite d-mandarin graphs in Chapter V. We find that in the case of quantum d-mandarin graphs, the extremal points are located at nonsymmetric points of the Brillouin zone where dispersion surfaces touch and the corresponding eigenfunction is zero on a vertex.

CHAPTER II

PRELIMINARIES: OPERATORS ON GRAPHS*

All graphs consist of a set of vertices V and a set of edges E where each edge connects two vertices. An edge that begins at vertex u and ends at vertex v is denoted by $(u, v) \in E$. If $(u, v) \in E$, we say that vertices u and v are *connected* and use the notation $u \sim v$. The *degree* of a vertex $v \in V$, denoted by d_v, is equal to the number of edges attached to it. A vertex of degree one is called a *leaf*.

A *path* is a sequence of edges $[e_1, e_2, \ldots, e_k]$ such that the vertex at the end of e_j is identical to the vertex at the beginning of e_{j+1}. A *cycle* is a path that begins and ends at the same vertex; in other words, the vertex at the beginning of e_1 is equal to the vertex at the end of e_k. In this paper, we consider all graphs to be *undirected*; that is, each edge may be traversed in either direction. Consequently, if there exists a path $\mathcal{P}$ from vertex v to u, then by traversing $\mathcal{P}$ in the opposite direction one has a path from u to v. While the graph itself is undirected, it will be necessary to assign direction to each edge in order to properly define operators and functions on graphs. We refer to the assigned direction as *positive* and the opposite direction as *negative*, as traversing an edge in the opposite direction typically switches the sign of the function or operator.

A graph is *finite* if it has a finite number of vertices and edges. The *first Betti number* of a graph is defined by

$$\beta = |E| - |V| + k$$

where k is the number of connected components and $|A|$ denotes the number of elements in the set A. Namely, if graph is connected (i.e., there exists a path from any vertex to

any other vertex), then $k = 1$. In this paper, we assume all graphs are connected unless stated otherwise. The first Betti number is equal to the rank of the fundamental group of a graph. Informally, it is equal to the number of "independent" cycles on a graph. A connected graph with $\beta = 0$ (i.e., no cycles) is called a *tree*.

In this dissertation, we will be analyzing the spectra and eigenfunctions of operators that act on functions whose domain is a graph. In this chapter, we will explicitly define what we mean by this in two cases: discrete graphs and metric (or quantum) graphs.

II.1 Operators on Discrete Graphs

A discrete graph Γ is completely defined by a set of vertices V and a set of edges E. Functions on discrete graphs are defined only on the vertices (not the edges). These functions can therefore be viewed as vectors in $\mathbb{R}^n$ or $\mathbb{C}^n$ where $|V| = n$. In order to represent functions whose domain is Γ as a vector, each vertex v is associated with an integer $1 \leq j \leq n$, and then $f(v)$ is in the jth component of the vector f. In particular, f is a function on Γ if

$$\sum_{v \in V} |f(v)|^2 = \|f\|_{l^2}^2 < \infty.$$

Since the functions may be viewed as vectors, the operators acting on these functions are matrices (in particular, $n \times n$ matrices). Such an operator is self-adjoint if and only if the corresponding matrix is self-adjoint. For example, the discrete Laplacian is given by the matrix

$$L_{u,v} = \begin{cases} -1 & u \sim v \\ d_u & u = v \\ 0 & \text{otherwise.} \end{cases}$$

9

The normalized Laplacian on a discrete graph is given by the matrix

$$\widetilde{L}_{u,v} = \begin{cases} -1/\sqrt{d_u d_v} & u \sim v \\ 1 & u = v \\ 0 & \text{otherwise.} \end{cases}$$

As these matrices are symmetric, these operators are self-adjoint, and their action on a function f can be written as

$$Lf(v) = -\sum_{u \sim v} f(u) + d_v f(v), \quad \text{or}$$

$$\widetilde{L}f(v) = -\sum_{u \sim v} \frac{1}{\sqrt{d_u d_v}} f(u) + f(v).$$

Suppose that two vertices $u, v \in E$ are connected by an edge $(u, v) \in E$. We consider a function f to have a zero on edge (u, v) if the function changes sign on the edge, which is equivalent to $f(u)f(v) < 0$. For each eigenfunction f_n of a self-adjoint operator H, we call this set of edges the *nodal set*, or in other words,

$$N(f_n) = \{(u, v) \in E : f_n(u)f_n(v) < 0\}.$$

We denote $\phi_n = |N(f_n)|$ and define the *nodal point count* as the sequence $\{\phi_n\}$. Furthermore, $\Gamma \backslash N(f_n)$ is a collection of disconnect subgraphs of Γ called *nodal domains*, and for each n we denote the number of such subgraphs by ν_n.

II.2 Operators on Metric Graphs

Here we use the notation and terminology found in [15].

A metric graph is uniquely defined by a set of vertices V, a set of edges E, and a set of real numbers L that assign length to each edge in E. We call a metric graph *compact*

if the graph is finite and each edge has finite length. We view each edge $e_j \in E$ as a one-dimensional interval of length l_j. Functions are defined everywhere on a metric graph (i.e., on the vertices and edges) and are in "tilde" function spaces where ~ represents the direct sum over each edge. For example,

$$\widetilde{H^k}(\Gamma) = \bigoplus_{e \in E} H^k(e)$$

is the space of all functions that are in the Sobolev space $H^k(e)$ for each edge in E. Intuitively, we can say $f \in \widetilde{H^k}(\Gamma)$ is equal to a different function on each edge, or in other words, $f = f_e \in H^k(e)$ on edge e of Γ. We define $\widetilde{L^k}(\Gamma)$ similarly. In some instances, it is useful to denote whether the function is real-valued or complex-valued. In these cases we use the notation

$$\widetilde{H^k}(\Gamma, \mathbb{R}) \qquad \text{and} \qquad \widetilde{H^k}(\Gamma, \mathbb{C})$$

to denote the real-valued and complex-valued functions of $\widetilde{H^k}(\Gamma)$ respectively.

On a metric graph Γ, we define the inner product as the sum of the inner product over each edge, or in other words

$$\langle f, g \rangle = \sum_{e \in E} \int_e f(x)\overline{g(x)} \, dx = \sum_{e \in E} \int_e f_e(x)\overline{g_e(x)} \, dx$$

since for any function h with domain Γ, $h = h_e$ on edge $e \in E$.

A *quantum graph* is a metric graph together with a differential operator H and associated vertex conditions which define the domain of functions $\mathcal{D}$ that H acts on. If the metric graph is a tree and the vertex conditions of the associated operator are local, then we call the graph a *quantum tree*.

An operator H with domain $\mathcal{D}$ is self-adjoint if $\langle Hf, g \rangle = \langle f, Hg \rangle$ for all functions $f, g \in \mathcal{D}$ and the domain of the adjoint H^* is also equal to $\mathcal{D}$. For example, the Laplacian is defined

11

by

$$L : f \to -\frac{d^2 f}{dx^2}$$

on functions in $\widetilde{H^2}(\Gamma)$ that satisfy the δ-type vertex conditions

$$\begin{cases} f(x) \text{ is continuous at v}, \\ \sum_{e \in E_v} \frac{df}{dx_e}(v) = \chi_v f(v), \qquad \chi_v \in \mathbb{R}, \end{cases} \tag{II.1}$$

at all vertices $v \in V$ where E_v is the set of edges attached to vertex v. We observe that

$$\begin{aligned} \langle Lf, g \rangle &= \sum_{e \in E} \int_e -f''(x)\overline{g(x)}\, dx \\ &= \sum_{e \in E} -f'(x)\overline{g(x)}\big|_e + \int_e f'(x)\overline{g'(x)}\, dx \\ &= \sum_{e \in E} -f'(x)\overline{g(x)}\big|_e + f(x)\overline{g'(x)}\big|_e - \int_e f(x)\overline{g''(x)}\, dx \\ &= \sum_{v \in V}\left(-\overline{g(v)}\sum_{e \in E_v} f'(v) + f(v)\sum_{e \in E_v}\overline{g'(v)}\right) - \sum_{e \in E}\int_e f(x)\overline{g''(x)}\, dx \\ &= \sum_{v \in V}\left(-\overline{g(v)}\chi_v f(v) + f(v)\overline{\chi_v g(v)}\right) - \sum_{e \in E}\int_e f(x)\overline{g''(x)}\, dx \\ &= \sum_{e \in E}\int_e f(x)(-\overline{g''(x)})\, dx = \langle f, Lg \rangle \end{aligned}$$

for all functions in the domain since $\chi_v \in \mathbb{R}$ $\forall v \in V$, and hence the operator is symmetric. Additionally, the adjoint operator has the same domain as the operator, and therefore the operator is self-adjoint. All local vertex conditions that render the Laplacian $-\frac{d^2}{dx^2}$ self-adjoint have been characterized and can be seen, for example, in Theorem 5 of [69] and Theorem 1.4.4 of [15].

On a metric graph, a function f has zeros at points $x \in \Gamma$ where $f(x) = 0$. For each eigenfunction f_n of a self-adjoint operator H, we call the set of points at which the eigenfunction

vanishes the *nodal set*, or in other words,

$$N(f_n) = \{x \in \Gamma : f_n(x) = 0\}.$$

If Dirichlet conditions are enforced at the vertices, we do not include these points in the nodal set. Once again we denote $\phi_n = |N(f_n)|$, and define the *nodal point count* as the sequence $\{\phi_n\}$. We call the collection of disconnected subgraphs $\Gamma \backslash N(f_n)$ *nodal domains*, and for each n we denote the number of such subgraphs by ν_n. The main difference is that in the discrete case the nodal set is a set of edges, and in the quantum case it is a set of points.

II.2.1   Generic Eigenvalues

An eigenvalue is called *simple* if its multiplicity is one. A simple eigenvalue whose corresponding eigenfunction is nonzero on all vertices of the graph is called a *generic eigenvalue*. Most known results on quantum graphs require a priori that the eigenvalues be generic. In this section, we analyze conditions that guarantee this is the case. We begin by stating a lemma that relates eigenvalues of operators that have slightly different vertex conditions. It can be found in [15] (Theorem 3.1.8 with slight modification). By δ-type conditions, we are referring to the conditions in (II.1).

Lemma II.1. *Let $\Gamma_{\chi'}$ be the quantum graph obtained from the graph Γ_χ by changing the coefficient of the δ-type condition at a vertex v from χ to χ' (conditions at all other vertices are fixed). If $-\infty < \chi < \chi' \leq \infty$ (where $\chi' = \infty$ corresponds to the Dirichlet condition at vertex v), then*

$$\lambda_n(\Gamma_\chi) \leq \lambda_n(\Gamma_{\chi'}) \leq \lambda_{n+1}(\Gamma_\chi). \tag{II.2}$$

If the eigenvalue $\lambda_n(\Gamma_{\chi'})$ is simple and its eigenfunction f is such that either $f(v)$ or $\sum f'(v)$ is nonzero, then the above inequalities can be made strict. If, in addition, $\chi' \neq \infty$,

the inequalities become

$$\lambda_n(\Gamma_\chi) < \lambda_n(\Gamma_{\chi'}) < \lambda_n(\Gamma_\infty) \le \lambda_{n+1}(\Gamma_\chi).$$

The following theorem is a generalization of Corollary 3.1.9 of [15].

Theorem II.1. *Let Γ be a graph with δ-type conditions at every internal vertex and extended δ-type conditions on all leaves. Suppose an eigenvalue λ of Γ has an eigenfunction f which is nonzero on all internal vertices of Γ. Further, assume that no zeros of f lie on the cycles of Γ. Then the eigenvalue λ is simple and f is eigenfunction number $\phi + 1$, where ϕ is the number of internal zeros of f.*

Remark 1. The condition that no zeros lie on the cycles of the graph Γ is equivalent to f having $\phi + 1$ nodal domains.

Proof. We use induction on the number of internal zeros of f to show that the eigenvalue is simple. If f has no internal zeros, then we know f corresponds to the groundstate eigenvalue, which is simple.

Now suppose f has $\phi > 0$ internal zeros. By way of contradiction, assume that λ is not simple. Choose an arbitrary zero ζ of f and another eigenfunction g. Cut Γ at ζ; making this cut will disconnect the graph into two subgraphs since ζ cannot lie on a cycle of Γ. On at least one of these subgraphs, g is nonzero and not a multiple of f (otherwise, f and g are not a linearly independent function). We will now analyze the eigenfunctions on this subgraph Γ'.

On the graph Γ', f and g satisfy the same δ-type conditions at all vertices except possibly the new leaf ζ. We denote by Γ'_τ as the graph Γ' with the conditions $\Phi'(\zeta) = \tau\Phi(\zeta)$. We know that (λ, f) is an eigenpair on Γ'_∞ and similarly, there exists χ such that (λ, g) is an eigenpair on Γ'_χ. However, since Γ'_∞ contains fewer internal zeros of f than Γ does, by the inductive hypothesis λ is simple on Γ'_∞ so $\chi \ne \infty$.

Observe that $f'(\zeta)$ is nonzero; if it was zero, the function f would be identically zero on the whole edge containing ζ and, therefore, at the end-vertices of the edge. Thus, the inequalities (II.2) with $\chi' = \infty$ become strict and Γ'_χ and Γ'_∞ cannot have the same eigenvalue λ. This demonstrates that λ is indeed a simple eigenvalue.

Now we show that f is eigenfunction number $n = \phi + 1$. By Remark 1 there are $\nu = \phi + 1$ nodal domains. Since λ is simple, we know from Theorem 5.2.8 of [15] that

$$n - \beta \leq \nu \leq n \qquad \text{and} \qquad n \leq \phi + 1 \leq n + \beta$$

where β is the Betti number of Γ. However, since $\nu = \phi + 1$, both inequalities hold only if $\nu = n = \phi + 1$ so f is indeed the eigenfunction number $\phi + 1$.

$\square$

II.2.2 The Wronskian on Quantum Graphs

In Chapters III and IV, we will need to relate values of functions and their derivatives at multiple vertices. We will accomplish this by using properties of the Wronskian on graphs. Here we consider the most general vertex conditions that keep our operator self-adjoint.

The *Wronskian* of two functions f_1 and f_2 evaluated at a point x_0 is defined as

$$W(f_1, f_2)(x_0) = f_1(x_0)f_2'(x_0) - f_1'(x_0)f_2(x_0).$$

Given any two functions f_1 and f_2 that satisfy the differential equation $f''(x) + b(x)f'(x) + c(x)f(x) = 0$ on an interval I, we know by Abel's identity that

$$W(f_1, f_2)(x) = W(f_1, f_2)(x_0)\exp\left(-\int_{x_0}^{x} b(t)\, dt\right).$$

Observe that if $b(x) \equiv 0$, then the Wronskian is constant everywhere on the interval. Also

notice that the Wronskian is a one-form; that is, its sign depends on direction.

We will first use the Wronskian to demonstrate a particular characteristic of eigenfunctions on graphs. Then we will show that the sum of Wronskians at any vertex with self-adjoint conditions is zero. Finally we will apply this result to the case in which all but two vertices have the same conditions.

Lemma II.2. *Suppose that Γ is a graph, H is a self-adjoint operator of the form $-\frac{d^2}{dx^2}+q(x)$ where $q : \Gamma \to \mathbb{R}$, and $f \in \widetilde{H^2}(\Gamma, \mathbb{C})$ is an eigenfunction of H. Then*

$$Im\big(f'(x)\overline{f(x)}\big)$$

is constant on each edge of Γ.

Proof. Since H is self-adjoint, f and $\overline{f}$ are both solutions to $-y''(x) + (q(x) - \lambda)y(x) = 0$ on each edge of Γ where λ is the eigenvalue corresponding to f. Applying Abel's identity with $b(x) \equiv 0$, one can see that the Wronskian $W(\overline{f}, f)$ is constant on each edge of Γ. One can then calculate that

$$
\begin{aligned}
W(\overline{f}, f)(x) &= \overline{f(x)}f'(x) - \overline{f'(x)}f(x) \\
&= \overline{f(x)}f'(x) - \overline{\overline{f(x)}f'(x)} = 2i\mathrm{Im}\big(\overline{f(x)}f'(x)\big),
\end{aligned}
$$

and hence $\mathrm{Im}(f'(x)\overline{f(x)})$ is constant on each edge of Γ.

$\square$

Lemma II.3. *Let Γ be a graph and suppose that $f_1, f_2 \in \widetilde{H^2}(\Gamma, \mathbb{C})$ are two solutions of $-f''(x) + (q(x) - \lambda)f(x) = 0$ on Γ that satisfy the same self-adjoint vertex conditions at vertex v. Then*

$$\sum_{e \in E_v} W_e(f_1, f_2)(v) = 0, \tag{II.3}$$

where E_v denotes the set of all edges attached to the vertex v and each Wronskian $W_e(f_1, f_2)$

16
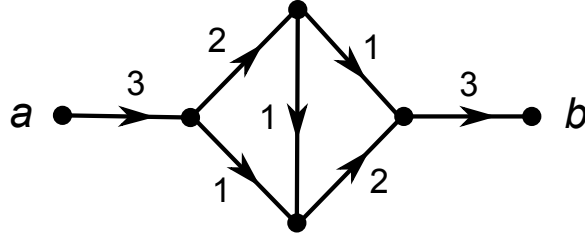
Figure II.1: Example of a flow on a graph. Let Γ be the directed graph above and let f be the function whose (constant) value on every edge is given by the number near each arrow. One can easily check that the function f constitutes a flow on Γ.

is taken outward from the vertex.

Proof. We denote the self-adjoint operator acting as $-\frac{d^2}{dx^2} + q(x)$ by H. Define a smooth compactly supported function ζ on Γ such that $\zeta \equiv 1$ in a neighborhood of the vertex v and zero at all other vertices of Γ. For the sake of convenience, we denote ζf_j by g_j. Since H is self-adjoint, we know that $\langle Hg_1, \overline{g_2} \rangle = \langle g_1, H\overline{g_2} \rangle$. Using this fact, integrating by parts, and carefully taking the direction of derivatives into account, we calculate that

$$
\begin{aligned}
0 &= \langle g_1, H\overline{g_2} \rangle - \langle Hg_1, \overline{g_2} \rangle \\
&= \sum_{e \in E} \int_e \left(-g_2''(x) + q(x)g_2(x) \right) g_1(x)\, dx - \int_e \left(-g_1''(x) + q(x)g_1(x) \right) g_2(x)\, dx \\
&= \sum_{e \in E} \int_e -g_2''(x)g_1(x)\, dx + \int_e g_1''(x)g_2(x)\, dx \\
&= \sum_{(u,w) \in E} \left(-g_2'(x)g_1(x) + g_1'(x)g_2(x) \right) \Big|_u^w + \sum_{e \in E} \int_e \left(g_2'(x)g_1'(x) - g_1'(x)g_2'(x) \right)\, dx \\
&= \sum_{e \in E_v} \left(g_1(v)g_2'(v) - g_1'(v)g_2(v) \right) = \sum_{e \in E_v} W_e(g_1, g_2)(v) = \sum_{e \in E_v} W_e(f_1, f_2)(v)
\end{aligned}
$$

since both g_1 and g_2 are zero near all other vertices of Γ and $g_j = f_j$ near vertex v.

$\square$

17

Lemma II.4. *Let a and b be two leaves (i.e., vertices of degree one) of a graph Γ and suppose that $f_1, f_2 \in \widetilde{H^2}(\Gamma, \mathbb{C})$ are two solutions of $-f''(x) + (q(x) - \lambda)f(x) = 0$ on Γ that satisfy the same self-adjoint vertex conditions at all vertices except a and b. Then $W(f_1, f_2)(a) = -W(f_1, f_2)(b)$.*

Proof. In graph theory, a *flow* between two vertices a and b is defined as a non-negative function on the edges of a directed graph Γ that satisfies Kirchhoff's current conservation condition at every vertex other than a and b, which can be stated as follows: the total current flowing into a vertex must equal the total current flowing out of it (see Figure II.1 for an example). Given a flow between a and b, it is a standard result of graph theory that the total current flowing into b is equal to the total current flowing out of a [24].

As the Wronskian is a one-form (i.e., it depends on direction) and constant on each edge, we assign a direction to each edge of Γ so that the Wonskian is always non-negative. Let E_v^+ denote the set of edges attached to vertex v that are directed into v and similarly let E_v^- denote the set of edges attached to v that are directed outward from v. In Lemma II.3, all Wronskians are taken outward from the vertex. Since the Wronskian is a one-form, (II.3) is equivalent to

$$\sum_{e \in E_v^-} W_e(f_1, f_2)(v) \; - \sum_{e \in E_v^+} W_e(f_1, f_2)(v) = 0$$

at all $v \in V \backslash \{a, b\}$ which means that the Wronskian satifies Kirchhoff's current conservation condition, and hence constitutes a flow. Therefore, we know that the flow into b equals the flow out of a so $W(f_1, f_2)(a) = -W(f_1, f_2)(b)$.

$\square$

CHAPTER III

STABILITY OF EIGENVALUES WITH RESPECT TO MAGNETIC

PERTURBATION*

In this chapter we analyze the connection between the nodal point count $\{\phi_n\}$ and stability of eigenvalues with respect to perturbation of a magnetic field. In particular, we focus on the main results of [13, 19] which state that if one considers eigenvalues of the the magnetic Schrödinger operator as functions of magnetic flux, zero magnetic flux is a critical point with Morse index equal to the nodal surplus $\phi_n - (n-1)$ of the corresponding eigenfunction. This was proven on discrete graphs in [13] and quantum graphs in [19]. Additionally, [26] provides an alternative proof in the discrete case and the first proof for a particular quantum graph (a circle). However, the latter proof used the known nodal point count of a circle, which made it impossible to generalize to general quantum graphs.

III.1   Discrete Graphs

Let $\Gamma = \{V, E\}$ be a finite discrete graph with vertex set V and edges E. We define the Schrödinger operator H^0 by

$$(H^0 f)(v) = -\sum_{u \sim v} f(u) + q(v) f(v)$$

where $q : V \to \mathbb{R}$ represents electric potential. The magnetic Schrödinger operator H^A is defined by

$$(H^A f)(v) = -\sum_{u \sim v} e^{iA_{u,v}} f(u) + q(v) f(v)$$

where $A : E \to \mathbb{R}$ represents magnetic potential. We may denote $A_{v,u}$ as simply A_e where e is the directed edge from v to u. To ensure that H^A is self-adjoint, we enforce the condition $A_{v,u} = A_e = -A_{-e} = -A_{u,v}$.

A cycle $\mathcal{C} = [e_1, e_2, \ldots, e_n]$ is a sequence of directed edges such that the end of edge e_k is the beginning of edge e_{k+1} for all $k = 1, 2, \ldots n - 1$ and the end of edge e_n is the beginning of edge e_1. The *magnetic flux* through a cycle $\mathcal{C}$ is defined as

$$\alpha_{\mathcal{C}} = \sum_{k=1}^{n} A_{e_k} \quad \mod 2\pi.$$

It turns out that the spectrum of H^A depends only on the magnetic flux through a set of basis cycles. In particular, choose a spanning tree $\mathbb{T}$ and let S be the set of edges in $\Gamma \backslash \mathbb{T}$. Notice that there are β edges in S where $\beta = |E| - |V| + 1$ is the first Betti number of Γ. One at a time, put each edge from S back into the graph and calculate the magnetic flux around the resulting cycle. Using a gauge transformation, one can show the following:

Lemma III.1. *The magnetic Schrödinger operator H^A is unitarily equivalent to the operator H^{α} defined by*

$$H^{\alpha}_{u,v} = \begin{cases} q(v) & \text{if } u = v \\ -1 & \text{if } (u,v) = e \in E \backslash S \\ -e^{\pm i\alpha_j} & \text{if } (u,v) = e_j \in S \end{cases}$$

where the sign is positive if $u < v$ and negative if $u > v$.

Consequently, any two operators that have the same flux through all cycles are unitarily equivalent. Henceforth, we consider eigenvalues as functions of magnetic flux $\boldsymbol{\alpha} = (\alpha_1, \alpha_2, \ldots, \alpha_{\beta})$.

For a simple n^{th} eigenvalue whose eigenvector is nonzero at vertices, we let ϕ_n denote the number of edges on the graph whose endpoints have different signs. Recall that on

20

a discrete graph, we associate this with the number of "zeros" an eigenvector has on the graph. We define the *nodal surplus* σ_n as

$$\sigma_n = \phi_n - (n-1).$$

Given this background, we are now able to present the main result of [13].

Theorem III.1. *If the nth eigenvalue of the Schrödinger operator H^0 is simple and the corresponding eigenvector f has no zero entries, then $\boldsymbol{\alpha} = (0, \ldots, 0)$ is a critical point of $\lambda_n(\boldsymbol{\alpha})$ whose Morse index is equal to the nodal surplus of f.*

As previously mentioned, an alternative proof can be found in [26].

III.2 Quantum Graphs

Let $\Gamma = \{V, E, L\}$ be a compact metric graph. We define the Schrödinger operator by

$$H^0 : f \to -\frac{d^2 f}{dx^2} + qf$$

where $q : \Gamma \to \mathbb{R}$ represents electric potential, and H^0 acts on functions from $\mathcal{D} \subset \widetilde{H^2}(\Gamma, \mathbb{R})$ that satisfy the δ-type vertex conditions

$$\begin{cases} f(x) \text{ is continuous at v}, \\ \sum_{e \in E_v} \frac{df}{dx_e}(v) = \chi_v f(v), \qquad \chi_v \in \mathbb{R} \end{cases} \tag{III.1}$$

for all $v \in V$. Here E_v denotes the set of all edges attached to vertex v, and x_e denotes the x coordinate on edge e. On vertices of degree one (i.e., *leaves*), we allow the Dirichlet condition $f(v) = 0$, which is formally equivalent to $\chi_v = \infty$. However, in this case we do not consider the eigenfunction to be zero on a vertex when either placing constraints on eigenfunctions or counting the zeros of an eigenfunction. This operator is self-adjoint,
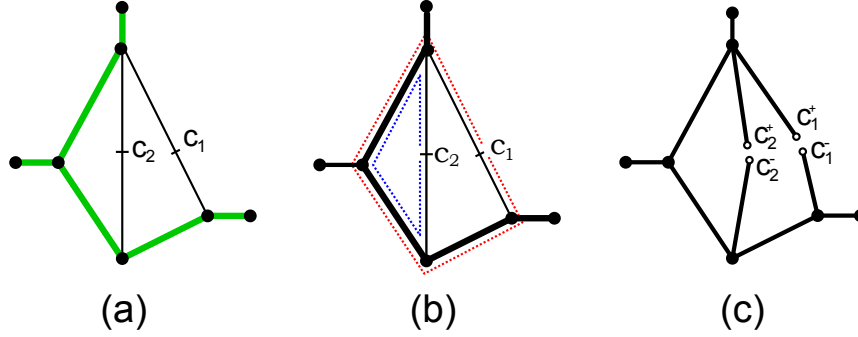
Figure III.1: The process of cutting a graph and calculating magnetic flux. (a) The chosen spanning tree (bold and green) and chosen cut points. (b) The unique paths (dashed and colored) over which we integrate magnetic potential to obtain magnetic flux. (c) The resulting tree graph.

bounded from below, and has a discrete set of (real) eigenvalues that can be ordered as

$$\lambda_1 \le \lambda_2 \le \ldots \le \lambda_n \le \ldots \quad .$$

The magnetic Schrödinger operator H^A is defined by

$$H^A : g \rightarrow -\left(\frac{d}{dx} - iA(x)\right)^2 g + qg$$

where the one-form $A(x)$ represents magnetic potential (as $A(x)$ changes sign with the orientation of the edge). The operator H^A acts on functions from $\mathcal{D}_A \subset \widetilde{H^2}(\Gamma, \mathbb{C})$ that satisfy

$$\begin{cases} g(x) \text{ is continuous at v}, \\ \sum_{e \in E_v}\left(\frac{dg}{dx_e}(v) - iA(v)g(v)\right) = \chi_v g(v), \qquad \chi_v \in \mathbb{R} \end{cases} \qquad \text{(III.2)}$$

for all $v \in V$.

We now describe how to compute the *magnetic flux* $\boldsymbol{\alpha} = (\alpha_1, \alpha_2, \ldots, \alpha_\beta)$ on a quantum graph. Choose a spanning tree of Γ and let S be the edges of Γ that are not in the spanning tree. It is well known that $|S| = \beta$, the first Betti number of Γ which is $\beta = |E| - |V| + 1$

22

and the rank of the fundamental group of the graph. Informally, β can be viewed as the number of independent cycles on a graph. Cut each edge $e_j \in S$ at an arbitrary point c_j to form two new vertices c_j^+ and c_j^-. The resulting graph will be a tree $\mathbb{T}$ (see Figure III.1). The following result can be found, for example, in [15, 62, 86].

Lemma III.2. *The magnetic Schrödinger operator H^A is unitarily equivalent to the operator H^α which is defined by*

$$H^\alpha : f \to -\frac{d^2 f}{dx^2} + qf$$

and acts on functions from $\mathcal{D}_\alpha \subset \widetilde{H^2}(\mathbb{T}, \mathbb{C})$ that satisfy the δ-type vertex conditions (III.1) on the vertices of $\mathbb{T}$ inherited from Γ and the conditions

$$
\begin{aligned}
f(c_j^-) &= e^{i\alpha_j} f(c_j^+) \\
f'(c_j^-) &= -e^{i\alpha_j} f'(c_j^+)
\end{aligned}
\tag{III.3}
$$

at the new vertices where the magnetic flux $\boldsymbol{\alpha} = (\alpha_1, \alpha_2, \ldots, \alpha_\beta)$ with

$$\alpha_j = \int_{c_j^-}^{c_j^+} A(x)\, dx \mod 2\pi$$

where the integral is taken over the unique path on Γ that does not pass through any other cut points c_k (see Figure III.1(b)).

Remark 2. The negative sign in the second equation of (III.3) is due to the convention that at the vertices c_j^+ and c_j^- of $\mathbb{T}$, the derivative is taken inward.

Proof. Define $\xi(x)$ such that $\xi'(x) = A(x)$, or in other words,

$$\xi(x) = \int_p^x A(x)\, dx \mod 2\pi$$

where p is an arbitrary point on Γ. The integral is taken along the unique path that does

23

not pass through any of the cut points $\{c_j\}_{j=1}^{\beta}$, or in other words, the unique path from p to x on the tree $\mathbb{T}$.

Suppose that g is an eigenfunction of H^A corresponding to the eigenvalue λ. We will demonstrate that $f := ge^{-i\xi}$ is an eigenfunction of H^α that corresponds to the same eigenvalue λ.

First we will show that $f \in \mathcal{D}_\alpha$. Since $g \in \mathcal{D}_A$, we know that g is continuous at all vertices of Γ, which means that f is also. Observe that

$$f'(x) = \big(g'(x) - iA(x)g(x)\big)e^{-i\xi(x)}. \tag{III.4}$$

Since g satisfies (III.2) at the vertices of Γ, we can see that

$$\sum_{e \in E_v} \frac{df}{dx_e}(v) = \sum_{e \in E_v} \left(\frac{dg}{dx_e}(v) - iA(v)g(v) \right) e^{-i\xi(v)} = \chi_v g(v)e^{-i\xi(v)} = \chi_v f(v)$$

and hence, f satisfies (III.1) at the vertices of Γ. We still need to show that f satisfies (III.3) at the new vertices. Since $g \in \mathcal{D}_A \subset \widetilde{H^2}(\Gamma, \mathbb{C})$, we know that g is continuous and has continuous derivatives at all cut points $\{c_j\}_{j=1}^{\beta}$. Therefore, $g(c_j^-) = g(c_j^+)$ and $g'(c_j^-) = -g'(c_j^+)$ for all $j = 1, 2, \ldots, \beta$. Notice that

$$-\xi(c_j^-) = \int_{c_j^-}^{p} A(x)\, dx = \int_{c_j^-}^{c_j^+} A(x)\, dx + \int_{c_j^+}^{p} A(x)\, dx = \alpha_j - \xi(c_j^+) \qquad \forall\ j = 1, 2, \ldots, \beta.$$

At the new vertices, we can now observe that

$$f(c_j^-) = g(c_j^-)e^{-i\xi(c_j^-)} = g(c_j^+)e^{i(\alpha_j - \xi(c_j^+))} = e^{i\alpha_j} f(c_j^+) \qquad \forall\ j = 1, 2, \ldots, \beta.$$

Since A is a one-form, we know that $A(c_j^-) = -A(c_j^+)$, and we can calculate that

$$
\begin{aligned}
f'(c_j^-) &= (g'(c_j^-) - iA(c_j^-)g(c_j^-))e^{-i\xi(c_j^-)} \\
&= -(g'(c_j^+) - iA(c_j^+)g(c_j^+))e^{i(\alpha_j - \xi(c_j^+))} = -e^{i\alpha_j}f'(c_j^+)
\end{aligned}
$$

for all $j = 1, 2, \ldots, \beta$. Hence, f is indeed in $\mathcal{D}_\alpha$.

To complete this proof, we must show that f is an eigenfunction of H^α corresponding to the eigenvalue λ. Continuing from (III.4), one can see that

$$
\begin{aligned}
f''(x) &= \frac{d}{dx}\left(\big(g'(x) - iA(x)g(x)\big)e^{-i\xi(x)} \right) \\
&= e^{-i\xi(x)}\frac{d}{dx}\big(g'(x) - iA(x)g(x)\big) - \big(g'(x) - iA(x)g(x)\big)\frac{d}{dx}e^{-i\xi(x)} \\
&= \left[\frac{d}{dx}\big(g'(x) - iA(x)g(x)\big) - iA(x)\big(g'(x) - iA(x)g(x)\big) \right]e^{-i\xi(x)} \\
&= \left[\left(\frac{d}{dx} - iA(x)\right)\big(g'(x) - iA(x)g(x)\big) \right]e^{-i\xi(x)} \\
&= \left[\left(\frac{d}{dx} - iA(x)\right)^2 g(x) \right]e^{-i\xi(x)}.
\end{aligned}
$$

This means that

$$
-f''(x) + q(x)f(x) = \left[-\left(\frac{d}{dx} - iA(x)\right)^2 g(x) + q(x)g(x) \right]e^{-i\xi(x)} = \lambda g(x)e^{-i\xi(x)} = \lambda f(x),
$$

and hence f is an eigenfunction of H^α corresponding to λ. Following the same procedure, one can show that if f is an eigenfunction of H^α, then $g := fe^{i\xi}$ is an eigenfunction of H^A. This proves that the operators are indeed unitarily equivalent.

$\square$

Henceforth, we denote H^α as the equivalence class of operators H^A that are unitarily equivalent to H^α.

For a simple n^{th} eigenvalue whose eigenfunction ψ is nonzero at vertices, we let ϕ_n denote the number of internal zeros of ψ on Γ. Recall that we define the *nodal surplus* σ_n as

$$\sigma_n = \phi_n - (n-1).$$

As in the discrete case, we consider the eigenvalues as functions of $\boldsymbol{\alpha}$ and are interested in the stability of the eigenvalues while perturbing the magnetic flux. The main result of this chapter is as follows:

Theorem III.2 ([19])**.** *Suppose that the nth eigenvalue of the Schrödinger operator H^0 is simple, and the corresponding eigenfunction ψ is nonzero at vertices and has ϕ_n internal zeros. We consider the perturbation H^A of H^0 by a magnetic field A with flux $\boldsymbol{\alpha} = (\alpha_1, \ldots, \alpha_\beta)$. Then $\boldsymbol{\alpha} = (0, \ldots, 0)$ is a non-degenerate critical point of $\lambda_n(\boldsymbol{\alpha})$ and its Morse index is equal to the nodal surplus $\phi_n - (n-1)$ of ψ.*

To prove this theorem, we first study the eigenvalues of an operator that has parameter-dependent δ-type vertex conditions at the newly formed vertices of the tree $\mathbb{T}$. The benefit of analyzing this operator instead of $H^{\boldsymbol{\alpha}}$ directly is that this operator has local vertex conditions. Hence, this operator is acting on functions defined on a quantum tree, and information is already known about eigenfunctions defined on quantum trees and their corresponding eigenvalues. We then relate these eigenvalues to the eigenvalues of an intermediate operator that can be viewed as the magnetic Schrödinger operator with complex magnetic potential. Finally, these eigenvalues will be related to the eigenvalues $\lambda_n(\boldsymbol{\alpha})$ of the magnetic Schrödinger operator with real magnetic potential.

Beginning with Γ, we form a tree $\mathbb{T}$ the same way we did when defining H^α (see Figure III.1 for details). Let $\boldsymbol{\gamma} = (\gamma_1, \ldots, \gamma_\beta) \in \mathbb{R}^\beta$. On the tree $\mathbb{T}$, we define the operator H^γ by

$$H^\gamma : f \to -\frac{d^2 f}{dx^2} + qf$$

on functions from $\mathcal{D}_\gamma \subset \widetilde{H^2}(\mathbb{T}, \mathbb{R})$ that satisfy the δ-type vertex conditions (III.1) on the vertices inherited from Γ and

$$
\begin{aligned}
f'(c_j^+) &= \gamma_j f(c_j^+) \\
f'(c_j^-) &= -\gamma_j f(c_j^-)
\end{aligned}
\tag{III.5}
$$

at the new vertices formed from cutting the graph. We consider eigenvalues of H^γ as functions of $\boldsymbol{\gamma}$.

We will now show that each eigenfunction ψ_n of H^0 gives rise to a critical point of $\lambda_m(\boldsymbol{\gamma})$ (for some m). This problem was first addressed in [7] while analyzing partitions of graphs. However, the results of [7] contained an a priori condition of non-degeneracy which renders them unsuitable for proving Theorem III.2. Here we remove this restriction and generalize the results of [7]. More details about this connection will be presented in Section III.3.

Let λ_n be a simple eigenvalue of H^0 with corresponding eigenfunction ψ. Assume that ψ is nonzero at the vertices and cut points of the graph (moving them if necessary). Since $\psi \in \mathcal{D} \subset \widetilde{H^2}(\Gamma, \mathbb{C})$, it is continuous with continuous first derivatives on Γ, and in particular at all cut points $\{c_j\}$. Considering ψ as a function acting on $\mathbb{T}$, we know that taking the direction of the derivative into account

$$\psi(c_j^+) = \psi(c_j^-) \quad \text{and} \quad \psi'(c_j^+) = -\psi'(c_j^-) \quad \forall \; j = 1, 2, \ldots, \beta.$$

Theorem III.3. *Suppose that the nth eigenvalue λ_n of the Schrödinger operator H^0 is simple, and the corresponding eigenfunction ψ is nonzero at vertices and has ϕ_n internal zeros. Define*

$$\widetilde{\gamma}_j := \frac{\psi'(c_j^+)}{\psi(c_j^+)} = -\frac{\psi'(c_j^-)}{\psi(c_j^-)}$$

and let $\widetilde{\boldsymbol{\gamma}} = (\widetilde{\gamma}_1, \ldots, \widetilde{\gamma}_\beta)$. Consider the eigenvalues of H^γ as functions of $\boldsymbol{\gamma}$. Then

1. *$\lambda_{\phi_n+1}(\widetilde{\boldsymbol{\gamma}}) = \lambda_n$,*

2. *$\boldsymbol{\gamma} = \widetilde{\boldsymbol{\gamma}}$ is a non-degenerate critical point of $\lambda_{\phi_n+1}(\boldsymbol{\gamma})$, and*

3. *the Morse index of the critical point $\widetilde{\boldsymbol{\gamma}}$ is $n - 1 + \beta - \phi_n$.*

III.2.2   Proof of Theorem III.3

In order to prove Theorem III.3, we first need to prove some preliminary results in the following subsections.

III.2.2.1   Quadratic Forms

The quadratic form of the operator H^0 on Γ is

$$h[f] = \sum_{e \in E(\Gamma)} \int_e |f'(x)|^2 + q(x)|f(x)|^2 \, dx + \sum_{v \in V(\Gamma)} \chi_v |f(v)|^2$$

with the domain

$$\mathcal{D} = \{f \in \widetilde{H^1}(\Gamma, \mathbb{R}) : f \text{ is continuous at all vertices of } \Gamma\}.$$

Dirichlet conditions, if any, are also imposed on $\mathcal{D}$. The quadratic form of H^γ on $\mathbb{T}$ is

$$h_{\boldsymbol{\gamma}}[f] = h[f] + \sum_{j=1}^{\beta} \gamma_j (|f(c_j^+)|^2 - |f(c_j^-)|^2) \qquad \text{(III.6)}$$

where β is the first Betti number of Γ. The quadratic form h_γ has the domain

$$\mathcal{D}_\gamma = \{f \in \widetilde{H^1}(\mathbb{T}, \mathbb{R}) : f \text{ is continuous at all vertices of } \mathbb{T}\}.$$

Observe that the domain $\mathcal{D}_\gamma$ is actually independent of γ and larger than the domain $\mathcal{D}$ since we no longer impose continuity at the cut points $\{c_j\}$. In particular,

$$\mathcal{D} = \{f \in \mathcal{D}_\gamma : f(c_j^+) = f(c_j^-) \text{ for all } j = 1, 2, \ldots, \beta\}.$$

Remark 3. Observe that any function $f \in \mathcal{D}_\gamma$ can be written as

$$f = f_0 + \sum_{j=1}^{\beta} s_j \rho_j$$

where $f_0 \in \mathcal{D}$, $s_j \in \mathbb{R}$ and $\rho_j \in \mathcal{D}_\gamma$ has a jump at c_j, but is continuous at all other cut points c_k, $k \neq j$ (i.e. each ρ_j represents one jump of the function f). In particular, for a given λ, we will use the family of functions $\rho_{j,\lambda}$ that satisfy

$$-\rho_{j,\lambda}''(x) + (q(x) - \lambda)\rho_{j,\lambda}(x) = 0$$

on every edge, the δ-type conditions (III.1) at the vertices of Γ, and the following conditions at the cut points:

$$\rho_{j,\lambda}(c_j^-) = 0 \qquad \text{and} \qquad \rho_{j,\lambda}(c_j^+) = 1, \tag{III.7}$$

$$\rho_{j,\lambda}(c_k^+) = \rho_{j,\lambda}(c_k^-) \qquad \text{and} \qquad \rho_{j,\lambda}'(c_k^+) = -\rho_{j,\lambda}'(c_k^-) \quad \forall \, k \neq j. \tag{III.8}$$

Notice that condition (III.8) ensures continuity of the function and derivative at all cut points (other than c_j).

Existence and uniqueness of the functions satisfying the above conditions is assured (see, for example [15], Section 3.5.2) provided λ stays away from the Dirichlet spectrum $\rho_{j,\lambda}(c_j^+) = 0$.

Since we are interested in λ close to the eigenvalue λ_n of H^0 on the uncut graph Γ, we check that λ_n does not belong to the Dirichlet spectrum described above. The corresponding "Dirichlet graph" can be viewed as the uncut graph with an extra Dirichlet condition imposed at the vertex c_j (in place of the Neumann condition effectively imposed there by H^0). However, by a simple extension of the interlacing theorem of [14, 15] (see Lemma II.1 for a precise formulation), one can see that the interlacing between Neumann and Dirichlet eigenvalues is strict since λ_n is assumed to be simple and the corresponding eigenfunction ψ is nonzero at the cut points.

III.2.2.2   Morse Index with Lagrange Multipliers

In the process of proving Theorem III.3, we will need to know the Morse index of the nth eigenpair (λ_n, ψ) of H^0. The lemma below will provide us with that information.

Lemma III.3. *Let A be a bounded from below self-adjoint operator acting on a real Hilbert space $\mathcal{H}$. Assume that A has only discrete spectrum below a certain Λ and its eigenvalues are ordered in increasing order. Let $h[f]$ be the quadratic form corresponding to A. If the nth eigenvalue $\lambda_n < \Lambda$ is simple and ψ is the corresponding eigenfunction of norm one, then the Lagrange functional*

$$L(\lambda, f) = h[f] - \lambda(\|f\|^2 - 1)$$

has a non-degenerate critical point at (λ_n, ψ) whose Morse index is n.

Proof. We split the Hilbert space $\mathcal{H}$ into the orthogonal sum $\mathcal{H}_- \oplus \mathcal{H}_0 \oplus \mathcal{H}_+$. Here the space $\mathcal{H}_-$ is the span of the first $n-1$ eigenfunctions of A, the space $\mathcal{H}_0$ is the span of the nth eigenfunction ψ, and $\mathcal{H}_+$ is their orthogonal complement. The quadratic form $h[f]$ is reduced by the decomposition $\mathcal{H} = \mathcal{H}_- \oplus \mathcal{H}_0 \oplus \mathcal{H}_+$, namely

$$h\left[f_- + f_0 + f_+\right] = h\left[f_-\right] + h\left[f_0\right] + h\left[f_+\right].$$

30

On $\mathcal{H}_-$, the quadratic form h is bounded from above. In particular,

$$h[f_-] \leq \lambda_{n-1}\|f_-\|^2 < \lambda_n\|f_-\|^2.$$

Similarly, on $\mathcal{H}_+$ the form h is bounded from below where

$$h[f_+] > \lambda_n\|f_+\|^2.$$

Finally, on $\mathcal{H}_0$ we have

$$h[f_0] = \lambda_n s^2,$$

where $f_0 = s\psi$ for some $s \in \mathbb{R}$.

To show that (λ_n, ψ) is a critical point and calculate its index, we evaluate

$$\delta L := L(\lambda_n + \delta\lambda, \psi + \delta f) - L(\lambda_n, \psi) = L(\lambda_n + \delta\lambda, \psi + \delta f) - \lambda_n$$

since $L(\lambda_n, \psi) = h[\psi] - \lambda_n(\|\psi\|^2 - 1) = h[\psi] = \lambda_n$. Expanding $\delta f = \delta f_- + s\psi + \delta f_+$ according to our decomposition of $\mathcal{H}$, we see that

$$
\begin{aligned}
\delta L &= L(\lambda_n + \delta\lambda, \psi + \delta f_- + s\psi + \delta f_+) - \lambda_n = L(\lambda_n + \delta\lambda, \delta f_- + (1+s)\psi + \delta f_+) - \lambda_n \\
&= h\left[\delta f_- + (s+1)\psi + \delta f_+\right] - (\lambda_n + \delta\lambda)\left(\|\delta f_- + (1+s)^2\psi + \delta f_+\|^2 - 1\right) - \lambda_n \\
&= h\left[\delta f_-\right] + h\left[(s+1)\psi\right] + h\left[\delta f_+\right] - (\lambda_n + \delta\lambda)\left(\|\delta f_-\|^2 + (1+s)^2 + \|\delta f_+\|^2 - 1\right) - \lambda_n \\
&= h\left[\delta f_-\right] + \lambda_n(1+s)^2 + h\left[\delta f_+\right] - (\lambda_n + \delta\lambda)\left(\|\delta f_-\|^2 + (1+s)^2 + \|\delta f_+\|^2\right) + \delta\lambda \\
&= h\left[\delta f_-\right] + h\left[\delta f_+\right] - (\lambda_n + \delta\lambda)\left(\|\delta f_-\|^2 + \|\delta f_+\|^2\right) + \left(1 - (1+s^2)\right)\delta\lambda \\
&= h\left[\delta f_-\right] + h\left[\delta f_+\right] - (\lambda_n + \delta\lambda)\left(\|\delta f_-\|^2 + \|\delta f_+\|^2\right) - (2s + s^2)\delta\lambda.
\end{aligned}
$$

Simplifying and completing squares, we obtain

$$\delta L = \left(h\left[\delta f_-\right] - \lambda_n \|\delta f_-\|^2 \right) - \frac{1}{2}(s + \delta\lambda)^2 + \frac{1}{2}(s - \delta\lambda)^2 + \left(h\left[\delta f_+\right] - \lambda_n \|\delta f_+\|^2 \right)$$
$$- \delta\lambda \left(\|\delta f_-\|^2 + \|\delta f_+\|^2 + s^2 \right),$$

where the third and fourth terms represent $-2s\delta\lambda$. We observe that all terms are quadratic or higher-order in terms of the "small" parameters $s, \delta\lambda, \delta f_+$ and δf_-. Therefore, we can see that (λ_n, ψ) is a critical point as claimed; take the derivative with respect to any of these parameters, and then the limit as all these parameters tend to zero is zero. The first two terms represent the negative part of the Hessian (as the second derivatives of all other terms are positive or zero). Their dimension is the dimension of $\mathcal{H}_-$ plus one. Thus the Morse index is $(n-1) + 1 = n$.

$\square$

We remark that in the finite-dimensional case, the Hessian of δL at the critical point is known as the "bordered Hessian" (see [92] for a brief history of the term).

III.2.2.3   Restriction to a Critical Manifold

We will also use the following simple result from [16].

Lemma III.4. *Let $X = Y \bigoplus Y'$ be a direct decomposition of a Banach space and $f : X \to \mathbb{R}$ be a smooth functional such that $(0,0) \in X$ is a critical point of Morse index $\mathrm{ind}(f)$.*

If for any y in a neighborhood of zero in Y, the point $(y, 0)$ is a critical point of f over the affine subspace $\{y\} \times Y'$, then the Hessian of f at the origin, as a quadratic form in X, is reduced by the decomposition $X = Y \bigoplus Y'$.

In particular,

$$\mathrm{ind}(f) = \mathrm{ind}(f|_Y) + \mathrm{ind}(f|_{Y'}),$$

32

where $\mathrm{ind}(f|_W)$ *is the Morse index of* 0 *as the critical point of the function* f *restricted to the space* W. *Moreover, if* $(0,0)$ *is a non-degenerate critical point of* f *on* X, *then* 0 *is non-degenerate as a critical point of* f *on* Y.

The subspace Y, which is the locus of the critical points of f over the affine subspaces $(y, \cdot)$, is called the *critical manifold*. In applications, the locus of the critical points with respect to a chosen direction is not usually a linear subspace. In this case, a simple change of variables is applied to reduce the situation to that of Lemma III.4 while the Morse index remains unchanged. This is, in fact, exactly what we will do in the following subsection.

III.2.2.4   Proof

In this subsection, λ is used as both an independent variable and a function (i.e, we continue to view the eigenvalue as a function of parameters). To reduce confusion, we denote the nth eigenvalue of H^0 by ξ. We let ψ denote the nth eigenfunction of H^0 and ϕ denote the number of internal zeros of ψ on Γ.

Proof of Part 1 of Theorem III.3. By design, ψ is an eigenfunction of H^{γ} when $\boldsymbol{\gamma} = \widetilde{\boldsymbol{\gamma}}$; the vertex conditions at the new vertices $c_j^{\pm}$ were specifically chosen to fit ψ. To see this, we consider ψ as a function in $\widetilde{H^2}(\mathbb{T}, \mathbb{R})$. Since ψ is an eigenfunction of H^0, we know that

$$-\psi''(x) + q(x)\psi(x) = \xi\psi(x)$$

on every edge of $\mathbb{T}$. It remains to show that $\psi \in \mathcal{D}_{\gamma}$. Since ψ satisfies the boundary conditions (III.1) on all vertices of Γ, we only need to check the vertex conditions at the new vertices $\{c_j^{\pm}\}$. Since $\psi \in \widetilde{H^2}(\Gamma, \mathbb{R})$, we know that

$$\psi(c_j^+) = \psi(c_j^-) \quad \text{and} \quad \psi'(c_j^+) = -\psi'(c_j^-) \quad \text{for } j = 1, \dots, \beta. \tag{III.9}$$

33

Hence, one can see that

$$\widetilde{\gamma}_j\psi(c_j^+) = \frac{\psi'(c_j^+)}{\psi(c_j^+)}\psi(c_j^+) = \psi'(c_j^+) \ \text{ and } \ -\widetilde{\gamma}_j\psi(c_j^-) = \frac{\psi'(c_j^-)}{\psi(c_j^-)}\psi(c_j^-) = \psi'(c_j^-)$$

so ψ is indeed in $\mathcal{D}_\gamma$ and an eigenfunction of $H^{\widetilde{\gamma}}$. From this we can conclude that ξ is in the spectrum of $H^{\widetilde{\gamma}}$.

Since ψ is nonzero on vertices (and cycles since $\mathbb{T}$ is a tree), Theorem II.1 tells us that the corresponding eigenvalue of $H^{\widetilde{\gamma}}$ is simple; also see [14, 90]. Eigenfunctions on a tree are Courant-sharp [14, 82, 90]; in other words, the nth eigenfunction has $n-1$ internal zeros. We use this property in reverse, concluding that ψ is the eigenfunction number $\phi+1$ of the quantum tree operator $H^{\widetilde{\gamma}}$.

$\square$

Proof of Part 2 of Theorem III.3. Here we prove that $\boldsymbol{\gamma} = \widetilde{\boldsymbol{\gamma}}$ is a critical point of $\lambda_{\phi+1}(\boldsymbol{\gamma})$.

Consider the Lagrange functional

$$F_3(\lambda, f, \boldsymbol{\gamma}) = h_{\boldsymbol{\gamma}}[f] - \lambda\left(\int_{\mathbb{T}} f^2(x)\,dx - 1\right)$$

where $h_{\boldsymbol{\gamma}}[f]$ is the quadratic form of the operator $H^{\boldsymbol{\gamma}}$, which is given by equation (III.6). The integral over the graph $\mathbb{T}$ is understood to be the sum of integrals over each edge of $\mathbb{T}$. Observe that $\lambda_{\phi+1}(\boldsymbol{\gamma}) =: \lambda(\boldsymbol{\gamma})$ is a restriction of F_3 onto a submanifold; namely,

$$\lambda(\boldsymbol{\gamma}) = F_3\Big(\lambda(\boldsymbol{\gamma}), f(\boldsymbol{\gamma}), \boldsymbol{\gamma}\Big), \tag{III.10}$$

where $f(\boldsymbol{\gamma})$ is the normalized $(\phi+1)^{th}$ eigenfunction of $H^{\boldsymbol{\gamma}}$. We will now show that $(\xi, \psi, \widetilde{\boldsymbol{\gamma}})$ is a critical point of F_3; the criticality of the function $\lambda_{\phi+1}(\boldsymbol{\gamma})$ will then follow immediately.

We know from Lemma III.3 that the eigenpair (ξ, ψ) is a critical point of the Lagrange

functional and therefore

$$\frac{\partial F_3}{\partial \lambda}\bigg|_{(\lambda, f, \gamma) = (\xi, \psi, \widetilde{\gamma})} = 0 \qquad \text{and} \qquad \frac{\partial F_3}{\partial f}\bigg|_{(\lambda, f, \gamma) = (\xi, \psi, \widetilde{\gamma})} = 0.$$

Additionally, we calculate from equation (III.6) that

$$\frac{\partial F_3}{\partial \gamma_j}\bigg|_{(\lambda, f, \gamma) = (\xi, \psi, \widetilde{\gamma})} = \psi^2(c_j^+) - \psi^2(c_j^-) = 0 \qquad \text{for } j = 1, \ldots, \beta,$$

since $\psi \in \widetilde{H^2}(\Gamma, \mathbb{R})$ satisfies (III.9). This proves that $\widetilde{\gamma}$ is a critical point of $\lambda_{\phi+1}(\gamma)$. The non-degeneracy of the critical point will follow from the proof of part 3.

$\square$

Proof of Part 3 of Theorem III.3. We will calculate the index of the critical point $\widetilde{\gamma}$ of $\lambda_{\phi+1}(\gamma)$ in two steps. We will first establish that the index of $(\xi, \psi, \widetilde{\gamma})$ as a critical point of F_3 is equal to $n + \beta$. Then we will apply Lemma III.4 to the restriction introduced in (III.10) in order to deduce the final result. As the second step is simpler, we start with it to illustrate our technique.

Index of the critical point $\gamma = \widetilde{\gamma}$ of $\lambda(\gamma)$. Assume we have already shown that $(\xi, \psi, \widetilde{\gamma})$ is a non-degenerate critical point of F_3 of index $n + \beta$. Define the following change of variables:

$$\begin{cases} \hat{\lambda} = \lambda - \lambda(\gamma), \\ \hat{f} = f - f(\gamma), \\ \hat{\gamma} = \gamma - \widetilde{\gamma}, \end{cases}$$

where $\lambda(\gamma)$ is the $(\phi + 1)^{th}$ eigenvalue of the operator H^γ and $f(\gamma)$ is the corresponding normalized eigenfunction. The eigenvalue $\lambda(\gamma)$ is simple when $\gamma = \widetilde{\gamma}$ (see the proof of part 1) and this property is preserved locally.

Since $\lambda(\widetilde{\gamma}) = \xi$ and $f(\widetilde{\gamma}) = \psi$, the critical point $(\xi, \psi, \widetilde{\gamma})$ corresponds to $(0, 0, \mathbf{0})$ in the new

35

variables. The change of variables is obviously non-degenerate, and therefore the Morse index of a critical point remains unchanged.

For every fixed γ, the function F_3 is the Lagrange functional of the operator H^γ. Hence, by Lemma III.3 we conclude that $(\lambda(\gamma), f(\gamma))$ is its non-degenerate critical point of Morse index $\phi + 1$. In the new variables, this translates to $(0, 0, \hat{\gamma})$ being a critical point with respect to the first two variables for any value of the third variable. Let $X = Y \bigoplus Y'$ where Y is the subspace spanned by $\hat{\gamma}$ and Y' is the subspace spanned by $(\hat{\lambda}, \hat{f})$. Now we can apply Lemma III.4 to conclude that $\hat{\gamma} = (0, \ldots, 0)$ is a non-degenerate critical point of $F_3(0, 0, \hat{\gamma})$. This critical point has Morse index

$$\mathrm{ind}(F_3|_Y) = \mathrm{ind}(F_3|_X) - \mathrm{ind}(F_3|_{Y'}) = (n + \beta) - (\phi + 1).$$

Since $\hat{\gamma} = (0, \ldots, 0)$ corresponds to $\gamma = \widetilde{\gamma}$ and $F_3(0, 0, \hat{\gamma}) = \lambda_{\phi+1}(\gamma)$, we obtain the desired conclusion. It remains to verify the assumption that $(\xi, \psi, \widetilde{\gamma})$ is a non-degenerate critical point of F_3 of index $n + \beta$.

Index of critical point of F_3. By Remark 3, any $f \in \mathcal{D}_\gamma$ can be written as

$$f = f_0 + \sum_{j=1}^{\beta} s_j \rho_{j,\lambda} =: f_0 + \boldsymbol{s} \cdot \boldsymbol{\rho_\lambda},$$

where $f_0 \in \mathcal{D}$ and each $\rho_{j,\lambda}$ satisfies $\rho_{j,\lambda}''(x) + (q(x) - \lambda)\rho_{j,\lambda}(x) = 0$. Therefore the Lagrange functional F_3 can be re-parameterized as follows:

$$F_4(\lambda, f_0, \boldsymbol{s}, \boldsymbol{\gamma}) := F_3\left(\lambda, f_0 + \boldsymbol{s} \cdot \boldsymbol{\rho_\lambda}, \boldsymbol{\gamma}\right)$$
$$= h_\gamma[f_0 + \boldsymbol{s} \cdot \boldsymbol{\rho_\lambda}] - \lambda\left(\int_{\mathbb{T}} (f_0 + \boldsymbol{s} \cdot \boldsymbol{\rho_\lambda})^2 \, dx - 1\right).$$

We let

$$R_j(\lambda) = \rho_{j,\lambda}'(c_j^+) + \rho_{j,\lambda}'(c_j^-),$$

36

and investigate F_4 as a function of $\boldsymbol{s}$ and $\boldsymbol{\gamma}$ while λ and f_0 are held fixed. We will now show that $(\boldsymbol{s}, \boldsymbol{\gamma}) = (\boldsymbol{0}, \boldsymbol{R}(\lambda))$ is a critical point. Indeed, one can observe that

$$\frac{\partial}{\partial s_j} \left(f_0(x) + \boldsymbol{s} \cdot \boldsymbol{\rho_\lambda}(x)\right)^2 \bigg|_{\boldsymbol{s}=\boldsymbol{0}} = 2 f_0(x) \rho_{j,\lambda}(x),$$

and similarly

$$\frac{\partial}{\partial s_j} \left(f_0'(x) + \boldsymbol{s} \cdot \boldsymbol{\rho_\lambda}'(x)\right)^2 \bigg|_{\boldsymbol{s}=\boldsymbol{0}} = 2 f_0'(x) \rho_{j,\lambda}'(x).$$

We can use integration by parts to calculate that

$$\frac{1}{2} \frac{\partial F_4}{\partial s_j} \bigg|_{\boldsymbol{s}=\boldsymbol{0}} = \int_{\mathbb{T}} \left(f_0'(x) \rho_{j,\lambda}'(x) + q(x) f_0(x) \rho_{j,\lambda}(x) - \lambda f_0(x) \rho_{j,\lambda}(x)\right) dx$$

$$+ \sum_{v \in V(\Gamma)} \chi_v f_0(v) \rho_{j,\lambda}(v) + \sum_{k=1}^{\beta} \gamma_k \left(f_0(c_k^+) \rho_{j,\lambda}(c_k^+) - f_0(c_k^-) \rho_{j,\lambda}(c_k^-)\right)$$

$$= \int_{\mathbb{T}} f_0(x) \left(-\rho_{j,\lambda}''(x) + (q(x) - \lambda) \rho_{j,\lambda}(x)\right) dx + \sum_{(u,w) \in E(\mathbb{T})} f_0(x) \rho_{j,\lambda}'(x) \bigg|_u^w$$

$$+ \sum_{v \in V(\Gamma)} \chi_v f_0(v) \rho_{j,\lambda}(v) + \gamma_j f_0(c_j^+).$$

The sum involving $\{\gamma_k\}$ simplified to a single term using the properties of $\rho_{j,\lambda}$ found in equations (III.7) and (III.8). By Remark 3, $\rho_{j,\lambda}$ satisfies $-\rho_{j,\lambda}''(x) + (q(x) - \lambda) \rho_{j,\lambda}(x) = 0$ so the integral disappears as well. Recall that derivatives are measured outward from the vertex, and therefore

$$\sum_{(u,w) \in E(\mathbb{T})} f_0(x) \rho_{j,\lambda}'(x) \bigg|_u^w = -\sum_{v \in V(\mathbb{T})} \sum_{e \in E_v} f_0(v) \rho_{j,\lambda}'(v).$$

Now we consider the vertices in $\mathbb{T}$ as the union of the vertices of Γ and the new cut vertices $\{c_k^\pm\}$. Continuing, we break the sum over all vertices in $\mathbb{T}$ into two partial sums and see

37

that

$$\frac{1}{2}\frac{\partial F_4}{\partial s_j}\bigg|_{\boldsymbol{s}=\boldsymbol{0}} = -\sum_{v\in V(\mathbb{T})}\sum_{e\in E_v} f_0(v)\rho'_{j,\lambda}(v) + \sum_{v\in V(\Gamma)} \chi_v f_0(v)\rho_{j,\lambda}(v) + \gamma_j f_0(c_j^+)$$

$$= -\sum_{v\in V(\Gamma)}\sum_{e\in E_v} f_0(v)\rho'_{j,\lambda}(v) - \sum_{k=1}^{\beta} f_0(c_k^+)\left(\rho'_{j,\lambda}(c_k^+) + \rho'_{j,\lambda}(c_k^-)\right)$$

$$+ \sum_{v\in V(\Gamma)} \chi_v f_0(v)\rho_{j,\lambda}(v) + \gamma_j f_0(c_j^+)$$

$$= -\sum_{v\in V(\Gamma)} f_0(v)\left(\sum_{e\in E_v}\rho'_{j,\lambda}(v)\right) - f_0(c_j^+)\left(\rho'_{j,\lambda}(c_j^+) + \rho'_{j,\lambda}(c_j^-)\right)$$

$$+ \sum_{v\in V(\Gamma)} \chi_v f_0(v)\rho_{j,\lambda}(v) + \gamma_j f_0(c_j^+)$$

since $f_0 \in \mathcal{D}$ is continuous across the cut vertices and $\rho_{j,\lambda}$ satisfies (III.8). Finally, we use the fact that $\rho_{j,\lambda}$ satisfies (III.1) to conclude that

$$\frac{1}{2}\frac{\partial F_4}{\partial s_j}\bigg|_{\boldsymbol{s}=\boldsymbol{0}} = -\sum_{v\in V(\Gamma)} \chi_v f_0(v)\rho_{j,\lambda}(v) - f_0(c_j^+)\left(\rho'_{j,\lambda}(c_j^+) + \rho'_{j,\lambda}(c_j^-)\right)$$

$$+ \sum_{v\in V(\Gamma)} \chi_v f_0(v)\rho_{j,\lambda}(v) + \gamma_j f_0(c_j^+)$$

$$= f_0(c_j^+)\left(\gamma_j - \rho'_{j,\lambda}(c_j^+) - \rho'_{j,\lambda}(c_j^-)\right).$$

This expression is equal to zero when $\gamma_j = R_j(\lambda)$.

Here we use the notation $f = f_0 + \boldsymbol{s}\cdot\boldsymbol{\rho_\lambda}$. The partial derivatives with respect to γ_j also vanish since

$$\frac{\partial F_4}{\partial \gamma_j}\bigg|_{\boldsymbol{s}=\boldsymbol{0}} = \left[f^2(c_j^+) - f^2(c_j^-)\right]_{\boldsymbol{s}=\boldsymbol{0}} = f_0^2(c_j^+) - f_0^2(c_j^-) = 0,$$

because the function $f_0 \in \mathcal{D}$ is continuous across the cut vertices $\{c_j\}$.

We will now calculate the Morse index of the critical point $(\boldsymbol{s},\boldsymbol{\gamma}) = (\boldsymbol{0},\boldsymbol{R})$. First we observe

that

$$\frac{\partial^2 F_4}{\partial \gamma_j \partial s_j}\bigg|_{s=0} = \frac{\partial}{\partial s_j}\left[f^2(c_j^+) - f^2(c_j^-)\right]\bigg|_{s=0} = 2f_0(c_j^+)$$

using the values of $\rho_{j,\lambda}$ at c_j^+ and c_j^- in equation (III.7). The Hessian is block-diagonal with β blocks of the form

$$\begin{bmatrix} \frac{\partial^2 F_4}{\partial \gamma_j \partial \gamma_j} & \frac{\partial^2 F_4}{\partial s_j \partial \gamma_j} \\ \frac{\partial^2 F_4}{\partial \gamma_j \partial s_j} & \frac{\partial^2 F_4}{\partial s_j \partial s_j} \end{bmatrix} = \begin{bmatrix} 0 & 2f_0(c_j^+) \\ 2f_0(c_j^+) & \cdot \end{bmatrix},$$

where the value of the second derivative with respect to s_j is irrelevant. Each block has a negative determinant and therefore contributes one negative and one positive eigenvalue. The Morse index is equal to the number of negative eigenvalues of the Hessian matrix, and therefore the total Morse index is β. Since the determinant is nonzero, the Hessian matrix is invertible (i.e., nonsingular), and thus the critical point is non-degenerate.

Finally, we observe that the critical manifold $(\lambda, f_0, \mathbf{0}, \mathbf{R}(\lambda))$ passes through the critical point $(\xi, \psi, \mathbf{0}, \widetilde{\boldsymbol{\gamma}})$. To show this, we need to verify that $R_j(\xi) = \widetilde{\gamma}_j$ when $f_0 = \psi$. By construction, ψ and $\rho_{j,\xi}$ satisfy the same differential equation $-g''(x) + (q(x) - \xi)g(x) = 0$ and the same vertex conditions at all vertices of $\mathbb{T}$ other than the leaves c_j^+ and c_j^- (since (III.8) is essentially enforcing continuity of $\rho_{j,\xi}$ at all other cut points). Hence, we can apply Lemma II.4 to the Wronskian of ψ and $\rho_{j,\xi}$ to obtain

$$\psi'(c_j^+)\rho_{j,\xi}(c_j^+) - \rho_{j,\xi}'(c_j^+)\psi(c_j^+) = -\psi'(c_j^-)\rho_{j,\xi}(c_j^-) + \rho_{j,\xi}'(c_j^-)\psi(c_j^-). \qquad \text{(III.11)}$$

Substituting the boundary values of $\rho_{j,\xi}$ from equation (III.7) and using the fact that ψ satisfies (III.9), (III.11) becomes

$$\psi'(c_j^+) - \rho_{j,\xi}'(c_j^+)\psi(c_j^+) = \rho_{j,\xi}'(c_j^-)\psi(c_j^+).$$

Rearranging this equation, we conclude that

$$\widetilde{\gamma}_j := \frac{\psi'(c_j^+)}{\psi(c_j^+)} = \rho'_{j,\xi}(c_j^+) + \rho'_{j,\xi}(c_j^-) =: R_j.$$

Using the non-degenerate change of variables

$$\begin{cases} \hat{\lambda} = \lambda - \xi, \\ \hat{f} = f_0 - \psi, \\ \hat{s} = s - \mathbf{0}, \\ \hat{\gamma} = \gamma - \mathbf{R}(\lambda), \end{cases}$$

we can once again apply Lemma III.4 with $Y = \left\{(\hat{\lambda}, \hat{f}, \mathbf{0}, \mathbf{0})\right\}$ and Y' being the subspace where $\hat{\lambda}$ and $\hat{f}$ are fixed. On the subspace Y, $F_4 = F_3 = h[f_0] - \lambda \left(\|f_0\|^2 - 1 \right)$, which is precisely the Lagrange functional for the operator H^0 with the correct domain. Since ξ is the nth eigenvalue of H^0, by Lemma III.3 the Lagrange functional has Morse index n at the point $(\lambda, f_0) = (\xi, \psi)$. We just calculated above that on the subspace Y' the Lagrange functional F_4 has Morse index β at the point $(\mathbf{0}, \widetilde{\gamma})$. Adding the two indices together we obtain the Morse index for the critical point $(\xi, \psi, \mathbf{0}, \widetilde{\gamma})$ of F_4 is $n + \beta$, which corresponds to the critical point $(\xi, \psi, \widetilde{\gamma})$ of F_3. This concludes our proof.

$\square$

III.2.3 Critical Points of $\lambda_n(\boldsymbol{\alpha})$

In this section we will show that $\boldsymbol{\alpha} = (0, \dots, 0)$ is a critical point of $\lambda(H^{\boldsymbol{\alpha}})$ and compute its Morse index, thus concluding the proof of Theorem III.2.

Theorem III.4. *Let $\sigma(\boldsymbol{\alpha})$ denote the spectrum of $H^{\boldsymbol{\alpha}}$ where $\boldsymbol{\alpha} = (\alpha_1, \ldots, \alpha_\beta) \in \mathbb{R}^\beta$. Then all points in the set*

$$\Sigma = \{(b_1, \ldots, b_\beta) : b_j \in \{-\pi, 0, \pi\}\}$$

are points of symmetry of $\sigma(\boldsymbol{\alpha})$; i.e., for all $\boldsymbol{\alpha} \in \mathbb{R}^\beta$ and for all $\boldsymbol{\varsigma} \in \Sigma$,

$$\sigma(\boldsymbol{\varsigma} - \boldsymbol{\alpha}) = \sigma(\boldsymbol{\varsigma} + \boldsymbol{\alpha}),$$

together with multiplicity.

Consequently, if $\lambda_n(\boldsymbol{\alpha})$ is the nth eigenvalue of $H^{\boldsymbol{\alpha}}$ that is simple at $\boldsymbol{\alpha} = \boldsymbol{\varsigma} \in \Sigma$, then $\boldsymbol{\varsigma}$ is a critical point of the function $\lambda_n(\boldsymbol{\alpha})$.

Proof. We will first show that if $f(x)$ is an eigenfunction of $H^{\boldsymbol{\varsigma}-\boldsymbol{\alpha}}$, then $\overline{f(x)}$ is an eigenfunction of $H^{\boldsymbol{\varsigma}+\boldsymbol{\alpha}}$. Since the operator $H^{\boldsymbol{\alpha}}$ is self-adjoint, we know that the eigenvalues are real. Taking the complex conjugate of the eigenvalue equation for $f(x)$ we see that $\overline{f(x)}$ satisfies the same equation; in particular,

$$-\frac{d^2 \overline{f(x)}}{dx^2} + q(x)\overline{f(x)} = \overline{-\frac{d^2 f(x)}{dx^2} + q(x)f(x)} = \overline{\lambda f(x)} = \lambda \overline{f(x)}$$

since $q(x)$ is real-valued. Similarly, all vertex conditions at the vertices inherited from Γ have real coefficients, and therefore $\overline{f(x)}$ satisfies them also. The only thing that remains to be verified is the vertex conditions at the cut vertices $\{c_j^\pm\}$.

Notice that for every $\boldsymbol{\varsigma} \in \Sigma$, ς_j is equal to either 0 or $\pm\pi$ so $e^{-2i\varsigma_j} = 1$ for all $j = 1, \ldots, \beta$. Therefore,

$$\overline{e^{i(\varsigma_j - \alpha_j)}} = e^{i(-\varsigma_j + \alpha_j)} = e^{-2i\varsigma_j} e^{i(\varsigma_j + \alpha_j)} = e^{i(\varsigma_j + \alpha_j)}.$$

Conjugating the vertex conditions of $H^{\varsigma-\alpha}$ at $c_j^\pm$ we obtain

$$\overline{f(c_j^-)} = \overline{e^{i(\varsigma_j - \alpha_j)} f(c_j^+)} = e^{i(\varsigma_j + \alpha_j)} \overline{f(c_j^+)},$$

and same for the derivative. Thus $\overline{f(x)}$ satisfies the vertex conditions of the operator $H^{\varsigma+\alpha}$.

Following the same procedure, given an eigenfunction $g(x)$ of $H^{\varsigma+\alpha}$, one can show that $\overline{g(x)}$ is an eigenfunction of $H^{\varsigma-\alpha}$. The spectra of these two operators are therefore identical.

Suppose that $\lambda_n(\alpha)$ is simple at $\alpha = \varsigma \in \Sigma$. By standard perturbation theory, we know that $\lambda_n(\alpha)$ is differentiable near ς. We can calculate that

$$\left.\frac{\partial \lambda_n(\alpha)}{\partial \alpha_j}\right|_{\alpha=\varsigma} = \lim_{\alpha_j \to 0} \frac{\lambda_n(\varsigma + \alpha_j) - \lambda_n(\varsigma - \alpha_j)}{2\alpha_j} = 0$$

due to symmetry for all $j = 1, \ldots, \beta$, and hence ς is a critical point of $\lambda_n(\alpha)$.

$\square$

III.2.3.2   A Non-Self-Adjoint Continuation

We now consider the operator $-\frac{d^2}{dx^2} + q(x)$ on the tree $\mathbb{T}$ with the δ-vertex conditions (III.1) on the vertices of Γ and the following conditions at the cut vertices $\{c_j^\pm\}$:

$$
\begin{aligned}
f(c_j^-) &= e^{\alpha_j} f(c_j^+), \\
f'(c_j^-) &= -e^{\alpha_j} f'(c_j^+),
\end{aligned}
\tag{III.12}
$$

i.e. the function has a jump in magnitude across the cut. It is easy to see that these conditions are obtained from (III.3) by changing α to $-i\alpha$. We will denote the operator with vertex conditions (III.12) at the vertices in $\mathbb{T}\backslash\Gamma$ by $H^{-i\alpha}$.

Remark 4. The operator of $H^{-i\alpha}$ is not self-adjoint for all $\alpha \in \mathbb{R}^\beta$. A simple example is

the interval $[0, \pi]$ with $q(x) = 0$ and the boundary conditions

$$f(0) = e^\alpha f(\pi) \qquad \text{and} \qquad f'(0) = e^\alpha f'(\pi),$$

which has complex eigenvalues when $\alpha \neq 0$. Indeed, the eigenvalues are easily calculated to be

$$\lambda_n = \left(2n \pm \frac{\alpha}{\pi} i\right)^2.$$

Lemma III.5. *If the eigenvalue λ_n of H^0 is simple, then locally around $\boldsymbol{\alpha} = (0, \ldots, 0)$ the eigenvalue $\lambda_n(-i\boldsymbol{\alpha})$ is real. The corresponding eigenfunction is real also.*

Proof. By standard perturbation theory [52] (also see [14] for results specifically on graphs), we know that $\lambda_n(-i\boldsymbol{\alpha})$ is an analytic function of $\boldsymbol{\alpha}$. Since λ_n is simple, $\lambda_n(-i\boldsymbol{\alpha})$ remains simple in a neighborhood of $\boldsymbol{\alpha} = (0, \ldots, 0)$. The operator $H^{-i\boldsymbol{\alpha}}$ has real coefficients, and therefore its complex eigenvalues must come in conjugate pairs. For this to happen, the real eigenvalue must first become double. Hence the eigenvalue $\lambda_n(-i\boldsymbol{\alpha})$ is real near $(0, \ldots, 0)$ since it is simple there.

$\square$

We note that since we imposed no restrictions on the eigenvalues below λ_n, some of them may turn complex as soon as $\boldsymbol{\alpha} \neq 0$. In this case, the kth eigenvalue $\lambda_k(-i\boldsymbol{\alpha})$ refers to the unique continuation of λ_k. Locally, this is the same as having the eigenvalues ordered by their real part.

III.2.3.3 Connection between H^γ and $H^{-i\boldsymbol{\alpha}}$

Locally around $\boldsymbol{\gamma} = \widetilde{\boldsymbol{\gamma}}$, we introduce a mapping $R : \boldsymbol{\gamma} \mapsto \boldsymbol{\alpha}$ such that $\lambda_{\phi+1}(\boldsymbol{\gamma}) = \lambda_n(-i\boldsymbol{\alpha})$ when $R(\boldsymbol{\gamma}) = \boldsymbol{\alpha}$.

For a given $\boldsymbol{\gamma}$, we find the $(\phi + 1)^{th}$ eigenfunction of $H^{\boldsymbol{\gamma}}$ and denote it by g. We then let

$$e^{\alpha_j} = \frac{g(c_j^-)}{g(c_j^+)}.$$

We will show that g is also an eigenfunction of $H^{-i\boldsymbol{\alpha}}$. The only difference between the operators $H^{\boldsymbol{\gamma}}$ and $H^{-i\boldsymbol{\alpha}}$ is the vertex conditions at the cut points $\{c_j^{\pm}\}$. It is obvious that $g(c_j^-) = e^{\alpha_j} g(c_j^+)$. Since g satisfies equation (III.5),

$$e^{\alpha_j} = \frac{g(c_j^-)}{g(c_j^+)} = \frac{-g'(c_j^-)/\gamma_j}{g'(c_j^+)/\gamma_j} = -\frac{g'(c_j^-)}{g'(c_j^+)},$$

which implies that $g'(c_j^-) = -e^{\alpha_j} g'(c_j^+)$, and thus g is indeed an eigenfunction of $H^{-i\boldsymbol{\alpha}}$.

A *diffeomorphism* is a bijection between two manifolds such that the function and its inverse are differentiable.

Lemma III.6. *The function R is a non-degenerate diffeomorphism. Therefore, the point $\boldsymbol{\alpha} = (0, \ldots, 0)$ is a critical point of the function $\lambda_n(-i\boldsymbol{\alpha})$ of index $n - 1 + \beta - \phi$.*

Proof. The eigenfunctions of $H^{\boldsymbol{\gamma}}$ are analytic functions of the parameters $\{\gamma_j\}$. Therefore R is a composition of analytic functions, and hence R is an analytic function in a neighborhood of $\widetilde{\boldsymbol{\gamma}}$. We can define R^{-1} by reversing the process, i.e. for a given $\boldsymbol{\alpha}$ find the (real) n^{th} eigenfunction φ of $H^{-i\boldsymbol{\alpha}}$ and let $\gamma_j = \varphi'(c_j^+)/\varphi(c_j^+)$. By the same argument, R^{-1} is an analytic function in a neighborhood of $(0, \ldots, 0)$, and therefore R is a non-degenerate diffeomorphism.

A diffeomorphism preserves Morse index and therefore the Morse index of $(0, \ldots, 0)$ of the function $\lambda_n(-i\boldsymbol{\alpha})$ is the same as the index of $\widetilde{\boldsymbol{\gamma}}$ of the function $\lambda_{\phi+1}(\boldsymbol{\gamma})$, which was computed to be $n - 1 + \beta - \phi$ in Theorem III.3.

$\square$

III.2.3.4   From $H^{-i\boldsymbol{\alpha}}$ to $H^{\boldsymbol{\alpha}}$

Proof of Theorem III.2. The function $\lambda_n(\boldsymbol{\alpha}) - \xi$ is analytic and, locally around $(0, \ldots, 0)$, quadratic in $\{\alpha_j\}$ because $(0, \ldots, 0)$ is a critical point so the linear term (i.e., the first derivative) is zero. Substituting $\boldsymbol{\alpha} \to -i\boldsymbol{\alpha}$ into the quadratic term results in an overall minus, that is

$$\lambda_n(-i\boldsymbol{\alpha}) - \xi = -\left(\lambda_n(\boldsymbol{\alpha}) - \xi\right) + \text{higher-order terms}.$$

Another way of viewing this is to analyze the Taylor expansions of both $\lambda_n(\boldsymbol{\alpha}) - \xi$ and $\lambda_n(-i\boldsymbol{\alpha}) - \xi$ at $\boldsymbol{\alpha} = (0, \ldots, 0)$. We only need to go to the quadratic term since this term provides information about the Morse index. The constant term in both cases is $\lambda_n(0, \ldots, 0) - \xi = 0$. Notice that

$$\frac{\partial}{\partial \alpha_j}\left(-i\boldsymbol{\alpha}\right) = -i\frac{\partial}{\partial \alpha_j}\boldsymbol{\alpha}.$$

We know that $\boldsymbol{\alpha} = (0, \ldots, 0)$ is a critical point of both $\lambda_n(\boldsymbol{\alpha})$ and $\lambda(-i\boldsymbol{\alpha})$, and hence both of the linear terms are zero because

$$\left.\frac{\partial \lambda_n(-i\boldsymbol{\alpha})}{\partial \alpha_j}\right|_{\boldsymbol{\alpha}=\mathbf{0}} = -i\left.\frac{\partial \lambda_n(\boldsymbol{\alpha})}{\partial \alpha_j}\right|_{\boldsymbol{\alpha}=\mathbf{0}} = 0 \qquad \text{for all } j = 1, \ldots \beta$$

where the $-i$ term came from using the chain rule. Now we look at the quadratic term. Using the chain rule again, one can see that

$$\left.\frac{\partial^2 \lambda_n(-i\boldsymbol{\alpha})}{\partial \alpha_j \partial \alpha_k}\right|_{\boldsymbol{\alpha}=\mathbf{0}} = (-i)^2 \left.\frac{\partial^2 \lambda_n(\boldsymbol{\alpha})}{\partial \alpha_j \partial \alpha_k}\right|_{\boldsymbol{\alpha}=\mathbf{0}} = -\left.\frac{\partial^2 \lambda_n(\boldsymbol{\alpha})}{\partial \alpha_j \partial \alpha_k}\right|_{\boldsymbol{\alpha}=\mathbf{0}} \qquad \text{for all } j, k = 1, \ldots \beta$$

since the functions $\lambda_n(-i\boldsymbol{\alpha})$ and $\lambda_n(\boldsymbol{\alpha})$ are equal at $\boldsymbol{\alpha} = (0, \ldots, 0)$. Consequently, the number of negative eigenvalues of the Hessian matrix of $\lambda_n(\boldsymbol{\alpha})$ (i.e., the Morse index of $\lambda_n(\boldsymbol{\alpha})$) is equal to the number of positive eigenvalues of the Hessian matrix H of $\lambda_n(-i\boldsymbol{\alpha})$. The number of positive eigenvalues of H is equal to the dimension of the space of variables (i.e, the dimension of $\boldsymbol{\alpha}$) minus the number of negative eigenvalues of H (i.e., the Morse

index of $\lambda_n(-i\boldsymbol{\alpha})$). Thus, the Morse index of $\lambda_n(\boldsymbol{\alpha})$ is equal to

$$\beta - (n - 1 + \beta - \phi) = \phi - (n - 1).$$

$\square$

III.3   Consequences to Graph Partitions

Theorem III.2 is interesting in its own right; there is no intuitive reason why the stability of the eigenvalue (with respect to magnetic perturbation) should be related to the number of zeros of the non-magnetic eigenfunction. It turns out that this theorem also provides additional information about critical partitions and the inverse nodal count problem. We will focus on the relation to critical partitions in this section and the consequence to the inverse nodal count problem in Section III.4.

In this chapter, we have been considering eigenvalues of different operators that are defined on (essentially) the same graph. In the study of partitions, we restrict ourselves to the Schrödinger operator H^0 and it is the graph that varies. In this section, we adjust our notation accordingly. We will refer to the nth eigenvalue of the Schödinger operator H^0 on the graph Γ as simply the nth eigenvalue of Γ, which we will denote by $\lambda_n(\Gamma)$.

A *proper m-partition* P of a quantum graph Γ is a set of m points lying on the edges (not the vertices) of the graph Γ. Enforcing Dirichlet conditions at these points separates the graph into a set of *partition subgraphs* which we denote $\{\Gamma_j\}$. The conditions on the vertices of each Γ_j are either (1) the same as they were on Γ at the old vertices or (2) Dirichlet at the new vertices. We define the energy functional

$$\Lambda(P) := \max_j \lambda_1(\Gamma_j) \tag{III.13}$$

where $\lambda_1(\Gamma_j)$ is the first eigenvalue of the partition subgraph Γ_j. Further, we call a proper

m-partition an *equipartition* if all subgraphs Γ_j share the same first eigenvalue, or in other words

$$\lambda_1(\Gamma_{j_i}) = \lambda_1(\Gamma_{j_k}), \qquad \text{for all } j_i, j_k.$$

A partition P is a candidate for the nodal set of an eigenfunction of Γ.

In this section, we analyze the stability of the energy functional Λ over the set of all equipartitions. First, we look at partitions that break all cycles in Section III.3.1. In this case, the main result is a direct consequence of Theorem III.3. Then in Section III.3.2, we look at what happens when partitions do not break all cycles. This case requires a more general version of Theorem III.3.

III.3.1   Partitions that Break All Cycles

It is easy to see that a proper m-partition breaks every cycle of Γ if and only if the number of the partition subgraphs, denoted by $\nu(P)$, is related to m by

$$\nu(P) = m - \beta + 1.$$

We start by considering eigenfunctions whose corresponding partition satisfies the above property. Eigenfunctions whose zeros do not break all cycles of Γ correspond to low values of λ, and it can easily be shown that there are only finitely many such eigenfunctions. We will handle these eigenfunctions in Section III.3.2 by introducing cut points only on those cycles which are broken by the zeros of the eigenfunction and adjusting the operator H^γ accordingly.

Suppose f is an eigenfunction of Γ corresponding to the eigenvalue λ. The partition defined by the nodal set of an eigenfunction (i.e., the set of points at which $f(x) = 0$) is an equipartition because on each partition subgraph the first eigenvalue is λ. In [7] it was shown that the set of m-equipartitions on Γ can be parameterized using β parameters $\{\gamma_j\}$

and the operator H^γ defined in Section III.2.1. In particular, the zeros of the $(m+1)^{th}$ eigenfunction of H^γ (transplanted to the original graph Γ) define an equipartition. With such parameterization, the energy $\Lambda(P)$ of the partition is simply the $(m+1)^{th}$ eigenvalue $\lambda_{m+1}(\boldsymbol{\gamma})$. The following result was first established on quantum graphs in [7]. Here we present a strengthened version that follows from Theorem III.3.

Corollary III.1. *Suppose the nth eigenvalue of Γ is simple and its eigenfunction ψ is nonzero on vertices. Denote by ϕ the number of zeros of ψ and by ν the number of its nodal domains. If the zeros of the eigenfunction break every cycle of Γ, then the ϕ-partition defined by the zeros of ψ is a non-degenerate critical point of the functional Λ on the set of equipartitions. The Morse index of this critical point is equal to $n - \nu$.*

Some remarks are in order. The "converse" fact that critical points of Λ correspond to eigenfunctions is easy to establish. The main difficulty lies in calculating the Morse index. In the main theorem of [7], the non-degeneracy of the critical point had to be assumed a priori. In Section III.2.2, we established that this actually follows from the other assumptions. Finally, the mapping R defined in Section III.2.3.3 essentially shows that the equipartitions can be parameterized using eigenfunctions of the "magnetic" Schrödinger operator with purely imaginary magnetic field.

III.3.2   Partitions that Do Not Break All Cycles

For eigenfunctions corresponding to low eigenvalues, the nodal set may not break all the cycles of the graph (see Figure III.2(a)). In this case, the parameterization of the nearby equipartitions is done via a modification of the operator H^γ. In this section, we describe this parameterization and point out changes in the proof of the analogue of Theorem III.3 that this new parameterization necessitates. An outline of the procedure has already appeared in [7, 18]; however some essential details were omitted there.

The eigenfunctions we are interested in here do not have a zero on every cycle. Hence, unlike the previous case for large eigenvalues where the corresponding eigenfunctions have
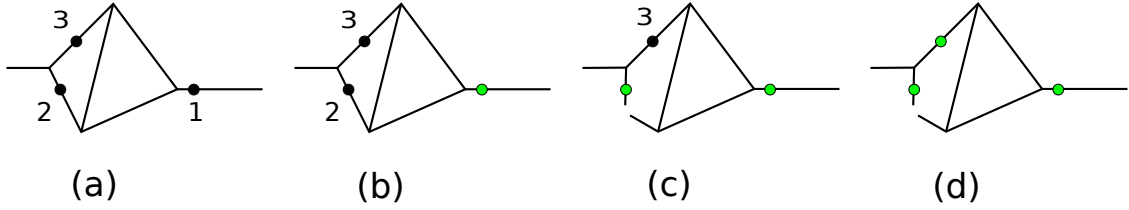
Figure III.2: A partition with surviving cycles. (a) Zeros, marked 1, 2, and 3, do not lie on all the cycles of the graph. To find cut points we consider the zeros in sequence. (b) Cutting the graph at zero 1 would disconnect it so we do nothing. (c) Cutting the graph at zero 2 would not disconnect it; therefore, a cut point is placed nearby. (d) Now, cutting the graph at zero 3 would disconnect the graph, so we do not introduce any more cut points.

at least one zero on every cycle, we must choose our cut points carefully to avoid cutting cycles that do not contain any zeros of the eigenfunction. To do this we look at the zeros of our eigenfunction ψ one at a time. If cutting the edge that contains the zero will disconnect the graph, we do nothing and remove this zero from consideration (see Figure III.2(b)). If cutting the edge that contains the zero will not disconnect the graph, then we cut that edge at a nearby point c_j at which ψ is nonzero, calling the new vertices c_j^+ and c_j^- as before (see Figure III.2(c)). Notice that the order in which we analyze the zeros does not matter; while the cut positions and resulting graph may vary, we will make the same number of cuts.

Let us consider the number of cuts η more explicitly. Denote the zero set of ψ by $\mathcal{N}$ and remove $\mathcal{N}$ from Γ to get the (disconnected) graph $\Gamma\backslash\mathcal{N}$. Let ν be the number of connected components $\{\Gamma_j\}$ after the cutting. Recall that the components Γ_j are the nodal domains of Γ with respect to ψ. Denote

$$\beta_{\Gamma\backslash\mathcal{N}} = \sum_{i=1}^{\nu} \beta_{\Gamma_j}$$

where β_κ is the Betti number of the graph κ. It is easy to see that

$$\eta = \beta_\Gamma - \beta_{\Gamma\backslash\mathcal{N}}.$$

49

Suppose we cut a graph Γ at a single point. The resulting Γ' has two new vertices and one new edge and therefore

$$|V_{\Gamma'}| - |E_{\Gamma'}| = |V_\Gamma| - |E_\Gamma| + 1.$$

In this case, we are making ϕ cuts (where $\phi = |\mathcal{N}| = \#$ of zeros of ψ), and hence

$$|V_{\Gamma \backslash \mathcal{N}}| - |E_{\Gamma \backslash \mathcal{N}}| = |V_\Gamma| - |E_\Gamma| + \phi. \tag{III.14}$$

For any graph $\mathbb{G}$, recall that

$$\beta_\mathbb{G} = |E_\mathbb{G}| - |V_\mathbb{G}| + k_\mathbb{G}$$

where $k_\mathbb{G}$ is the number of connected components of $\mathbb{G}$. Hence from equation (III.14) it is obvious that

$$k_{\Gamma \backslash \mathcal{N}} - \beta_{\Gamma \backslash \mathcal{N}} = k_\Gamma - \beta_\Gamma + \phi,$$

or in other words

$$\eta = \left(\beta_\Gamma - \beta_{\Gamma \backslash \mathcal{N}}\right) = k_\Gamma + \phi - k_{\Gamma \backslash \mathcal{N}} = 1 + \phi - \nu. \tag{III.15}$$

For further details, see Lemma 5.2.1 of [15]. Now we continue with an alternative statement of Theorem III.3.

Theorem III.5. *Suppose the nth eigenvalue λ_n of the Schrödinger operator H^0 is simple, and that the corresponding eigenfunction ψ is nonzero at vertices. We denote by ϕ the number of internal zeros and by ν the number of nodal domains of ψ on Γ. Let $c_j^\pm$, $j = 1, \ldots, \eta$, be the cut points created by following the procedure above, where $\eta = 1 + \phi - \nu$.*

Let H^γ, $\boldsymbol{\gamma} = (\gamma_1, \ldots, \gamma_\eta)$, be the operator obtained from H^0 by imposing the additional conditions

$$\begin{aligned} f'(c_j^+) &= \gamma_j f(c_j^+), \\ f'(c_j^-) &= -\gamma_j f(c_j^-), \end{aligned} \tag{III.16}$$

50

at the cut points.

Define

$$\widetilde{\gamma_j} := \frac{\psi'(c_j^+)}{\psi(c_j^+)} = -\frac{\psi'(c_j^-)}{\psi(c_j^-)}$$

and let $\widetilde{\gamma} = (\widetilde{\gamma_1}, \ldots, \widetilde{\gamma_\beta})$. Consider the eigenvalues of H^γ as functions of γ. Then

    1. $\lambda_{\phi+1}(\widetilde{\gamma}) = \lambda_n$,

    2. $\gamma = \widetilde{\gamma}$ is a non-degenerate critical point of $\lambda_{\phi+1}(\gamma)$, and

    3. the Morse index of the critical point $\widetilde{\gamma}$ is $n - \nu$.

We will prove Theorem III.5 after explaining its significance to the question of equipartitions.

Theorem III.6. *Suppose the nth eigenvalue of Γ is simple and its eigenfunction ψ is nonzero on vertices. Denote by ϕ the number of internal zeros of ψ and by ν the number of its nodal domains. Then the ϕ-equipartitions in the vicinity of the nodal partition of ψ are parameterized by the variables $\gamma = (\gamma_1, \ldots, \gamma_\eta)$.*

The nodal partition of ψ corresponds to the point $\widetilde{\gamma} = (\tilde{\gamma}_1, \ldots, \tilde{\gamma}_\eta)$ and is a non-degenerate critical point of the functional Λ on the set of equipartitions. The Morse index of this critical point is equal to $n - \nu$.

The mapping from $(\gamma_1, \ldots, \gamma_\eta)$ to the equipartitions is constructed as follows (see [7] for more details): the partition in question is generated by the zeros of the $(\phi + 1)^{th}$ eigenfunction of the operator H^γ placed upon the original graph Γ. Indeed, the groundstates of the nodal domains can be obtained by cutting the eigenfunction at zeros and gluing the cut points together (conditions (III.16) ensure the gluing is possible). To verify that all equipartitions are obtainable in this way we simply reverse the process and construct an eigenfunction of H^γ from the groundstates of the nodal domains. The gluing is now done

at zeros, and it can be done recursively (since all cycles with zeros on them have been cut).

Once the parameterization of the equipartitions is accomplished, the Morse index result follows immediately from Theorem III.5. Below we only include the parts of the proof that differ from Theorem III.3.

Proof of Theorem III.5. In the proof of Theorem III.3 (Section III.2.2), the fact that H^γ is an operator on functions whose domain is a tree was used to show that its eigenvalue is simple and to find the sequence number of λ in the spectrum. Theorem II.1 allows us to do the same with a graph with fewer cuts.

Indeed, on the cut graph Γ_γ, ψ is nonzero on all cycles and internal vertices, and therefore by Theorem II.1 the eigenvalue is simple and has number $\phi + 1$ in the spectrum of $H^{\widetilde{\gamma}}$. Since the eigenvalue is simple, we can still apply Lemma III.3. The rest of the proof goes through, with the amendment that the index of the critical point of F_3 is $n + \eta$, since we now have η cuts instead of β cuts. Using equation (III.15), we finally conclude that the Morse index of the critical point is

$$(n + \eta) - (\phi + 1) = n + (1 + \phi - \nu) - \phi - 1 = n - \nu.$$

$\square$

III.4 Consequences to the Inverse Nodal Count Problem

In this section we will focus on the consequence Theorem III.2 has regarding the inverse nodal count problem. Namely, given the nodal count of a graph, can one determine its structure?

Here we recall a few necessary definitions from Chapter II. Let $f_n(x)$ denote the nth eigenfunction of the Schrödinger operator H^0 on a finite graph Γ. We call the zeros of f_n the *nodal set*. The number of such zeros is denoted by ϕ_n and we call the sequence $\{\phi_n\}$

the *nodal point count*. The number of subgraphs formed by removing the nth nodal set from Γ is denoted by ν_n. A *generic eigenvalue* is a simple eigenvalue whose corresponding eigenfunction is nonzero on vertices. We will use the following notation:

$$\mathcal{N} = \{n : \lambda_n \text{ is a generic eigenvalue}\}.$$

A *Neumann metric graph* Γ is a graph with no magnetic or electric potential along with the vertex conditions

$$\begin{cases} f(x) \text{ is continuous at } v \text{ and} \\ \sum_{e \in E_v} \frac{df}{dx_e}(v) = 0 \end{cases}$$

at all vertices v of Γ, which you may recognize is (III.1) with $\chi_v = 0$. The following theorem partially solves the inverse nodal count problem on quantum graphs.

Theorem III.7 (Band,[6]). *Suppose Γ is a Neumann metric graph with at least one generic eigenvalue greater than zero. Then there are infinitely many generic eigenvalues and exactly one of the following is true:*

1. *Γ is a tree and for all $n \in \mathcal{N}$, $\phi_n = n - 1$ and $\nu_n = n$, or*

2. *Γ is not a tree and both sets $\{n \in \mathcal{N} : \phi_n > n - 1\}$ and $\{n \in N : \nu_n < n\}$ are infinite.*

The proof relies heavily on Theorem III.2; it uses the fact that the Morse index of $\lambda_n(\boldsymbol{\alpha})$ is equal to the nodal surplus of the corresponding eigenfunction at $\boldsymbol{\alpha} = (0, \ldots, 0)$. Namely, it shows that if the nodal surplus (and hence the Morse index) is zero for all $n \in \mathcal{N}$, then $\beta = 0$, and hence the graph must be a tree. There is also a discrete graph analogue of Theorem III.7 whose proof relies on Theorem III.1.

It is worth mentioning that Theorem III.7 can be restated as the following: either Γ is a tree or infinitely many ϕ_n differ from n. Consequently, it is not possible for only finitely many ϕ_n to differ from n, or in other words, it is not possible to be "close" to a tree's nodal point count without actually being a tree.

CHAPTER IV

CRITICAL POINTS OF THE DISPERSION RELATION OF INFINITE PERIODIC

GRAPHS

An infinite graph is called $\mathbb{Z}^k$-*periodic* if it is equipped with an action of the free abelian group $\mathbb{Z}^k$ (see Definition 4.1.1 of [15] for details). Given an infinite $\mathbb{Z}^k$-periodic graph $\mathbb{G}$, a fundamental domain $\mathbb{W}$ is a connected subgraph of $\mathbb{G}$ that satisfies the following properties:

1. the union of all $\mathbb{Z}^k$ shifts of $\mathbb{W}$ covers all of $\mathbb{G}$, and

2. different shifted copies of $\mathbb{W}$ have either

   - no vertices in common in the discrete case, or

   - only finitely many points in common in the quantum case, none of which are vertices.

Notice that two vertices are connected in $\mathbb{W}$ if and only if they are attached in $\mathbb{G}$. Let $s_j(v)$ denote the vertex in $\mathbb{G}$ resulting from shifting the vertex v in the positive $j^{th}\mathbb{Z}^k$ direction. In the case of a discrete graph, we define the ordered vertex pair $(v, u) \in \mathbb{W}$ to be the jth *quasi-connected pair* if the vertex $s_j(v)$ is connected to u in $\mathbb{G}$ (Figure IV.1). We denote the set of all quasi-connect pairs by QC. In the quantum case, we define the ordered vertex pair $(v_j^+, v_j^-) \in \mathbb{W}$ to be the jth *quasi-identified pair* if they are identified by the same point after a shift in the positive $j^{th}\mathbb{Z}^k$ direction, or in other words $s_j(v_j^+) = v_j^-$ (Figure IV.2). The main difference is that in the discrete case the shifted vertex is connected, but in the quantum case it is identical. We will only be considering infinite periodic graphs with one quasi-identified or quasi-connected pair in each direction.
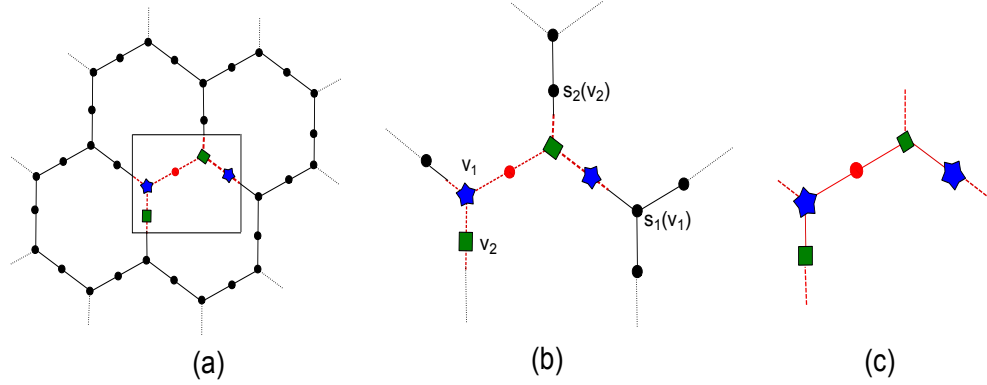
Figure IV.1: Fundamental domain of an infinite periodic discrete graph. (a) An infinite $\mathbb{Z}^2$-periodic graph with chosen fundamental domain inside the box. (b) A zoomed in view of the infinite graph with quasi-connected and shifted vertices marked. (c) The chosen fundamental domain with quasi-connected vertices marked with the same shape/color.
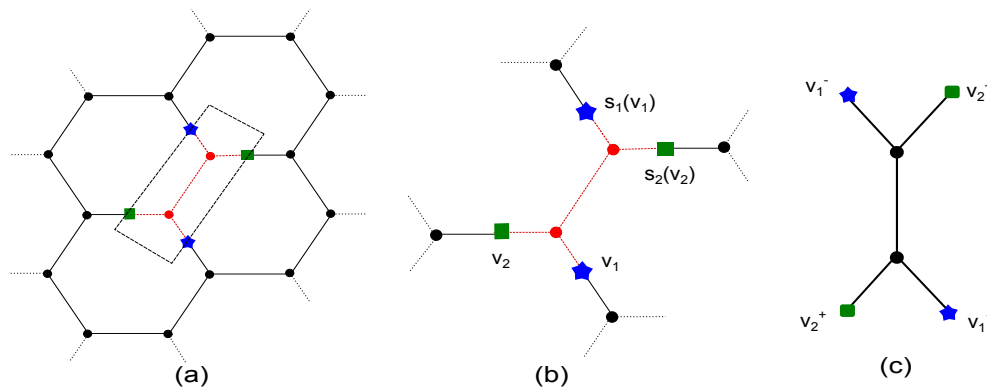

Figure IV.2: Fundamental domain of an infinite periodic quantum graph. (a) An infinite $\mathbb{Z}^2$-periodic graph with chosen fundamental domain inside the box. (b) A zoomed in view of the infinite graph with quasi-identified and shifted vertices marked. (c) The chosen fundamental domain with quasi-identified vertices marked with the same shape/color.

In this chapter, we will first provide a brief introduction to Floquet-Bloch theory in Section IV.1. Floquet-Bloch theory provides a way to determine the spectrum of an operator H that acts on functions whose domain is an infinite periodic graph. This is accomplished by calculating the spectrum of a related operator $H^{\boldsymbol{\alpha}}$ which acts on functions that are defined on a finite fundamental domain, and then taking the union over all possible parameters $\{\boldsymbol{\alpha}\}$. Eigenvalues of this related operator can therefore be viewed as functions of parameters. We will analyze critical points of the eigenvalues with respect to these parameters in the case of discrete graphs in Section IV.2 and quantum graphs in Section IV.3.

IV.1 Floquet-Bloch Theory

The following is a brief summary of Floquet-Bloch theory that focuses on the aspects we will be using later in this chapter. The interested reader can find more details in [66] and Chapter 4 of [15].

IV.1.1 Floquet Transform

Suppose we have the ordinary Schrödinger operator on an infinite $\mathbb{Z}^k$-periodic graph with no magnetic potential. Recall that in the discrete case this operator is defined by

$$(Hf)(v) = -\sum_{u \sim v} f(u) + q(v)f(v) \tag{IV.1}$$

where $q : V \to \mathbb{R}$ is $\mathbb{Z}^k$-periodic and represents electric potential. In the quantum case, we defined the Schrödinger operator as

$$H : f \to -\frac{d^2 f}{dx^2} + qf \tag{IV.2}$$

on functions from $\mathcal{D} \subset \widetilde{H^2}(\Gamma, \mathbb{R})$ that satisfy

$$\begin{cases} f(x) \text{ is continuous at v,} \\ \sum_{e \in E_v} \frac{df}{dx_e}(v) = \chi_v f(v), \qquad \chi_v \in \mathbb{R} \end{cases} \qquad \text{(IV.3)}$$

for all $v \in V$ where $q : \Gamma \to \mathbb{R}$ is $\mathbb{Z}^k$-periodic and represents electric potential.

The Floquet transform of (IV.1) acts on the finite discrete graph $\mathbb{W}$ the same way H acted on $\mathbb{G}$, but we need to add the condition that when moving from v to $s_j(v)$ (which is connected to u), we multiply the function by $e^{i\alpha_j}$. Observe that if $s_j(v)$ is connected to u, then the vertex obtained by shifted u in the negative $j^{th} \mathbb{Z}^k$ direction is connected to v, or in other words $s_{-j}(u)$ is connected to v. Hence, when moving from u to v, we need to multiply the function by $e^{-i\alpha_j}$. Let C be the connectivity matrix of $\mathbb{W}$ and Q be the diagonal matrix representing real electric potential on $\mathbb{W}$. Observe that Q is enough information to uniquely define the electric potential everywhere on $\mathbb{G}$ since q is $\mathbb{Z}^k$-periodic. The transformed operator defined on the vertices of $\mathbb{W}$ is $H^{\boldsymbol{\alpha}} = Q - C - M^{\boldsymbol{\alpha}}$ where

$$M^{\boldsymbol{\alpha}}_{v,u} = \begin{cases} e^{i\alpha_j} & \text{if } (v,u) \text{ is the } j^{th} QC \text{ pair} \\ e^{-i\alpha_j} & \text{if } (u,v) \text{ is the } j^{th} QC \text{ pair} \\ 0 & \text{otherwise.} \end{cases}$$

Similarly, the Floquet transform of (IV.2, IV.3) acts on the finite quantum graph $\mathbb{W}$ the same way H acted on $\mathbb{G}$. This time, we need to add the condition that when moving from v_j^+ to v_j^-, the function is multiplied by $e^{i\alpha_j}$. This means that the transformed operator acts as (IV.2) on functions from $\widetilde{H^2}(\mathbb{W}, \mathbb{C})$ that satisfy (IV.3) at the non-quasi-identified vertices of $\mathbb{W}$ and

$$\begin{aligned} f(v_j^-) &= e^{i\alpha_j} f(v_j^+), \\ f'(v_j^-) &= -e^{i\alpha_j} f'(v_j^+) \end{aligned} \qquad \text{(IV.4)}$$

at the quasi-identified vertices. Notice that we do not have "negative" shift terms as we did with discrete graphs since multiplying the above equations by $e^{-i\alpha_j}$ accounts for this case.

Observe that in both cases, these operators are very similar to the discrete and differential operators $H^{\boldsymbol{\alpha}}$ defined in Chapter III. There are, however, two differences. The first is in the physical interpretation. In Chapter III, $\boldsymbol{\alpha}$ represented magnetic flux, and here it represents a position in the infinite graph $\mathbb{G}$. Second, the operators have different domains. In Chapter III, the operator acted on functions whose domain was a tree. Here the functions act on $\mathbb{W}$, which may or may not be a tree. However, observe that if $\mathbb{W}$ has a cycle, we can cut it at an arbitrary (nonzero) point and fix the corresponding $\alpha_j = 0$, which is equivalent to continuity at the point or "gluing" the cut points together. As these differences are minor, we will continue to use the same notation $H^{\boldsymbol{\alpha}}$ in this chapter.

IV.1.2 Spectral Bands

To find the spectrum of an operator whose domain is functions that are defined on an infinite periodic graph, one needs to find eigenvalues of the Floquet transform for all possible values of the transform. Informally, Floquet-Bloch theory says that we can compute the spectrum of the Schrödinger operator on the $\mathbb{Z}^k$-infinite graph $\mathbb{G}$ by taking the union of the spectrum of $H^{\boldsymbol{\alpha}}$ on a fundamental domain $\mathbb{W}$ for all $\boldsymbol{\alpha} \in [-\pi, \pi]^k$, which is called the *Brillouin zone*. We will make this concept precise in this section.

Suppose the Schrödinger operator ((IV.1) in the discrete case or (IV.2, IV.3) in the quantum case) is acting on functions whose domain is an infinite $\mathbb{Z}^k$-periodic graph $\mathbb{G}$. We define the *spectral band* I_j corresponding to the jth eigenvalue as follows:

$$I_j = \{\lambda : \lambda = \lambda_j(\boldsymbol{\alpha}) \text{ for some } \boldsymbol{\alpha} \in [-\pi, \pi]^k\}.$$

The spectrum of H is

$$\sigma = \bigcup_{j=1}^{n} I_j,$$

in the discrete case where n is the number of vertices of the fundamental domain $\mathbb{W}$ and

$$\sigma = \bigcup_{j} I_j$$

in the quantum case. Notice that in the quantum case the operator H is unbounded, which will result in infinitely many spectral bands $I_j = [a_j, b_j]$ with $\lim_{j \to \infty} a_j = \infty$. We call this representation the *band-gap structure*. We call the boundary (i.e., maximum and minimum value) of each spectral band a *spectral edge*. The multi-valued function $\boldsymbol{\alpha} \to \sigma$ is called the *dispersion relation* and its graph is called the *dispersion curve*. The bands I_j may be separated, which results in spectral gaps in the dispersion curve.

Most literature refers to "interior" and "exterior" or "boundary" points of the Brillouin zone. To make these terms more precise, we will refer to Theorem III.4. Recall that the theorem says that $H^{\varsigma - \boldsymbol{\alpha}}$ and $H^{\varsigma + \boldsymbol{\alpha}}$ have the same spectrum (in the case of a finite quantum graph) for all

$$\varsigma \in \Sigma = \left\{ (b_1, \ldots, b_\beta) : b_j \in \{-\pi, 0, \pi\} \right\}.$$

In our case, $\varsigma = (b_1, b_2, \ldots, b_k)$ for an infinite $\mathbb{Z}^k$-periodic graph; as mentioned previously, all other b_j (i.e., $j = k+1, \ldots, \beta$) are zero. We will call all $\varsigma \in \Sigma$ *symmetric points*; all other points in the Brillouin zone are called *nonsymmetric points*. In terms of the traditional nomenclature, symmetric points are equivalent to exterior or boundary points whereas all nonsymmetric points are considered interior points.

In this chapter, we explore cases in which the spectral bands touch at nonsymmetric points of the Brillouin zone. As mentioned in Section I.3, this is rare, as most touching points appear at symmetric points of the Brillouin zone.

IV.2   Infinite Periodic Discrete Graphs

Functions defined on the fundamental domain $\mathbb{W}$ are in $\mathbb{C}^n$, where n is the number of vertices of $\mathbb{W}$. Let $\boldsymbol{\gamma} = (\gamma_1, \gamma_2, \ldots, \gamma_k) \in \mathbb{R}^k$ and define the operator $H^{\boldsymbol{\gamma}} = Q - C - M^{\boldsymbol{\gamma}}$ on $\mathbb{C}^n$ where once again Q is a diagonal matrix with real entries representing electric potential, C is the connectivity matrix of $\mathbb{W}$, and here $M^{\boldsymbol{\gamma}}$ is the diagonal matrix

$$
M^{\boldsymbol{\gamma}}_{v,v} = \begin{cases} \gamma_j & \text{if } (v,u) \text{ is the } j^{th} QC \text{ vertex pair} \\[2mm] \frac{1}{\gamma_j} & \text{if } (u,v) \text{ is the } j^{th} QC \text{ vertex pair} \\[2mm] 0 & \text{otherwise.} \end{cases}
$$

Observe that the matrix $H^{\boldsymbol{\gamma}}$ is self-adjoint and has real entries. Therefore, for each eigenvalue λ_n one can choose a representative eigenvector with real entries. We are now ready to present the main theorem of this chapter for the case of discrete graphs.

Theorem IV.1. *Suppose the infinite $\mathbb{Z}^k$-periodic discrete graph $\mathbb{G}$ has no magnetic potential and only one quasi-connected vertex pair in each direction, $\lambda_n(\boldsymbol{\alpha})$ has a critical point $\boldsymbol{\alpha}^*$ that is not at a symmetric point of the Brillouin zone (i.e., $\exists j$ such that $\alpha_j^* \neq 0, \pm\pi$), the eigenvalue $\lambda_n(\boldsymbol{\alpha}^*)$ is simple, and the corresponding eigenvector f is nonzero at all quasi-connected vertex pairs. Then $\lambda = \lambda_n(\boldsymbol{\alpha}^*)$ is a degenerate eigenvalue of $H^{\widetilde{\boldsymbol{\gamma}}}$ where $\widetilde{\gamma}_j = e^{i\alpha_j^*} \frac{f(u)}{f(v)} \in \mathbb{R}$ and (v,u) is the jth quasi-connected vertex pair.*

IV.2.1   Proof of Theorem IV.1

Before we can prove Theorem IV.1, we first need to collect and prove a few lemmas. Since we defined the operator $H^{\boldsymbol{\gamma}}$ for $\boldsymbol{\gamma} \in \mathbb{R}^k$, we will first verify that $\widetilde{\gamma}_j$ is real.

Lemma IV.1. *Suppose that the infinite $\mathbb{Z}^k$-periodic discrete graph $\mathbb{G}$ has no magnetic potential and only one quasi-connected vertex pair in each direction. If $\boldsymbol{\alpha}^*$ is a critical point of $\lambda_n(\boldsymbol{\alpha})$ and $\lambda_n(\boldsymbol{\alpha}^*)$ is a simple eigenvalue, then the eigenvector f of norm one*

corresponding to $\lambda_n(\boldsymbol{\alpha}^*)$ *satisfies*

$$e^{i\alpha_j^*} f(u)\overline{f(v)} \in \mathbb{R} \qquad \forall j = 1, 2, \ldots, k$$

where (v, u) *is the* j^{th} *quasi-connected vertex pair.*

Proof. By standard perturbation theory (see, for example, [52]), since $\lambda_n(\boldsymbol{\alpha}^*)$ is a simple eigenvalue of $H^{\boldsymbol{\alpha}}$, we know that the function $\lambda_n(\boldsymbol{\alpha})$ is smooth (indeed analytic and therefore differentiable) around $\boldsymbol{\alpha} = \boldsymbol{\alpha}^*$. Let $f_{\boldsymbol{\alpha}}$ be an eigenvector of norm one corresponding to $\lambda_n(\boldsymbol{\alpha})$. We define $f := f_{\boldsymbol{\alpha}^*}$ and know that $\lambda_n(\boldsymbol{\alpha}) = (H^{\boldsymbol{\alpha}} f)\overline{f^T} := (H^{\boldsymbol{\alpha}} f, f)$. Since $H^{\boldsymbol{\alpha}}$ is self-adjoint and $\boldsymbol{\alpha}^*$ is a critical point of $\lambda_n(\boldsymbol{\alpha})$, we can use the chain rule to calculate that

$$
\begin{aligned}
\frac{\partial}{\partial \alpha_j} \lambda_n(\boldsymbol{\alpha})\bigg|_{\boldsymbol{\alpha}=\boldsymbol{\alpha}^*} &= \frac{\partial}{\partial \alpha_j}(H^{\boldsymbol{\alpha}} f_{\boldsymbol{\alpha}}, f_{\boldsymbol{\alpha}})\bigg|_{\boldsymbol{\alpha}=\boldsymbol{\alpha}^*} \\
&= \left[\left(\frac{\partial H^{\boldsymbol{\alpha}}}{\partial \alpha_j} f_{\boldsymbol{\alpha}}, f_{\boldsymbol{\alpha}}\right) + \left(H^{\boldsymbol{\alpha}} \frac{\partial f_{\boldsymbol{\alpha}}}{\partial \alpha_j}, f_{\boldsymbol{\alpha}}\right) + \left(H^{\boldsymbol{\alpha}} f_{\boldsymbol{\alpha}}, \frac{\partial f_{\boldsymbol{\alpha}}}{\partial \alpha_j}\right)\right]\bigg|_{\boldsymbol{\alpha}=\boldsymbol{\alpha}^*} \\
&= \left[\left(\frac{\partial H^{\boldsymbol{\alpha}}}{\partial \alpha_j} f_{\boldsymbol{\alpha}}, f_{\boldsymbol{\alpha}}\right) + \left(\frac{\partial f_{\boldsymbol{\alpha}}}{\partial \alpha_j}, H^{\boldsymbol{\alpha}} f_{\boldsymbol{\alpha}}\right) + \left(H^{\boldsymbol{\alpha}} f_{\boldsymbol{\alpha}}, \frac{\partial f_{\boldsymbol{\alpha}}}{\partial \alpha_j}\right)\right]\bigg|_{\boldsymbol{\alpha}=\boldsymbol{\alpha}^*} \\
&= \left[\left(\frac{\partial H^{\boldsymbol{\alpha}}}{\partial \alpha_j} f_{\boldsymbol{\alpha}}, f_{\boldsymbol{\alpha}}\right) + \left(\frac{\partial f_{\boldsymbol{\alpha}}}{\partial \alpha_j}, \lambda_n(\boldsymbol{\alpha}) f_{\boldsymbol{\alpha}}\right) + \left(\lambda_n(\boldsymbol{\alpha}) f_{\boldsymbol{\alpha}}, \frac{\partial f_{\boldsymbol{\alpha}}}{\partial \alpha_j}\right)\right]\bigg|_{\boldsymbol{\alpha}=\boldsymbol{\alpha}^*} \\
&= \left(\frac{\partial H^{\boldsymbol{\alpha}}}{\partial \alpha_j} f_{\boldsymbol{\alpha}}, f_{\boldsymbol{\alpha}}\right)\bigg|_{\boldsymbol{\alpha}=\boldsymbol{\alpha}^*} + \lambda_n(\boldsymbol{\alpha})\left[\left(\frac{\partial f_{\boldsymbol{\alpha}}}{\partial \alpha_j}, f_{\boldsymbol{\alpha}}\right) + \left(f_{\boldsymbol{\alpha}}, \frac{\partial f_{\boldsymbol{\alpha}}}{\partial \alpha_j}\right)\right]\bigg|_{\boldsymbol{\alpha}=\boldsymbol{\alpha}^*} \\
&= \left(\frac{\partial H^{\boldsymbol{\alpha}}}{\partial \alpha_j} f_{\boldsymbol{\alpha}}, f_{\boldsymbol{\alpha}}\right)\bigg|_{\boldsymbol{\alpha}=\boldsymbol{\alpha}^*} + \lambda_n(\boldsymbol{\alpha}) \frac{\partial}{\partial \alpha_j}(f_{\boldsymbol{\alpha}}, f_{\boldsymbol{\alpha}})\bigg|_{\boldsymbol{\alpha}=\boldsymbol{\alpha}^*} \\
&= \left(\frac{\partial H^{\boldsymbol{\alpha}^*}}{\partial \alpha_j} f, f\right) = 0
\end{aligned}
$$

because $\lambda_n(\boldsymbol{\alpha})$ is real and the eigenvectors are normalized to one (so $\frac{\partial}{\partial \alpha_j}(f_{\boldsymbol{\alpha}}, f_{\boldsymbol{\alpha}}) = 0$). As

the matrices Q and C are independent of $\boldsymbol{\alpha}$, we have that

$$\left(\frac{\partial H^{\boldsymbol{\alpha}}}{\partial \alpha_j}\right)_{v,u} = -\left(\frac{\partial M^{\boldsymbol{\alpha}}}{\partial \alpha_j}\right)_{v,u} = \begin{cases} -ie^{i\alpha_j} & \text{if } (v,u) \text{ is the } j^{th} QC \text{ vertex pair} \\ ie^{-i\alpha_j} & \text{if } (u,v) \text{ is the } j^{th} QC \text{ vertex pair} \\ 0 & \text{otherwise.} \end{cases}$$

Therefore, since $\boldsymbol{\alpha}^*$ is a critical point of $\lambda_n(\boldsymbol{\alpha})$, one can see that

$$\begin{aligned} \frac{\partial}{\partial \alpha_j}\lambda_n(\boldsymbol{\alpha})\Big|_{\boldsymbol{\alpha}=\boldsymbol{\alpha}^*} = \left(\frac{\partial H^{\boldsymbol{\alpha}^*}}{\partial \alpha_j}f, f\right) &= -ie^{i\alpha_j^*}f(u)\overline{f(v)} + ie^{-i\alpha_j^*}f(v)\overline{f(u)} \\ &= -i[e^{i\alpha_j^*}f(u)\overline{f(v)} - \overline{e^{i\alpha_j^*}f(u)\overline{f(v)}}] \\ &= 2\text{Im}(e^{i\alpha_j^*}f(u)\overline{f(v)}) = 0, \end{aligned}$$

which completes the proof.

$\square$

Lemma IV.2. *Suppose that $\mathbb{G}$ is an infinite $\mathbb{Z}^k$-periodic discrete graph and $\boldsymbol{\alpha}^*$ is a critical point of $\lambda_n(\boldsymbol{\alpha})$. If the eigenvector f of $H^{\boldsymbol{\alpha}^*}$ corresponding to $\lambda = \lambda_n(\boldsymbol{\alpha}^*)$ is nonzero at all quasi-connected vertex pairs, then f is also an eigenvector of $H^{\widetilde{\gamma}}$ corresponding to the same eigenvalue λ where $\widetilde{\gamma}_j = e^{i\alpha_j^*}\frac{f(u)}{f(v)} \in \mathbb{R}$ and (v,u) is the jth quasi-connected vertex pair.*

Proof. We will complete this proof by demonstrating that $H^{\widetilde{\gamma}}f = H^{\boldsymbol{\alpha}^*}f = \lambda f$. Using the definitions of the operators, one can see that this is equivalent to showing

$$H^{\widetilde{\gamma}}f = (Q - C)f - M^{\widetilde{\gamma}}f = (Q - C)f - M^{\boldsymbol{\alpha}^*}f = H^{\boldsymbol{\alpha}^*}f = \lambda f,$$

or in other words

$$M^{\widetilde{\gamma}}f = M^{\boldsymbol{\alpha}^*}f.$$

Suppose that (v,u) is the jth quasi-connected vertex pair. Then $\gamma_j^* = e^{i\alpha_j^*}\frac{f(u)}{f(v)}$. At v we

62

have

$$(M^{\widetilde{\gamma}}f)(v) = M^{\widetilde{\gamma}}_{v,v}f(v) = \gamma_j^* f(v)$$
$$= e^{i\alpha_j^*}\frac{f(u)}{f(v)}f(v)$$
$$= e^{i\alpha_j^*}f(u) = (M^{\boldsymbol{\alpha}^*}f)(v).$$

Similarly, at u we have

$$(M^{\widetilde{\gamma}}f)(u) = M^{\widetilde{\gamma}}_{u,u}f(u) = \frac{1}{\gamma_j^*}f(u)$$
$$= e^{-i\alpha_j^*}\frac{f(v)}{f(u)}f(u)$$
$$= e^{-i\alpha_j^*}f(v) = (M^{\boldsymbol{\alpha}^*}f)(u).$$

If w is not in any quasi-connected pair, then it is easy to see that

$$(M^{\widetilde{\gamma}}f)(w) = 0 = (M^{\boldsymbol{\alpha}^*}f)(w).$$

Combining these cases, we see that $M^{\widetilde{\gamma}}f = M^{\boldsymbol{\alpha}^*}f$ and hence, f is an eigenvector of $H^{\widetilde{\gamma}}$.

$\square$

Proof of Theorem IV.1. By Lemma IV.2, the eigenvector f of $H^{\boldsymbol{\alpha}^*}$ is also an eigenvector of $H^{\widetilde{\gamma}}$ (corresponding to the same eigenvalue $\lambda = \lambda_n(\boldsymbol{\alpha}^*)$). By assumption, there exists j such that $\alpha_j^* \neq 0, \pm\pi$ which implies that f is a complex-valued vector since it satisfies

$$e^{i\alpha_j^*}f(u)\overline{f(v)} \in \mathbb{R}$$

by Lemma IV.1. We know that $H^{\widetilde{\gamma}}$ is a self-adjoint operator with real entries, which means its eigenvectors should be real-valued. Therefore, the real and imaginary parts of f must both be eigenvectors of $H^{\widetilde{\gamma}}$ which implies that λ is a degenerate eigenvalue of $H^{\widetilde{\gamma}}$. $\square$

The following corollary is the main result of this section.

Corollary IV.1. *Suppose the infinite $\mathbb{Z}^k$-periodic discrete graph $\mathbb{G}$ has no magnetic potential and only one quasi-connected vertex pair in each direction, the chosen fundamental domain $\mathbb{W}$ is a tree, $\lambda_n(\boldsymbol{\alpha})$ has a critical point $\boldsymbol{\alpha}^*$ that is not at a symmetric point of the Brillouin zone (i.e., $\exists j$ such that $\alpha_j^* \neq 0, \pm\pi$), the eigenvalue $\lambda_n(\boldsymbol{\alpha}^*)$ is simple, and the corresponding eigenvector f is nonzero at all quasi-connected vertex pairs. Then the corresponding eigenvector f is zero on at least one internal vertex of $\mathbb{W}$.*

Proof. By Theorem IV.1, $\lambda_n(\boldsymbol{\alpha}^*)$ is a multiple eigenvalue of $H^{\widetilde{\gamma}}$, which acts on functions whose domain is the tree $\mathbb{W}$. When an operator that acts on functions whose domain is a tree has a multiple eigenvalue, there exists an internal vertex at which all eigenvectors from the corresponding eigenspace vanish [34]. By Lemma IV.2, f is one such eigenvector of $H^{\widetilde{\gamma}}$ corresponding to the multiple eigenvalue $\lambda_n(\boldsymbol{\alpha}^*)$ and hence, it must be zero on at least one internal vertex of $\mathbb{W}$. Furthermore, the degree of that vertex must be greater than or equal to three [34].

$\square$

IV.3   Infinite Periodic Quantum Graphs

Beginning with the fundamental domain $\mathbb{W}$, merge the vertices of each quasi-identified pair (v_j^+, v_j^-) to form a new vertex v_j and denote the resulting graph by $\mathbb{D}$. When connecting vertices, do not change relative lengths. For example, if there is length l_1 between vertices a and v_1^- and length l_2 between vertices b and v_1^+, then in the graph $\mathbb{D}$ the length of the path from a to b that passes through v_1 must be $l_1 + l_2$ (see Figure IV.3). The following easy result is equivalent to Lemma III.2 and can be found, for example, in [15, 62, 86].

Lemma IV.3. *The operator $H^{\boldsymbol{\alpha}}$ is unitarily equivalent to the operator $H^A : \widetilde{H^2}(\mathbb{D}, \mathbb{C}) \to \widetilde{L^2}(\mathbb{D}, \mathbb{C})$, which is defined as $-\left(\frac{d}{dx} - iA(x)\right)^2 + q(x)$ on every edge where $A(x)$ is a one-form*
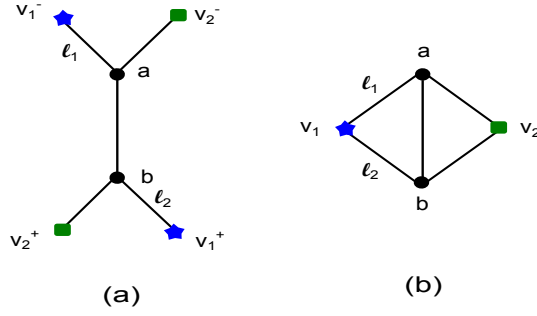
Figure IV.3: Merging quasi-identified vertices of a fundamental domain. (a) The fundamental domain with quasi-identified vertices marked with the same shape/color. The length from v_1^- to a is l_1 and the length from v_1^+ to b is l_2. (b) The graph $\mathbb{D}$ formed by merging the quasi-identified vertices. Notice that the length of the path from a to b through v_1 is $l_1 + l_2$.

on $\mathbb{D}$ that satisfies

$$\alpha_j = \int_{v_j^-}^{v_j^+} A(x) \mod 2\pi$$

for any path on $\mathbb{W}$ between v_j^- and v_j^+, along with the vertex conditions

$$
\begin{cases}
g(x) \text{ is continuous at } v, \\
\sum_{e \in E_v} \left(\frac{d}{dx} - iA(v) \right) g(v) = \chi_v g(v), \qquad \chi_v \in \mathbb{R}.
\end{cases}
$$

Remark 5. The parameters α_j are path independent because there is no magnetic potential on our graph, and hence the integral of $A(x)$ around any cycle in $\mathbb{W}$ is zero.

In the discrete case, we required that the eigenfunction be nonzero on all quasi-connected vertices to avoid γ_j being equal to zero or infinity. In the quantum case, we will only require that the eigenfunction is not identically zero on any edge attached to quasi-identified vertices. We do this by moving the quasi-identified vertices to a place on the edge at which the eigenfunction is nonzero and define γ_j there. In the following, we will make this restriction and construction precise.

65

By Lemma IV.3, it is easy to see that the eigenvalues depend only on the integral of the one-form $A(x)$ through the cycles that were formed by merging the quasi-identified pairs. Therefore, we can cut each one of these cycles at any point and enforce the $\boldsymbol{\alpha}$ vertex conditions (IV.4) there without changing the spectrum. Namely, we will cut the cycle at a point at which the eigenfunction is nonzero to avoid γ_j being zero or infinity.

Remark 6. Recall that in the process of proving Lemma III.2 (which is equivalent to Lemma IV.3), we showed that if g is an eigenfunction of H^A, then $f := g e^{-i\xi}$ is an eigenfunction of $H^{\boldsymbol{\alpha}}$ where

$$\xi(x) = \int_p^x A(x)\, \mathrm{d}x.$$

Let g be an eigenfunction of H^A, and let f be the eigenfunction of the unitarily equivalent operator $H^{\boldsymbol{\alpha}}$ as constructed in Remark 6. We know by this construction that $|f| = |g|$ and hence, $f(x) = 0$ if and only if $g(x) = 0$. On an edge attached to vertex v_j, we choose a point c_j such that the eigenfunction g is nonzero at c_j. We then cut $\mathbb{D}$ at the points $\{c_j\}_{j=1}^k$ to form the graph $\mathbb{W}'$ (see Figure IV.4). Observe that we cut k (not necessarily equal to β, the first Betti number of $\mathbb{W}$) edges, and hence $\mathbb{W}'$ may not be a tree; in fact, $\mathbb{W}'$ will have the same number of cycles $\mathbb{W}$ does. We will analyze the unitarily equivalent operator $H^{\boldsymbol{\alpha}} : \widetilde{H^2}(\mathbb{W}', \mathbb{C}) \to \widetilde{L^2}(\mathbb{W}', \mathbb{C})$ which again acts as $-\frac{d^2}{dx^2} + q(x)$ on every edge but now has the boundary conditions

$$
\begin{aligned}
f(c_j^-) &= e^{i\alpha_j} f(c_j^+), \\
f'(c_j^-) &= -e^{i\alpha_j} f'(c_j^+)
\end{aligned}
\tag{IV.5}
$$

at the new vertices formed by the cuts and (IV.3) at the other vertices. It is easy to see from the graph $\mathbb{D}$ that

$$\int_{c_j^-}^{c_j^+} A(x) \mod 2\pi = \int_{v_j^-}^{v_j^+} A(x) \mod 2\pi = \alpha_j,$$
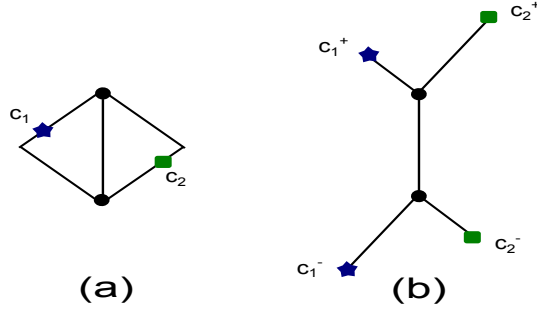
and hence these are the same $\{\alpha_j\}$ as (IV.4).

Figure IV.4: Forming $\mathbb{W}'$ from $\mathbb{D}$. (a) A graph $\mathbb{D}$ based off of the fundamental domain from Figure IV.3(a) with chosen cut points. (b) The resulting graph $\mathbb{W}'$ after cutting $\mathbb{D}$ at the chosen points. Observe that if $\mathbb{G}$ is a Z^k-periodic graph, we only cut k edges so the resulting graph $\mathbb{W}'$ may not be a tree.

Let $\boldsymbol{\gamma} = (\gamma_1, \gamma_2, \ldots, \gamma_k) \in \mathbb{R}^k$ and define the operator $H^{\boldsymbol{\gamma}} : \widetilde{H^2}(\mathbb{W}', \mathbb{C}) \to \widetilde{L^2}(\mathbb{W}', \mathbb{C})$, which acts as $-\frac{d^2}{dx^2} + q(x)$ on every edge, along with the vertex conditions

$$
\begin{aligned}
f'(c_j^+) &= \gamma_j f(c_j^+), \\
f'(c_j^-) &= -\gamma_j f(c_j^-)
\end{aligned}
\tag{IV.6}
$$

at the cut points and (IV.3) at all other vertices of $\mathbb{W}'$. Now we are ready to present the analogue of Theorem IV.1 for the case of a quantum graph.

Theorem IV.2. *Suppose the infinite $\mathbb{Z}^k$-periodic quantum graph $\mathbb{G}$ has no magnetic potential and only one quasi-identified vertex pair in each direction, $\lambda_n(\boldsymbol{\alpha})$ has a critical point $\boldsymbol{\alpha}^*$ that is not at a symmetric point of the Brillouin zone (i.e., $\exists j$ such that $\alpha_j^* \neq 0, \pm\pi$), the eigenvalue $\lambda_n(\boldsymbol{\alpha}^*)$ is simple, and the corresponding eigenfunction f is not identically zero on edges attached to quasi-identified vertices. Then $\lambda = \lambda_n(\boldsymbol{\alpha}^*)$ is a degenerate eigenvalue of $H^{\widetilde{\gamma}}$ where $\widetilde{\gamma}_j = \frac{f'(c_j^+)}{f(c_j^+)} \in \mathbb{R}$.*

Remark 7. Notice that if the the eigenfunction f is nonzero at all quasi-identified vertices, then we can take $\widetilde{\gamma}_j = \frac{f'(v_j^+)}{f(v_j^+)}$, which is analogous to the case we had in Theorem IV.1.

67

IV.3.1   Proof of Theorem IV.2

The proof of Theorem IV.2 will follow the same basic structure as the proof of Theorem IV.1 in Section IV.2.1. In particular, we will show that $\widetilde{\gamma} \in \mathbb{R}^k$ and f is also an eigenfunction of $H^{\widetilde{\gamma}}$. Since the vertex conditions of $H^{\widetilde{\gamma}}$ have real coefficients and $H^{\widetilde{\gamma}}$ acts on functions whose domain is a quantum tree, its eigenfunctions can be chosen to be real-valued. However, f is complex-valued which means that λ is a degenerate eigenvalue of $H^{\widetilde{\gamma}}$. First we collect preliminary lemmas to demonstrate that these details are true.

By standard perturbation theory (see, for example, [52]), we know that if $\lambda_n(\boldsymbol{\alpha}^*)$ is a simple eigenvalue of $H^{\boldsymbol{\alpha}^*}$, then the function $\lambda_n(\boldsymbol{\alpha})$ is smooth (indeed analytic) around $\boldsymbol{\alpha} = \boldsymbol{\alpha}^*$. Therefore, we can take derivatives with respect to α_j and analyze critical points. The following lemma demonstrates that $\widetilde{\gamma} \in \mathbb{R}^k$.

Lemma IV.4. *Suppose that the infinite $\mathbb{Z}^k$-periodic quantum graph $\mathbb{G}$ has no magnetic potential and only one quasi-identified vertex pair in each direction. If $\boldsymbol{\alpha}^*$ is a critical point of $\lambda_n(\boldsymbol{\alpha})$ and $\lambda_n(\boldsymbol{\alpha}^*)$ is a simple eigenvalue, then the eigenfunction f corresponding to $\lambda_n(\boldsymbol{\alpha}^*)$ satisfies*

$$f'(c_j^+)\overline{f(c_j^+)} \in \mathbb{R} \quad \forall j = 1, 2, \ldots, k.$$

Proof. By perturbation theory, $\lambda(\boldsymbol{\alpha})$ is analytic near $\boldsymbol{\alpha}^*$. Hence, we can calculate derivatives near $\boldsymbol{\alpha}^*$ and know that

$$\frac{d\lambda_n(\boldsymbol{\alpha})}{d\boldsymbol{\alpha}}\bigg|_{\boldsymbol{\alpha}=\boldsymbol{\alpha}^*} = \frac{\partial\lambda_n(\boldsymbol{\alpha}^* + t\boldsymbol{\delta\alpha})}{\partial t}\bigg|_{t=0} = 0.$$

By Lemma IV.3, this is equivalent to

$$\frac{\partial\lambda_n(\boldsymbol{\alpha}^* + t\boldsymbol{\delta\alpha})}{\partial t}\bigg|_{t=0} = \frac{\partial\lambda_n(A^* + tB)}{\partial t}\bigg|_{t=0} = 0$$

68

for any continuous function $B(x)$ that satisfies

$$\int_{c_j^-}^{c_j^+} B(x) \mod 2\pi = \delta\alpha_j \quad \text{for all } j = 1, 2, \ldots, k.$$

Let g_t be an eigenfunction of norm one corresponding to $\lambda_n(A^* + tB)$. We define $g :=$ $g_0 = fe^{i\xi}$ (by Remark 6), and for the sake of notation denote $\lambda_n(A^* + tB) := \lambda_t \in \mathbb{R}$ (so $\lambda_0 = \lambda_n(A^*) = \lambda_n(\alpha^*)$). Since H^A is self-adjoint, we can use the chain rule to calculate that

$$
\begin{aligned}
\frac{\partial}{\partial t}\lambda_n(A^* + tB)\Big|_{t=0} &= \frac{\partial}{\partial t}\langle H^{A^*+tB} g_t, g_t\rangle\Big|_{t=0} \\
&= \left[\left\langle \frac{\partial H^{A^*+tB}}{\partial t} g_t, g_t\right\rangle + \left\langle H^{A^*+tB}\frac{\partial g_t}{\partial t}, g_t\right\rangle + \left\langle H^{A^*+tB} g_t, \frac{\partial g_t}{\partial t}\right\rangle\right]\Big|_{t=0} \\
&= \left[\left\langle \frac{\partial H^{A^*+tB}}{\partial t} g_t, g_t\right\rangle + \left\langle \frac{\partial g_t}{\partial t}, H^{A^*+tB} g_t\right\rangle + \left\langle H^{A^*+tB} g_t, \frac{\partial g_t}{\partial t}\right\rangle\right]\Big|_{t=0} \\
&= \left[\left\langle \frac{\partial H^{A^*+tB}}{\partial t} g_t, g_t\right\rangle + \left\langle \frac{\partial g_t}{\partial t}, \lambda_t g_t\right\rangle + \left\langle \lambda_t g_t, \frac{\partial g_t}{\partial t}\right\rangle\right]\Big|_{t=0} \\
&= \left[\left\langle \frac{\partial H^{A^*+tB}}{\partial t} g_t, g_t\right\rangle + \lambda_t\left(\left\langle \frac{\partial g_t}{\partial t}, g_t\right\rangle + \left\langle g_t, \frac{\partial g_t}{\partial t}\right\rangle\right)\right]\Big|_{t=0} \\
&= \left[\left\langle \frac{\partial H^{A^*+tB}}{\partial t} g_t, g_t\right\rangle + \lambda_t \frac{\partial}{\partial t}\langle g_t, g_t\rangle\right]\Big|_{t=0} \\
&= \left\langle \frac{\partial H^{A^*+tB}}{\partial t} g_t, g_t\right\rangle\Big|_{t=0} = 0 \qquad\qquad\qquad\qquad\qquad \text{(IV.7)}
\end{aligned}
$$

because λ_t is real and all g_t have fixed norm one so $\frac{\partial}{\partial t}\langle g_t, g_t\rangle = 0$. This result is a particular case of the Hellmann-Feynman Theorem [33].

One can also calculate that

$$
\begin{aligned}
H^{A^*+tB} f(x) &= -\left(\frac{d}{dx} - i(A^*(x) + tB(x))\right)^2 f(x) \\
&= -\left(\frac{d}{dx} - i(A^*(x) + tB(x))\right)\left(f'(x) - i\big(A^*(x) + tB(x)\big)f(x)\right)
\end{aligned}
$$

69

$$= - \left(f''(x) - i\frac{d}{dx}\left(\left(A^*(x) + tB(x) \right) f(x) \right) - i\left(A^*(x) + tB(x) \right) f'(x) \right.$$
$$\left. - \left(A^*(x) + tB(x) \right)^2 f(x) \right)$$
$$= -f''(x) + i\left(A^{*\prime}(x) + tB'(x) \right) f(x) + 2i\left(A^*(x) + tB(x) \right) f'(x)$$
$$+ \left(A^{*2}(x) + 2tA^*(x)B(x) + t^2 B^2(x) \right) f(x)$$

for any function f in the domain. This means that

$$H^{A^*+tB} = -\frac{d^2}{dx^2} + i\left(A^{*\prime}(x) + tB'(x) \right) + 2i\left(A^*(x) + tB(x) \right)\frac{d}{dx}$$
$$+ \left(A^{*2}(x) + 2tA^*(x)B(x) + t^2 B^2(x) \right),$$

and therefore

$$\left. \frac{\partial H^{A^*+tB}}{\partial t} \right|_{t=0} = iB'(x) + 2iB(x)\frac{d}{dx} + 2A^*(x)B(x). \tag{IV.8}$$

For each $j = 1, 2, \ldots, k$, we choose $\boldsymbol{\delta\alpha} = (0, \ldots, \delta\alpha_j, \ldots, 0)$ and $B_j(x) \in \widetilde{H}^1(\mathbb{D}, \mathbb{R})$ that is compactly supported on edge e_j of $\mathbb{D}$ near c_j (i.e., $B_j(v) = 0$ for all vertices of $\mathbb{D}$) and satisfies

$$\int_{c_j^-}^{c_j^+} B_j(x)\, dx \mod 2\pi = \delta\alpha_j \neq 0.$$

Combining equations (IV.7) and (IV.8), one can see that

$$\left. \frac{\partial}{\partial t}\lambda_n(A^* + tB) \right|_{t=0} = \sum_{e \in E(\mathbb{D})} \int_e iB_j'(x)g(x)\overline{g(x)}\, dx + \int_e 2iB_j(x)g'(x)\overline{g(x)}\, dx$$
$$+ \int_e 2A^*(x)B_j(x)g(x)\overline{g(x)}\, dx$$
$$= \sum_{(u,v) \in E(\mathbb{D})} iB_j(x)|g(x)|^2\big|_u^v + \sum_{e \in E(\mathbb{D})} \left(-\int_e iB_j(x)\frac{d}{dx}(g(x)\overline{g(x)})\, dx \right.$$
$$\left. + \int_e \left(2iB_j(x)g'(x)\overline{g(x)} + 2A^*(x)B_j(x)g(x)\overline{g(x)} \right) dx \right)$$

$$= \sum_{(u,v)\in E(\mathbb{D})} iB_j(x)|g(x)|^2\big|_u^v + \sum_{e\in E(\mathbb{D})} \left(-\int_e iB_j(x)g(x)\overline{g'(x)}\,dx\right.$$
$$\left. + \int_e \left(iB_j(x)g'(x)\overline{g(x)} + 2A^*(x)B_j(x)g(x)\overline{g(x)}\right)dx\right)$$

using integration by parts where $E(\mathbb{D})$ is the edge set of $\mathbb{D}$. Since $B_j(x)$ is zero at all vertices of $\mathbb{D}$ and compactly supported on e_j, all of the boundary terms disappear and the sum is reduced to one term. Continuing, we calculate that

$$\frac{\partial}{\partial t}\lambda_n(A^* + tB)\bigg|_{t=0} = \int_{e_j} iB_j(x)g'(x)\overline{g(x)} - iB_j(x)g(x)\overline{g'(x)} + 2A^*(x)B_j(x)g(x)\overline{g(x)}$$

$$= \int_{e_j} B_j(x)\left(ig'(x)\overline{g(x)} - ig(x)\overline{g'(x)} + 2A^*(x)g(x)\overline{g(x)}\right)dx$$

$$= \int_{e_j} B_j(x)\left(\left(A^*(x)g(x) + ig'(x)\right)\overline{g(x)} + \left(A^*(x)\overline{g(x)} - i\overline{g'(x)}\right)g(x)\right)dx$$

$$= \int_{e_j} B_j(x)\left(\left(ig'(x) + A^*(x)g(x)\right)\overline{g(x)} + \overline{\left(ig'(x) + A^*(x)g(x)\right)\overline{g(x)}}\right)dx$$

$$= \int_{e_j} 2B_j(x)\mathrm{Re}\left(\left(ig'(x) + A^*(x)g(x)\right)\overline{g(x)}\right)dx$$

$$= \int_{e_j} 2B_j(x)\mathrm{Re}\left(i\left(g'(x) - iA^*(x)g(x)\right)\overline{g(x)}\right)dx$$

$$= -\int_{e_j} 2B_j(x)\mathrm{Im}\left(\left(g'(x) - iA^*(x)g(x)\right)\overline{g(x)}\right)dx = 0 \qquad \text{(IV.9)}$$

since $A(x)$ is real-valued. By construction and Remark 6, we know that $f = ge^{-i\xi}$, and hence one can observe that

$$\mathrm{Im}(f'(x)\overline{f(x)}) = \mathrm{Im}\left(\left(g'(x) - iA^*(x)g(x)\right)\overline{g(x)}\right). \qquad \text{(IV.10)}$$

Since f is an eigenfunction of the self-adjoint operator H^α, we know by Lemma II.2 that this value is equivalent to a Wronskian and therefore is constant on each edge of $\mathbb{W}'$. We will show that it is also constant on each edge of $\mathbb{D}$. We only need to check the edges that differ, which are the edges that contain a cut point. The edge e_j, which contains c_j, is formed by merging edges e_j^+ and e_j^- of $\mathbb{W}'$. By Lemma II.3, we know that the sum of

the Wronskians at c_j taken in the outgoing direction is zero, and therefore the Wronskian on edge e_j^+ is equal to the negative of the Wronskian on edge e_j^-. Since both Wronskians are measured outward from c_j, we need to flip the direction on edge e_j^- to measure the Wronskian on edge e_j of $\mathbb{D}$ (see Figure IV.5). As the Wronskian is a one-form that depends on direction, this flip ensures that the Wronskain (IV.10) is constant on each edge e_j of $\mathbb{D}$.

Since $\text{Im}\big((g'(x) - iA^*(x)g(x))\overline{g(x)}\big)$ is constant on e_j, we can pull it outside of the integral. We now continue from equation (IV.9) and observe that

$$\frac{\partial \lambda(\boldsymbol{\alpha}^* + t\boldsymbol{\delta\alpha})}{\partial t}\bigg|_{t=0} = \text{Im}\Big((g'(c_j) - iA^*(c_j)g(c_j))\overline{g(c_j)}\Big) \int_{e_j} B_j(x)\,\mathrm{d}x = 0. \qquad \text{(IV.11)}$$

Recall that we chose $B_j(x)$ such that $\int_{e_j} B_j(x)\,dx \mod 2\pi \neq 0$. This means that (IV.11) implies

$$\text{Im}\Big((g'(c_j) - iA^*(c_j)g(c_j))\overline{g(c_j)}\Big) = \text{Im}\Big(f'(c_j^+)\overline{f(c_j^+)}\Big) = 0,$$

which completes our proof.

$\square$

Proof of Theorem IV.2. Let $\widetilde{\gamma}_j = \frac{f'(c_j^+)}{f(c_j^+)}$ where f is an eigenfunction of $H^{\boldsymbol{\alpha}^*}$. We know by Lemma IV.4 that $\widetilde{\boldsymbol{\gamma}} \in \mathbb{R}^k$. We also know that f satisfies $-\frac{d^2}{dx^2} + q(x)$ on $\mathbb{W}'$ and the δ-type vertex conditions (IV.3) on all vertices that are not cut vertices. We will show that f also satisfies (IV.6) at $\{c_j^\pm\}$ and this will prove that f is also an eigenfunction of $H^{\widetilde{\gamma}}$. Since f satisfies (IV.5), we know that

$$\alpha_j^* = \frac{f(c_j^-)}{f(c_j^+)} = -\frac{f'(c_j^-)}{f'(c_j^+)},$$

and therefore

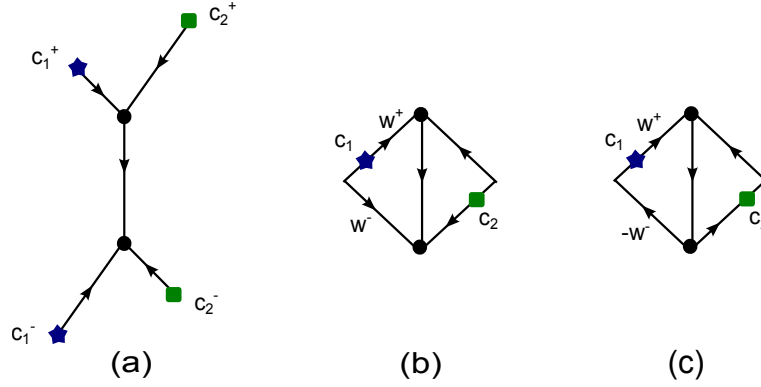$$\frac{f'(c_j^+)}{f(c_j^+)} = \widetilde{\gamma}_j = -\frac{f'(c_j^-)}{f(c_j^-)}.$$

Figure IV.5: Calculating the Wronskain on $\mathbb{D}$. (a) A fundamental domain $\mathbb{W}'$ based off of the infinite $\mathbb{Z}^2$-periodic graph from Figure IV.2 showing the direction of the Wronskian (which is taken to be positive in the direction outgoing from the vertices of interest). (b) The resulting graph $\mathbb{D}$ after merging the quasi-identical vertices. The letters above the edges $e_1^{\pm}$ denote the constant value of the Wronskian, and the arrows denote the direction of the Wronskian. (c) Flipping the direction of some "minor" edges to form the edges e_j that pass through c_j. Notice that the value of the Wronskian at c_1 is $w^+ = -w^-$.

It is now easy to see that

$$\widetilde{\gamma}_j f(c_j^+) = \frac{f'(c_j^+)}{f(c_j^+)} f(c_j^+) = f'(c_j^+) \quad \text{and} \quad -\widetilde{\gamma}_j f(c_j^-) = \frac{f'(c_j^-)}{f(c_j^-)} f(c_j^-) = f'(c_j^-),$$

and hence f satisfies (IV.6).

The self-adjoint operator $H^{\widetilde{\gamma}}$ is real-valued with real vertex conditions and it acts on functions defined on a quantum tree. Therefore its eigenfunctions can be chosen to be real-valued functions. However, since there exists j such that $\alpha_j^* \neq 0, \pm\pi$, f is not real-valued (since f satisfies (IV.5)). This implies that the real and imaginary parts of f are both eigenfunctions, meaning that the corresponding eigenvalue λ must be a degenerate eigenvalue of $H^{\widetilde{\gamma}}$.

$\square$

Corollary IV.2. *Suppose the infinite $\mathbb{Z}^k$-periodic quantum graph $\mathbb{G}$ has no magnetic potential and only one quasi-identified vertex pair in each direction, the chosen fundamental domain $\mathbb{W}$ is a tree, $\lambda_n(\boldsymbol{\alpha})$ has a critical point $\boldsymbol{\alpha}^*$ that is not at a symmetric point of the Brillouin zone (i.e., $\exists j$ such that $\alpha_j^* \neq 0, \pm\pi$), the eigenvalue $\lambda_n(\boldsymbol{\alpha}^*)$ is simple, and the corresponding eigenfunction f is not identically zero on edges attached to quasi-identified vertices. Then f is zero on at least one internal vertex of $\mathbb{W}$ that has degree three or higher.*

Proof. While $H^{\boldsymbol{\alpha}}$ and H^{γ} are formally defined on $\mathbb{W}'$, to simplify this proof, here we consider them to be defined on $\mathbb{W}$. The argument still holds since (1) $\mathbb{W}$ is a tree if and only if $\mathbb{W}'$ is a tree and (2) all vertices of degree three or higher are identical in both $\mathbb{W}$ and $\mathbb{W}'$ (only the quasi-identified leaves differ). When an eigenvalue of an operator that acts on functions whose domain is a quantum tree is multiple, there exists an internal vertex of degree three or higher at which all eigenfunctions from the eigenspace vanish (Corollary 3.1.9 of [15]; also see [14]). During the proof of Theorem IV.2, it was shown that f is an eigenfunction of $H^{\widetilde{\gamma}}$ corresponding to the multiple eigenvalue $\lambda_n(\boldsymbol{\alpha}^*)$ and hence, it must be zero on at least one internal vertex of $\mathbb{W}$ of degree three or higher.

$\square$

Recall that interior extrema of spectral bands are uncommon, as most occur on the boundary of the Brillouin zone. The main results of this chapter are Corollaries IV.1 and IV.2, which provide further details about what is happening at these interior (or nonsymmetric) critical points. In particular, we have shown that when the fundamental domain is a tree, the eigenfunction corresponding to a nonsymmetric critical point of $\lambda_n(\boldsymbol{\alpha})$ is zero on at least one internal vertex. We will build on this idea in Chapter V where we study touching points between dispersion surfaces. For particular cases, we will calculate where touching points occur by analyzing eigenfunctions that are zero on an internal vertex.

CHAPTER V

EXTREMAL AND DEGENERATE POINTS IN THE DISPERSION SURFACES OF

MANDARIN GRAPHS

In this chapter, we focus on extremal points of dispersion surfaces of mandarin graphs. We first state new results regarding where these extrema occur, as well as properties of the corresponding eigenfunctions, in the case of quantum d-mandarin graphs in Section V.1. Then in Section V.2, we use this information to calculate the location of touching points between dispersion surfaces for both discrete and quantum d-mandarin graphs.

V.1   Extremal Points of the Mandarin Graph

A *d-mandarin graph* is a graph consisting of two vertices and d edges. In this section, we focus on quantum d-mandarin graphs. Edge lengths are chosen such that the eigenvalues are simple and the corresponding eigenfunctions are nonzero on vertices [17, 36]; we call such a graph *generic*. The two vertices are assumed to have the Neumann conditions

$$\begin{cases} f(x) \text{ is continuous at v}, \\ \sum_{e \in E_v} \frac{df}{dx_e}(v) = 0 \qquad \text{for all vertices with } d_v > 1, \end{cases} \qquad (V.1)$$

where d_v is the degree of vertex v. In other words, these are the conditions (III.1) with $\chi_v = 0$. As defined, it is a multi-graph (as there are multiple edges connecting the same vertices), but one can easily turn it into a simple graph by adding vertices of degree 2 on the edges. At these new vertices, one may enforce the Neumann conditions above or the anti-Neumann conditions

$$f(v_-) = -f(v_+) \qquad \text{and} \qquad f'(v_-) = f'(v_+).$$

Notice that these conditions are equivalent to the conditions (III.3) of H^α at cut points with $\alpha_j = \pi$.

Suppose that f is the nth eigenfunction of the Schrödinger operator on Γ, and f has ϕ_n internal zeros. Recall that the *nodal surplus* is defined as $\sigma_n = \phi_n - (n-1)$, and the corresponding eigenvalue λ_n is *generic* if it is simple and f is nonzero on vertices. It has been shown that $0 \le \sigma_n \le \beta$ [7, 12]. The following strengthened version of this inequality for the case of a quantum d-mandarin graph is found in [9].

Theorem V.1. *Let Γ be a quantum mandarin graph with d edges, some of which have anti-Neumann conditions imposed in the middle. If the nth eigenvalue λ_n of the Schrödinger operator is generic and $n > 1$, then the nodal surplus satisfies*

$$1 \le \sigma_n \le \beta - 1 = d - 2.$$

We now consider the operator H^α on a (cut) finite quantum d-mandarin graph. The eigenvalue $\lambda_n(\boldsymbol{\alpha})$ can then be viewed as a function of $\boldsymbol{\alpha} = (\alpha_1, \alpha_2, \ldots, \alpha_\beta)$. It was shown in Section III.2.3.1 (specifically Theorem III.4) that $H^{\varsigma - \alpha}$ and $H^{\varsigma + \alpha}$ have the same spectrum for all

$$\varsigma \in \Sigma = \{(b_1, \ldots, b_\beta) : b_j \in \{-\pi, 0, \pi\}\}.$$

Henceforth, we refer to the vectors in Σ as *symmetric points* and all other vectors as *nonsymmetric points*. By Theorem III.2, we know that the Morse index of $\lambda_n(\boldsymbol{\alpha})$ at a symmetric point is equal to the nodal surplus of the corresponding eigenfunction. Combining this with Theorem V.1, we know that on a quantum mandarin graph

$$1 \le \text{MI}\big(\lambda_n(\varsigma)\big) \le \beta - 1$$

where $\text{MI}\big(\lambda_n(\varsigma)\big)$ is the Morse index of $\lambda_n(\boldsymbol{\alpha})$ at a symmetric point ς. This implies that no symmetric points are extrema of $\lambda_n(\boldsymbol{\alpha})$ (with the exception of $\lambda_1(\mathbf{0})$) since extrema
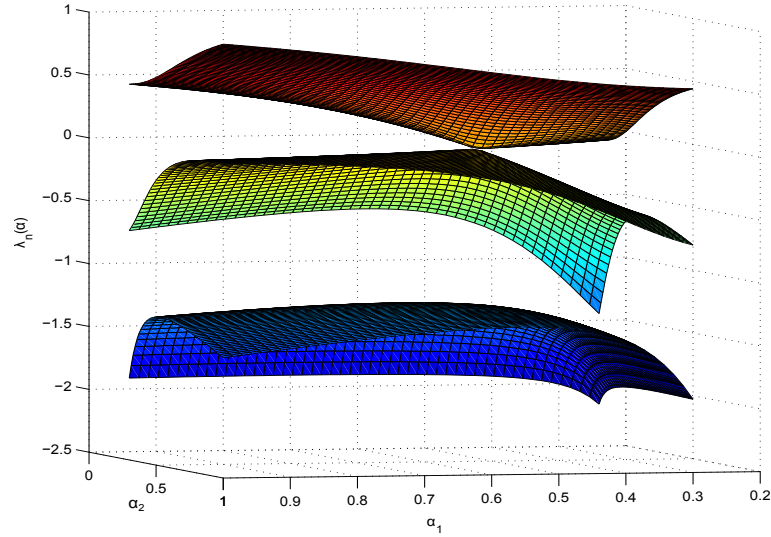
76

Figure V.1: An example of dispersion surfaces. Here $\boldsymbol{\alpha} = (\alpha_1, \alpha_2)$, and hence the surface is two-dimensional. Notice the Dirac conical touching point between the second and third surfaces. At that critical point, the second and third eigenvalues are identical.

of $\lambda_n(\boldsymbol{\alpha})$ have a Morse index of 0 or β. Consequently, the extrema of $\lambda_n(\boldsymbol{\alpha})$ cannot be achieved at the symmetric points (or on boundary) of the Brillouin zone $[-\pi, \pi]^\beta$, and hence must be located at nonsymmetric points (or in the interior).

A *dispersion surface* associated with $\lambda_n(\boldsymbol{\alpha})$ is the surface formed by plotting $\lambda_n(\boldsymbol{\alpha})$ for all $\boldsymbol{\alpha}$ in the Brillouin zone (see Figure V.1). The following theorem is the main result of this section and informs us that the dispersion surfaces have special properties at these nonsymmetric extrema points [9].

Theorem V.2. *For a generic quantum mandarin graph, all extrema of $\lambda_n(\boldsymbol{\alpha})$, apart from the minimum of λ_1, are achieved at points where two dispersion surfaces touch.*

Theorem IV.2 along with Corollary IV.2 led us to conclude that in the case of infinite periodic quantum graphs, a special role is played by eigenfunctions that have zeros on vertices. The related result below, which can be seen in [9], considers the same situation in the case of finite quantum graphs.

77

Theorem V.3. *Suppose Γ is a finite quantum graph with first Betti number β. If $\lambda_n(\boldsymbol{\alpha})$ has a nonsymmetric critical point $\boldsymbol{\alpha}^* = (\alpha_1^*, \alpha_2^* \ldots, \alpha_\beta^*)$ (i.e., there exists j such that $\alpha_j^* \neq 0, \pm\pi$), then the eigenfunction corresponding to $\lambda_n(\boldsymbol{\alpha}^*)$ is equal to zero at a vertex of the graph.*

As discussed previously, we know by Theorems V.1 and III.2 that extrema occur at nonsymmetric points of the Brillouin zone. We now know from Theorem V.3 that at nonsymmetric extrema of $\lambda(\boldsymbol{\alpha})$, the corresponding eigenfunction is zero at a vertex. Finally, Theorem V.2 informs us that all extrema occur where dispersion surfaces touch. Therefore, in the case of a quantum d-mandarin graph, wherever the dispersion surfaces touch, the corresponding eigenfunction must be zero on a vertex.

V.2   Calculating Degenerate Points of the Mandarin Graph

Here we construct two linearly independent eigenfunctions of the same operator, demonstrating that the dispersion surfaces of a mandarin graph do touch. In light of the discussion above, we know dispersion surfaces touch when the eigenfunction is zero on a vertex, so the linearly independent eigenfunctions we construct here will satisfy this property.

V.2.1   Discrete 3-Mandarin Graph

While the previous results of this chapter pertain to quantum graphs, we first provide an example with a discrete graph for simplicity.

We consider the discrete graph Γ in Figure V.2(a), which is a 3-mandarin graph with additional vertices. Observe that Γ is top/bottom symmetric; we restrict the magnetic potential $q : V \to \mathbb{R}$ so that it is also; namely, we set $q(v_4) = q(v_1)$. On Γ, we consider the
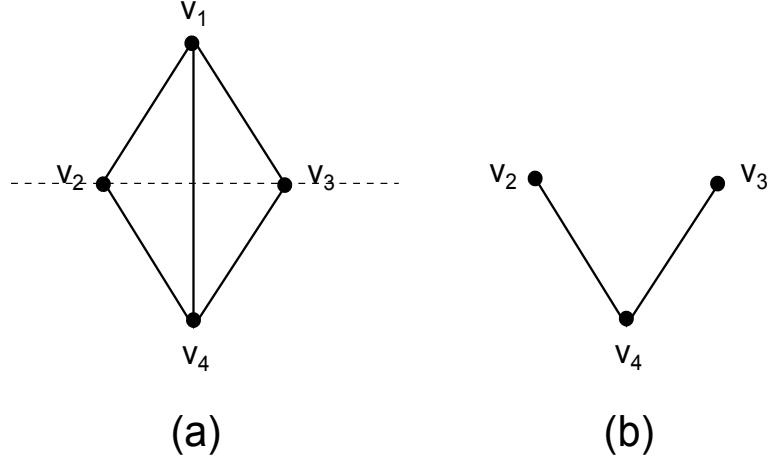
Figure V.2: Discrete 3-mandarin graph with additional vertices. (a) Notice that the graph Γ is top/bottom symmetric. (b) Resulting graph after Dirlichet conditions are enforced at v_1.

operator

$$
H^{\boldsymbol{\alpha}} = \begin{bmatrix}
q(v_1) & -e^{i\alpha_1} & -e^{i\alpha_2} & -1 \\
-e^{-i\alpha_1} & q(v_2) & 0 & -1 \\
-e^{-i\alpha_2} & 0 & q(v_3) & -1 \\
-1 & -1 & -1 & q(v_1)
\end{bmatrix},
$$

where $\boldsymbol{\alpha} \in [-\pi, \pi]^2$. Notice that this is precisely the operator $H^{\boldsymbol{\alpha}}$ that was defined in Lemma III.1 on the graph in Figure V.2(a). We will now look for $\boldsymbol{\alpha}^*$ at which the dispersion surfaces touch. We already noted that in the quantum graph case, the corresponding eigenfunction must be zero on a vertex. Therefore, while searching for touching points, we enforce Dirlichet conditions at vertex v_1, which is equivalent to considering the subgraph without v_1 and the adjacent edges (see Figure V.2(b)). On this subgraph, we consider the restricted operator

$$
H = \begin{bmatrix}
q(v_2) & 0 & -1 \\
0 & q(v_3) & -1 \\
-1 & -1 & q(v_1)
\end{bmatrix}.
$$

79

The matrix H is self-adjoint and has real entries. Therefore, the eigenvalues are real, and the eigenvectors can be chosen to have real entries. Suppose that

$$
f' = \begin{pmatrix} f(v_2) \\ f(v_3) \\ f(v_4) \end{pmatrix} \qquad \in \mathbb{R}^3
$$

is an eigenvector of H corresponding to the real eigenvalue λ. If

$$
f = \begin{pmatrix} 0 \\ f(v_2) \\ f(v_3) \\ f(v_4) \end{pmatrix}
$$

is an eigenvector of H^α, then we know by the first row of H^α that the entries of f' must satisfy

$$
e^{i\alpha_1} f(v_2) + e^{i\alpha_2} f(v_3) + f(v_4) = 0, \tag{V.2}
$$

which is equivalent to

$$
e^{i\alpha_2} = -\frac{f(v_4) + e^{i\alpha_1} f(v_2)}{f(v_3)}.
$$

Consequently, we know that f is an eigenvector of H^α only if

$$
1 = \left| \frac{f(v_4) + e^{i\alpha_1} f(v_2)}{f(v_3)} \right|^2 = \frac{(f(v_4) + f(v_2)\cos(\alpha_1))^2 + (f(v_2)\sin(\alpha_1))^2}{f^2(v_3)},
$$

or in other words,

$$
|\cos(\alpha_1)| = \left| \frac{f^2(v_3) - f^2(v_4) - f^2(v_2)}{2f(v_2)f(v_4)} \right| \le 1. \tag{V.3}
$$

Whether this is true or not for some eigenvector f' of H depends on the chosen electric

potential q; we will discuss this further in Subsection V.2.1.1. If (V.3) holds, we set

$$\alpha_1^* = \cos^{-1}\left(\frac{f^2(v_3) - f^2(v_4) - f^2(v_2)}{2f(v_2)f(v_4)}\right) \quad \text{and} \quad \alpha_2^* = -i\ln\left(-\frac{f(v_4) + e^{i\alpha_1}f(v_2)}{f(v_3)}\right).$$

We have constructed f to be an eigenvector of H^{α^*} corresponding to eigenvalue λ (since f' is an eigenvector of H corresponding to λ that satisfies (V.2)) so we know that

$$\begin{cases} e^{i\alpha_1^*}f(v_2) + e^{i\alpha_2^*}f(v_3) + f(v_4) & = 0, \\ q(v_2)f(v_2) - f(v_4) & = \lambda f(v_2), \\ q(v_3)f(v_3) - f(v_4) & = \lambda f(v_3), \\ -f(v_2) - f(v_3) + q(v_1)f(v_4) & = \lambda f(v_4). \end{cases} \tag{V.4}$$

Equation (V.2) implies that

$$\overline{e^{i\alpha_1^*}f(v_2) + e^{i\alpha_2^*}f(v_3) + f(v_4)} = e^{-i\alpha_1}f(v_2) + e^{-i\alpha_2}f(v_3) + f(v_4) = 0.$$

Using this and (V.4), one can easily show that

$$H^{\alpha^*}\begin{pmatrix} f(v_4) \\ e^{-i\alpha_1^*}f(v_2) \\ e^{-i\alpha_2^*}f(v_3) \\ 0 \end{pmatrix} = \begin{pmatrix} q(v_1)f(v_4) - e^{i\alpha_1^*}(e^{-i\alpha_1^*}f(v_2)) - e^{i\alpha_2^*}(e^{-i\alpha_2^*}f(v_3)) \\ -e^{-i\alpha_1^*}f(v_4) + q(v_2)e^{-i\alpha_1^*}f(v_2) \\ -e^{-i\alpha_2^*}f(v_4) + q(v_3)e^{-i\alpha_2^*}f(v_3) \\ -\left(f(v_4) + e^{-i\alpha_1^*}f(v_2) + e^{-i\alpha_2^*}f(v_3)\right) \end{pmatrix}$$

$$= \begin{pmatrix} -f(v_2) - f(v_3) + q(v_1)f(v_4) \\ e^{-i\alpha_1^*}\left(q(v_2)f(v_2) - f(v_4)\right) \\ e^{-i\alpha_2^*}\left(q(v_3)f(v_3) - f(v_4)\right) \\ -\left(f(v_4) + e^{-i\alpha_1^*}f(v_2) + e^{-i\alpha_2^*}f(v_3)\right) \end{pmatrix} = \lambda\begin{pmatrix} f(v_4) \\ e^{-i\alpha_1^*}f(v_2) \\ e^{-i\alpha_2^*}f(v_3) \\ 0 \end{pmatrix}.$$

81

Hence,

$$\tilde{f} = \begin{pmatrix} f(v_4) \\ e^{-i\alpha_1^*} f(v_2) \\ e^{-i\alpha_2^*} f(v_3) \\ 0 \end{pmatrix}$$

is also an eigenvector of H^{α^*} corresponding to the same eigenvalue λ. Assuming we chose f' such that $f(v_4) \neq 0$ (see the Subsection V.2.1.1 for details), we have two linearly independent eigenvectors, which implies that the dispersion surfaces touch at α^*.

V.2.1.1   Existence of Eigenvectors

We now consider the question: do such eigenvectors exist? In other words, does there exist f' that satisfies (V.3) and is nonzero at v_4 so we obtain another linearly independent eigenvector by "flipping" it? Here we will demonstrate with a specific example that these eigenvectors may exist and that their existence depends on the electric potential q.

We consider the same graph (Figure V.2) and operator H^{α} above, but now for simplicity we enforce the condition that $q(v_2) = q(v_3)$. We will analyze eigenvectors f' of

$$H = \begin{bmatrix} q(v_2) & 0 & -1 \\ 0 & q(v_2) & -1 \\ -1 & -1 & q(v_1) \end{bmatrix}.$$

The eigenvalues are

$$\begin{cases} \lambda_1 = q(v_2), \\ \lambda_2 = \frac{q(v_1)+q(v_2)+\sqrt{\left(q(v_1)-q(v_2)\right)^2+8}}{2}, \quad \text{and} \\ \lambda_3 = \frac{q(v_1)+q(v_2)-\sqrt{\left(q(v_1)-q(v_2)\right)^2+8}}{2} \end{cases}$$

with the corresponding eigenvectors

$$f_1' = \begin{pmatrix} -1 \\ 1 \\ 0 \end{pmatrix}, \ f_2' = \begin{pmatrix} (\lambda_3 - q(v_2))/2 \\ (\lambda_3 - q(v_2))/2 \\ 1 \end{pmatrix}, \ \text{and } f_3' = \begin{pmatrix} (\lambda_2 - q(v_2))/2 \\ (\lambda_2 - q(v_2))/2 \\ 1 \end{pmatrix}.$$

The first eigenvector does not solve our problem since $f_1'(v_4) = 0$, and hence "flipping" will not result in another eigenvector that is linearly independent. Instead we will concentrate on the third eigenvector, which is nonzero at v_4. The same procedure works for the second eigenvector, but the calculations are more complicated so we choose the third one for simplicity. It remains to show that f_3' satisfy (V.3). Observe that since $f_3'(v_2) = f_3'(v_3)$, (V.3) simplifies to

$$\left| \frac{-f(v_4)}{2f(v_2)} \right| \leq 1,$$

which is equivalent to

$$|f(v_4)| \leq 2|f(v_2)|. \tag{V.5}$$

Inputting the values of f_3', (V.5) becomes

$$1 \leq |\lambda_2 - q(v_2)| = \left| \frac{q(v_1) - q(v_2) + \sqrt{\left(q(v_1) - q(v_2)\right)^2 + 8}}{2} \right|.$$

It is easy to see that this inequality holds for many values of $q(v_1)$ and $q(v_2)$; in particular, it clearly holds whenever $q(v_1) - q(v_2) \geq 0$.

V.2.2   Quantum 3-Mandarin Graph

As explained previously, one can conclude from the results of Section V.1 that on a d-mandarin quantum graph, all extrema occur at nonsymmetric points of the Brillouin zone, the corresponding eigenfunctions are zero on an internal vertex, and the dispersion surfaces touch at these extrema. Below we calculate touching points by analyzing eigenfunctions
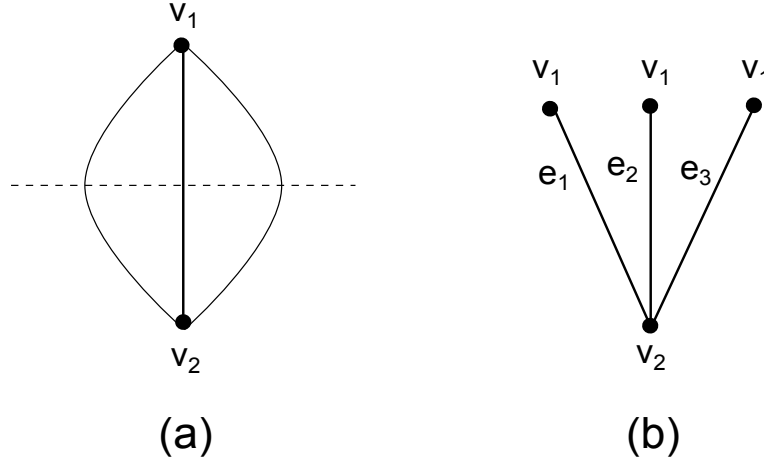
83

Figure V.3: Quantum 3-mandarin graph. (a) Notice that the graph is top/bottom symmetric. (b) The resulting graph after Dirichlet conditions are enforced at v_1 with the edges labeled e_j.

that are zero on an internal vertex.

In particular, we consider the 3-mandarin quantum graph in Figure V.3(a), and assume there are Neumann conditions at the vertices. Consider the operator H^α; recall that we define this operator on functions whose domain is a tree. In Chapter IV, we saw that it does not matter where we cut the cycles. In this case, we will cut both of them at v_1; this can be done formally by taking limits. The result is a star graph (Figure V.3(b)) with the following conditions at v_1:

$$\begin{cases} f_1(v_1) = f_2(v_1) = f_3(v_1) \\ e^{i\alpha_1} f_1'(v_1) + e^{i\alpha_2} f_2'(v_1) + f_3'(v_1) = 0 \end{cases} \quad \text{(V.6)}$$

where f_j denotes the function f on edge e_j. Now we can formally define H^α on the star graph as the differential operator $-\frac{d^2}{dx^2} + q(x)$ on each edge, conditions (V.6) at v_1 and regular Neumann conditions (V.1) at v_2. Since eigenfunctions corresponding to touching points of the dispersion surfaces are zero on a vertex, we also enforce Dirichlet conditions at v_1, which is equivalent to setting the first line of equations of (V.6) equal to zero. If f

is an eigenfunction of $H^{\boldsymbol{\alpha}}$ with these conditions, it must satisfy

$$e^{i\alpha_2} = -\frac{e^{i\alpha_1}f_1'(v_1) + f_3'(v_1)}{f_2'(v_1)}$$

or in other words

$$1 = \left|\frac{e^{i\alpha_1}f_1'(v_1) + f_3'(v_1)}{f_2'(v_1)}\right|^2 = \frac{|f_1'(v_1)|^2 + |f_3'(v_1)|^2 + 2\cos(\alpha_1)f_1'(v_1)f_3'(v_3)}{|f_2'(v_1)|^2}. \qquad \text{(V.7)}$$

One can see that (V.7) has a solution if and only if

$$|\cos(\alpha_1)| = \left|\frac{|f_2'(v_1)|^2 - |f_1'(v_1)|^2 - |f_3'(v_1)|^2}{2f_1'(v_1)f_3'(v_1)}\right| \leq 1. \qquad \text{(V.8)}$$

As in the discrete case, whether this condition holds or not depends on the electric potential $q(x)$. When (V.8) does hold, we define

$$\alpha_1^* = \cos^{-1}\left(\frac{|f_2'(v_1)|^2 - |f_1'(v_1)|^2 - |f_3'(v_1)|^2}{2f_1'(v_1)f_3'(v_1)}\right) \quad \text{and} \quad \alpha_2^* = -i\ln\left(-\frac{e^{i\alpha_1}f_1'(v_1) + f_3'(v_1)}{f_2'(v_1)}\right).$$

By construction, f is an eigenfunction of $H^{\boldsymbol{\alpha}^*}$.

Suppose that f is an eigenfunction of $H^{\boldsymbol{\alpha}^*}$ that corresponds to the eigenvalue λ and is nonzero at v_2. Let κ denote the standard vertical reflection operator and define $\hat{f} := \kappa f$. It is easy to observe that $\hat{f}$ is an eigenfunction of $H^{-\boldsymbol{\alpha}^*}$ corresponding to λ; the sign of $\boldsymbol{\alpha}^*$ changes since the function (and hence, magnetic flux, which is a one-form) is "flipped". Finally, $\overline{\hat{f}}$ is an eigenfunction of $H^{\boldsymbol{\alpha}^*}$ corresponding to λ. However, it is a different function from f (since f is zero at v_1 and $\overline{\hat{f}}$ is zero at v_2) which means that λ is a degenerate eigenvalue.

CHAPTER VI

CONCLUSIONS

In Chapter III, we analyzed the stability of eigenvalues of the magnetic Schrödinger oper-
ator as the magnetic potential was varied. In particular, we showed that the Morse index
at symmetric points is equal to the nodal surplus of the corresponding eigenfunction in the
case of quantum graphs. This result had already been established on discrete graphs in [13]
and on a circle quantum graph in [26]. Those proofs, however, could not be used directly
in the general quantum graph case; a completely new approach was needed to analyze the
intermediate operator H^γ, which can be seen in Section III.2.2.

It was first shown in [7] that the set of equipartitions can be parameterized using the
β parameters $\boldsymbol{\gamma} = (\gamma_1, \gamma_2, \ldots, \gamma_\beta)$ and the operator H^γ. In particular, the zeros of the
$(m+1)^{th}$ eigenfunction of H^γ define an m-equipartition. The energy functional Λ is defined
as the maximal first eigenvalue over all partition subgraphs. The main result of [7] states
that the zeros of an eigenfunction are a critical point of Λ over the set of equipartitions
with Morse index equal to the nodal deficiency. Theorem III.3 allowed us to strengthen
this result. Namely, we were able to remove the a priori condition of non-degeneracy, and
we extended the theorem to the case in which removing all zeros of the eigenfunction from
the graph does not break all the cycles.

The main result of Chapter III is Theorem III.2, which demonstrates a relationship between
the stability of an eigenvalue and the nodal surplus of the corresponding eigenfunction. This
result itself is interesting, as there is little intuition as to why these things are related. The
result, however, has already proven fruitful in studying other problems related to nodal
counts. Band used Theorem III.2 to partially solve the inverse nodal count problem [6].
Namely, he used it to prove that either a quantum graph is a tree and the nodal surplus

is always zero or the quantum graph is not a tree and the nodal surplus is nonzero for infinitely many eigenfunctions; see Section III.4 and Theorem III.7 for details.

In Chapter IV, we analyzed critical points of the dispersion relation of discrete and quantum infinite periodic graphs. Using Floquet-Bloch theory, we studied the spectrum of the Schrödinger operator on infinite periodic graphs by analyzing eigenvalues of $H^{\boldsymbol{\alpha}}$ on a fundamental domain. It turned out that critical points of $\lambda_n(\boldsymbol{\alpha})$ corresponded to degenerate eigenvalues of $H^{\boldsymbol{\gamma}}$ (which also acts on functions whose domain is the finite fundamental domain). This in turn led us to conclude the main result of this chapter: if the fundamental domain is a tree, any critical point of $\lambda_n(\boldsymbol{\alpha})$ that occurs inside the Brillouin zone corresponds to an eigenfunction that is zero on at least one internal vertex.

This idea was pursued further in Chapter V where we analyzed extrema of eigenvalues of the magnetic Schrödinger operator on d-mandarin graphs. It was proven in [9] that extrema of the mandarin graph occur inside the Brillouin zone, these extrema occur where dispersion surfaces touch, and the corresponding eigenfunction at an interior extremal point is zero on at least one vertex. In Section V.2, we used this information to explicitly calculate where touching points occur. Specifically, we analyzed eigenfunctions of a 3-mandarin graph (in both the discrete and quantum case) that are zero on a vertex. We then found necessary conditions the eigenfunction must satisfy in order for it to correspond to an extremal point. When these conditions were satisfied, we calculated extremal points $\boldsymbol{\alpha}^*$ and two corresponding linearly independent eigenfunctions, which demonstrates that the dispersion surfaces do in fact touch at the extremal point.

REFERENCES

[1] M. AIZENMAN, R. SIMS, AND S. WARZEL, *Absolutely continuous spectra of quantum tree graphs with weak disorder*, Comm. Math. Phys., 264 (2006), pp. 371–389.

[2] M. AIZENMAN AND S. WARZEL, *Persistence under weak disorder of AC spectra of quasi-periodic Schrödinger operators on trees graphs*, Mosc. Math. J., 5 (2005), pp. 499–506.

[3] S. ALEXANDER, *Superconductivity of networks. A percolation approach to the effects of disorder*, Phys. Rev. B, 27 (1983), pp. 1541–1557.

[4] C. AMOVILLI, F. LEYS, AND N. MARCH, *Electronic energy spectrum of two-dimensional solids and a chain of C atoms from a quantum network model*, J. Math. Chem., 36 (2004), pp. 93–112.

[5] P. ANDERSON, *New method for scaling theory of localization. II. Multichannel theory of a "wire" and possible extension to higher dimensionality*, Phys. Rev. B, 23 (1981), pp. 4828–4836.

[6] R. BAND, *Nodal count $\{0, 1, 2, 3, \ldots\}$ implies the graph is a tree*, Phi. Trans. R. Soc. A, 372 (2014), pp. 2012.0504, 24.

[7] R. BAND, G. BERKOLAIKO, H. RAZ, AND U. SMILANSKY, *The number of nodal domains on quantum graphs as a stability index of graph partitions*, Comm. Math. Phys., 311 (2012), pp. 815–838.

[8] R. BAND, G. BERKOLAIKO, AND U. SMILANSKY, *Dynamics of nodal points and the nodal count on a family of quantum graphs*, Ann. Henri Poincaré, 13 (2012), pp. 145–184.

[9] R. BAND, G. BERKOLAIKO, AND T. WEYAND, *Anomalous nodal domain count and singularities in the dispersion relation of honeycomb graphs*, (2014). In preparation.

[10] R. BAND, I. OREN, AND U. SMILANSKY, *Nodal domains on graphs—how to count them and why?*, in Analysis on Graphs and Its Applications, vol. 77 of Proceedings of

Symposia in Pure Mathematics, Amer. Math. Soc., Providence, RI, 2008, pp. 5–27.

[11] R. BAND, O. PARZANCHEVSKI, AND G. BEN-SHACH, *The isospectral fruits of representation theory: quantum graphs and drums*, J. Phys. A, 42 (2009), pp. 175202, 42.

[12] G. BERKOLAIKO, *A lower bound for nodal count on discrete and metric graphs*, Comm. Math. Phys., 278 (2008), pp. 803–819.

[13] G. BERKOLAIKO, *Nodal count of graph eigenfunctions via magnetic perturbation*, Anal. PDE, 6 (2013), pp. 1213–1233.

[14] G. BERKOLAIKO AND P. KUCHMENT, *Dependence of the spectrum of a quantum graph on vertex conditions and edge lengths*, in Spectral Geometry, vol. 84 of Proceedings of Symposia in Pure Mathematics, Amer. Math. Soc., Providence, RI, 2012, pp. 117–137.

[15] G. BERKOLAIKO AND P. KUCHMENT, *Introduction to quantum graphs*, vol. 186 of Mathematical Surveys and Monographs, Amer. Math. Soc., Providence, RI, 2013.

[16] G. BERKOLAIKO, P. KUCHMENT, AND U. SMILANSKY, *Critical partitions and nodal deficiency of billiard eigenfunctions*, Geom. Funct. Anal., 22 (2012), pp. 1517–1540.

[17] G. BERKOLAIKO AND W. LIU, *Genericity of eigenpairs of a quantum graph*, (2014). In preparation.

[18] G. BERKOLAIKO, H. RAZ, AND U. SMILANSKY, *Stability of nodal structures in graph eigenfunctions and its relation to the nodal domain count*, J. Phys. A, 45 (2012), pp. 165203, 16.

[19] G. BERKOLAIKO AND T. WEYAND, *Stability of eigenvalues of quantum graphs with respect to magnetic perturbation and the nodal count of the eigenfunctions*, Phi. Trans. R. Soc. A, 372 (2014), pp. 2012.0522, 24.

[20] T. BIYIKOĞLU, *A discrete nodal domain theorem for trees*, Linear Algebra Appl., 360 (2003), pp. 197–205.

[21] G. BLUM, S. GNUTZMANN, AND U. SMILANSKY, *Nodal domains statistics — a criterion for quantum chaos*, Phys. Rev. Lett., 88 (2002), pp. 114101, 4.

[22] E. BOGOMOLNY AND C. SCHMIT, *Percolation model for nodal domains of chaotic*

wave functions, Phys. Rev. Lett., 88 (2002), pp. 114102, 4.

[23] E. BOGOMOLNY AND C. SCHMIT, *Random wavefunctions and percolation*, J. Phys. A, 40 (2007), pp. 14033–14043.

[24] B. BOLLOBÁS, *Modern graph theory*, vol. 184 of Graduate Texts in Mathematics, Springer-Verlag, New York, NY, 1998.

[25] J. CHALKER AND P. CODDINGTON, *Percolation, quantum tunnelling and the integer hall effect*, J. Phys. C, 21 (1988), pp. 2665–2679.

[26] Y. COLIN DE VERDIÈRE, *Magnetic interpretation of the nodal defect on graphs.* Preprint available at `arXiv:1201.1110v2 [math-ph]`, 2012.

[27] R. COURANT AND D. HILBERT, *Methods of mathematical physics. Vol. I*, Interscience Publishers, Inc., New York, NY, 1953.

[28] B. DAVIES, G. L. GLADWELL, J. LEYDOLD, AND P. STADLER, *Discrete nodal domain theorems*, Linear Algebra Appl., 336 (2001), pp. 51–60.

[29] N.T. DO AND P. KUCHMENT, *Quantum graph spectra of a graphyne structure*, NanoMMTA, 2 (2013), pp. 107–123.

[30] P. EXNER, P. KUCHMENT, AND B. WINN, *On the location of spectral edges in $\mathbb{Z}$-periodic media*, J. Phys. A, 43 (2010), pp. 474022, 8.

[31] P. EXNER AND O. POST, *Convergence of spectra of graph-like thin manifolds*, J. Geom. Phys., 54 (2005), pp. 77–115.

[32] C. FEFFERMAN AND M. WEINSTEIN, *Honeycomb lattice potentials and Dirac points*, J. Amer. Math. Soc., 25 (2012), pp. 1169–1220.

[33] R. FEYNMAN, *Forces in molecules*, Phys. Rev., 56 (1939), pp. 340–343.

[34] M. FIEDLER, *Eigenvectors of acyclic matrices*, Czechoslovak Math. J., 25 (1975), pp. 607–618.

[35] A. FIGOTIN AND P. KUCHMENT, *Spectral properties of classical waves in high-contrast periodic media*, SIAM J. Appl. Math., 58 (1998), pp. 683–702.

[36] L. FRIEDLANDER, *Genericity of simple eigenvalues for a metric graph*, Israel J. Math., 146 (2005), pp. 149–156.

[37] S. Gnutzmann, P. Karageorge, and U. Smilansky, *Can one count the shape of a drum?*, Phys. Rev. Lett., 97 (2006), pp. 090201, 4.

[38] S. Gnutzmann and U Smilansky, *Quantum graphs: Applications to quantum chaos and universal spectral statistics*, Adv. Phys., 55 (2006), pp. 527–625.

[39] S. Gnutzmann, U. Smilansky, and N. Sondergaard, *Resolving isospectral 'drums' by counting nodal domains*, J. Phys. A, 38 (2005), pp. 8921–8933.

[40] S. Gnutzmann, U. Smilansky, and J. Weber, *Nodal counting on quantum graphs*, Waves Random Media, 14 (2004), pp. S61–S73.

[41] N. Goldman and P. Gaspard, *Quantum graphs and the integer quantum hall effect*, Phys. Rev. B, 77 (2008), pp. 024302, 10.

[42] P. Harper, *Single band motion of conduction electrons in a uniform magnetic field*, Proc. Phys. Soc. A, 68 (1955), pp. 874–878.

[43] J. Harrison, P. Kuchment, A. Sobolev, and B. Winn, *On occurrence of spectral edges for periodic operators inside the Brillouin zone*, J. Phys. A, 40 (2007), pp. 7597–7618.

[44] B. Helffer, T. Hoffmann-Ostenhof, and S. Terracini, *Nodal domains and spectral minimal partitions*, Ann. Inst. H. Poincaré Anal. Non Linéaire, 26 (2009), pp. 101–138.

[45] H. Hezari and Z. Wang, *Lower bounds for volumes of nodal sets: an improvement of a result of Sogge-Zelditch*, in Spectral Geometry, vol. 84 of Proceedings of Symposia in Pure Mathematics, Amer. Math. Soc., Providence, RI, 2012, pp. 229–235.

[46] P. Hislop and O. Post, *Anderson localization for radial tree-like quantum graphs*, Waves Random Complex Media, 19 (2009), pp. 216–261.

[47] D. Hofstadter, *Energy levels and wave functions of Bloch electrons in rational and irrational magnetic fields*, Phys. Rev. B, 14 (1976), pp. 2239–2249.

[48] O. Hul, S. Bauch, P. Pakoński, N. Savytskyy, K. Życzkowski, and L. Sirko, *Experimental simulation of quantum graphs by microwave networks*, Phys. Rev. E, 69 (2004), pp. 056205, 7.

[49] O. Hul, M. Ławniczak, S. Bauch, and L. Sirko, *Simulation of quantum graphs by microwave networks*, in Analysis on Graphs and Its Applications, vol. 77 of Proceedings of Symposia in Pure Mathematics, Amer. Math. Soc., Providence, RI, 2008, pp. 595–615.

[50] A. Iantchenko and E. Korotyaev, *Schrödinger operator on the zigzag half-nanotube in magnetic field*, Math. Model. Nat. Phenom., 5 (2010), pp. 175–197.

[51] M. Kac, *Can one hear the shape of a drum?*, Amer. Math. Monthly, 73 (1966), pp. 1–23.

[52] T. Kato, *Perturbation theory for linear operators*, Springer-Verlag, Berlin, Germany, 2nd ed., 1976.

[53] B. Kim and H. Choi, *Graphyne: Hexagonal network of carbon with versatile Dirac cones*, Phys. Rev. B, 86 (2012), pp. 115435, 5.

[54] A. Klein, *Absolutely continuous spectrum in the Anderson model on the Bethe lattice*, Math. Res. Lett., 1 (1994), pp. 399–407.

[55] A. Klein, *Extended states in the Anderson model on the Bethe lattice*, Adv. Math., 133 (1998), pp. 163–184.

[56] R. Klesse and M. Metzler, *Spectral compressibility at the metal-insulator transition of the quantum Hall effect*, Phys. Rev. Lett., 79 (1997), pp. 721–724.

[57] F. Klopp and K. Pankrashkin, *Localization on quantum graphs with random vertex couplings*, J. Stat. Phys., 131 (2008), pp. 651–673.

[58] F. Klopp and K. Pankrashkin, *Localization on quantum graphs with random edge lengths*, Lett. Math. Phys., 87 (2009), pp. 99–114.

[59] A. Kolovsky and G. Mantica, *Driven Harper model*, Phys. Rev. B, 86 (2012), pp. 054306, 4.

[60] E. Korotyaev and A. Kutsenko, *Zigzag nanoribbons in external electric and magnetic fields*, Int. J. Comput. Sci. Math., 3 (2010), pp. 168–191.

[61] E. Korotyaev and I. Lobanov, *Schrödinger operators on zigzag nanotubes*, Ann. Henri Poincaré, 8 (2007), pp. 1151–1176.

[62] V. KOSTRYKIN AND R. SCHRADER, *Quantum wires with magnetic fluxes*, Comm. Math. Phys., 237 (2003), pp. 161–179.

[63] T. KOTTOS AND U. SMILANSKY, *Quantum chaos on graphs*, Phys. Rev. Lett., 79 (1997), pp. 4794–4797.

[64] T. KOTTOS AND U. SMILANSKY, *Periodic orbit theory and spectral statistics for quantum graphs*, Ann. Phys., 274 (1999), pp. 76–124.

[65] Y. KRAUS AND O. ZILBERBERG, *Topological equivalence between the Fibonacci quasicrystal and the Harper model*, Phys. Rev. Lett., (2012), pp. 116404, 5.

[66] P. KUCHMENT, *Floquet theory for partial differential equations*, vol. 60 of Operator Theory: Advances and Applications, Birkhäuser Verlag, Basel, Switzerland, 1993.

[67] P. KUCHMENT, *The mathematics of photonic crystals*, in Mathematical Modeling in Optical Science, vol. 22 of Frontiers in Applied Mathematics, SIAM, Philadelphia, PA, 2001, pp. 207–272.

[68] P. KUCHMENT, *Graph models for waves in thin structures*, Waves Random Media, 12 (2002), pp. R1–R24.

[69] P. KUCHMENT, *Quantum graphs: an introduction and a brief survey*, in Analysis on Graphs and Its Applications, vol. 77 of Proceedings of Symposia in Pure Mathematics, Amer. Math. Soc., Providence, RI, 2008, pp. 291–312.

[70] P. KUCHMENT AND L. KUNYANSKY, *Differential operators on graphs and photonic crystals*, Adv. Comput. Math., 16 (2002), pp. 263–290.

[71] P. KUCHMENT AND O. POST, *On the spectra of carbon nano-structures*, Comm. Math. Phys., 275 (2007), pp. 805–826.

[72] P. KUCHMENT AND H. ZENG, *Convergence of spectra of mesoscopic systems collapsing onto a graph*, J. Math. Anal. Appl., 258 (2001), pp. 671–700.

[73] M. ŁAWNICZAK, S. BAUCH, O. HUL, AND L. SIRKO, *Experimental investigation of properties of hexagon networks with and without time reversal symmetry*, Phys. Scr., 2009 (2009), pp. 014050, 5.

[74] M. ŁAWNICZAK, O. HUL, S. BAUCH, AND L. SIRKO, *Experimental simulation of*

quantum graphs by microwave networks – closed and open systems, CMSIM, 1 (2011), pp. 105–118.

[75] F. Nazarov and M. Sodin, *On the number of nodal domains of random spherical harmonics*, Amer. J. Math., 131 (2009), pp. 1337–1357.

[76] K. Novoselov, *Nobel lecture: Graphene: Materials in the flatland*, Rev. Mod. Phys., 83 (2011), pp. 837–849.

[77] K. Pankrashkin, *Localization effects in a periodic quantum graph with magnetic field and spin-orbit interaction*, J. Math. Phys., 47 (2006), pp. 112105, 17.

[78] K. Pankrashkin, *Localization in a quasiperiodic model on quantum graphs*, in Analysis on Graphs and Its Applications, vol. 77 of Proceedings of Symposia in Pure Mathematics, Amer. Math. Soc., Providence, RI, 2008, pp. 459–467.

[79] O. Parzanchevski and R. Band, *Linear representations and isospectrality with boundary conditions*, J. Geom. Anal., 20 (2010), pp. 439–471.

[80] L. Pauling, *The diamagnetic anisotropy of aromatic molecules*, J. Chem. Phys., 4 (1936), pp. 673–677.

[81] Å. Pleijel, *Remarks on Courant's nodal line theorem*, Comm. Pure Appl. Math., 9 (1956), pp. 543–550.

[82] Y. Pokornyĭ, V. Pryadiev, and A. Al′-Obeĭd, *On the oscillation of the spectrum of a boundary value problem on a graph*, Mat. Zametki, 60 (1996), pp. 468–470.

[83] O. Post, *Branched quantum wave guides with Dirichlet boundary conditions: the decoupling case*, J. Phys. A, 38 (2005), pp. 4917–4931.

[84] M. Reed and B. Simon, *Methods of modern mathematical physics. IV. Analysis of operators*, Academic Press, New York, NY, 1978.

[85] J. Rubinstein and M. Schatzman, *Asymptotics for thin superconducting rings*, J. Math. Pures Appl., 77 (1998), pp. 801–820.

[86] R. Rueckriemen, *Recovering quantum graphs from their Bloch spectrum*. To appear in the Annales de l′Institut Fourier; preprint available at `arXiv:1101.6002`, 2011.

[87] K. Ruedenberg and C. Scherr, *Free-electron network model for conjugated sys-*

tems. I. Theory, J. Chem. Phys., 21 (1953), pp. 1565–1581.

[88] R. Saito, G. Dresselhaus, and M. Dresselhaus, *Physical properties of carbon nanotubes*, Imperial College Press, London, England, 1998.

[89] Y. Saito, *The limiting equation for Neumann Laplacians on shrinking domains*, Electron. J. Differential Equations, 2000 (2000), pp. 1–25.

[90] P. Schapotschnikow, *Eigenvalue and nodal properties on quantum graph trees*, Waves Random Complex Media, 16 (2006), pp. 167–178.

[91] C. Sogge and S. Zelditch, *Lower bounds on the Hausdorff measure of nodal sets*, Math. Res. Lett., 18 (2011), pp. 25–37.

[92] D. Spring, *On the second derivative test for constrained local extrema*, Amer. Math. Monthly, 92 (1985), pp. 631–643.

[93] C. Sturm, *Mémoire sur une classe d'équations à différences partielles*, J. Math. Pures Appl., 1 (1836), pp. 373–444.

[94] T. Sunada, *Discrete geometric analysis*, in Analysis on Graphs and Its Applications, vol. 77 of Proceedings of Symposia in Pure Mathematics, Amer. Math. Soc., Providence, RI, 2008, pp. 51–83.

[95] E. van Dam and W. Haemers, *Which graphs are determined by their spectrum?*, Linear Algebra Appl., 373 (2003), pp. 241–272.

APPENDIX

GLOSSARY

*Words that appear in a definition in italics are defined elsewhere in this glossary.

Brillouin Zone – The set of all points in $[-\pi, \pi]^k$ for an infinite $\mathbb{Z}^k$-periodic graph, or set of all points in $[-\pi, \pi]^\beta$ when referring to the operator $H^{\boldsymbol{\alpha}}$ acting on a finite graph where β is the *first Betti number* of the original (uncut) graph.

Compact Graph – A *metric graph* that has a finite number of vertices and edges and each edge has finite length.

Cycle – A *path* on a graph that begins and ends at the same vertex.

Degenerate Critical Point – A critical point of a function at which the corresponding *Hessian matrix* is singular, or in other words, a point at which all partial first derivatives and the determinant of the *Hessian matrix* are zero.

Degenerate Eigenvalue – An eigenvalue with multiplicity greater than one. In this case, there exists more than one linearly independent eigenfunction corresponding to the same eigenvalue.

Degree – The number of edges attached to a vertex.

Discrete Graph – A graph completely defined by a set of vertices V and a set of edges E connecting the vertices. Functions are defined only on vertices. See page 8 for details.

Dispersion Relation – The multi-valued function that maps $\boldsymbol{\alpha}$ to the spectrum of the Schrödinger operator on an infinite periodic graph. See pages 47–48 for details.

Dispersion Surface – Graph of $\lambda_n(\boldsymbol{\alpha})$ for all $\boldsymbol{\alpha}$ in the *Brillouin zone*. This can also be viewed as the graph of the nth *spectral band*. See page 63 for an example.

First Betti Number – The rank of the fundamental group of a graph. It is also equal to the number of edges that must be broken in order to form a *tree* with the same number of connected components as the original graph. We denote this number by β and it is equal to

$$\beta = |E| - |V| + k$$

where $|E|$ is the number of edges, $|V|$ is the number of vertices, and k is the number of connected components of the graph. In the case of a connected graph (which is

typically the case in this dissertation), the formula simplifies to

$$\beta = |E| - |V| + 1.$$

Informally, the first Betti number can be viewed as the number of "independent" cycles of a graph.

Generic Eigenvalue – A *simple eigenvalue* whose corresponding eigenfunction is nonzero on all vertices of the graph.

Generic Graph – A graph Γ such that all eigenvalues of the Schrödinger operator on Γ are *generic eigenvalues*.

Hessian Matrix – An $n \times n$ matrix of second partial derivatives of f, where f is a function of n variables. In particular, the j, k entry at the point $\boldsymbol{x} = (x_1, x_2, \ldots, x_n)$ is of the form

$$H_{j,k} = \frac{\partial^2 f(\boldsymbol{x})}{\partial x_j \partial x_k}.$$

Leaf – A vertex of *degree* one.

Magnetic Flux – The total magnetic potential around a set of basis *cycles* of a graph. To see the steps to calculate it, see page 17 for the discrete graphs and pages 18–19 for quantum graphs.

Metric Graph – A graph defined by a set of vertices V, edges E, and real numbers L that assigns length to each edge. See page 9 for details.

Nodal Deficiency – The difference between the expected and actual number of *nodal domains*, which is equal to

$$n - \nu_n$$

where ν_n is the number of *nodal domains* of the nth eigenfunction.

Nodal Domains – The connected components formed by "cutting" the graph at *zeros of an eigenfunction*. In the discrete case, these components are formed by removing the edges that contain a zero of the eigenfunction, and in the quantum case, Dirichlet conditions are enforced at the *zeros of the eigenfunction*.

Nodal Point Count – The sequence $\{\phi_n\}$ where ϕ_n is the number of *zeros of the nth eigenfunction*.

Nodal Set – The set of *zeros of an eigenfunction*. This is a set of edges in the discrete case and a set of points in the quantum case.

Nodal Surplus – The difference between the expected and actual number of *zeros*

of an eigenfunction. This number is denoted by σ_n and is equal to

$$\sigma_n = \phi_n - (n-1)$$

where ϕ_n is the number of *zeros of the nth eigenfunction.*

Path – A sequence of edges $[e_1, e_2, \ldots, e_k]$ such that the vertex at the end of e_j is identical to the vertex at the beginning of edge e_{j+1}.

Quantum Graph – A *metric graph* along with a differential operator and associated vertex conditions. Functions are defined everywhere on the vertices and edges. See pages 9–10 for details.

Quantum Tree – A *metric graph* that is a *tree* and the vertex conditions of the associated operator are local.

Simple Eigenvalue – An eigenvalue with multiplicity one; i.e., a non-degenerate eigenvalue.

Spectral Band – The set of all n^{th} eigenvalues $\lambda_n(\boldsymbol{\alpha})$, for a fixed n, over all $\boldsymbol{\alpha}$ in the *Brillouin zone.* See pages 47–48 for details.

Symmetric Point – A vector whose entries are all $-\pi, 0,$ or π, or in other words, a vector in

$$\Sigma = \{(b_1, \ldots, b_n) : b_j \in \{-\pi, 0, \pi\}\}.$$

When analyzing the eigenvalues $\lambda_n(\boldsymbol{\alpha})$ of a finite graph, $n = \beta$, the *first Betti number* of the original (uncut) graph. When analyzing an infinite $\mathbb{Z}^k$-periodic graph, $n = k$. These points are traditional called "exterior" or "boundary" points of the *Brillouin zone.*

Tree – A graph with no *cycles*, or in other words, a graph whose *first Betti number* β is zero.

Zeros of a Function – In the case of a discrete graph, we say that a function has a zero on an edge if the sign of the function changes on that edge. In particular, f has a zero on edge $(u, v) \in E$ if

$$f(u)f(v) < 0.$$

In the case of a quantum graph, a function f is zero at a point x on the graph at which $f(x) = 0$.